Technical Report REMR-CS-44
June 1994

US Army Corps
of Engineers
Waterways Experiment
Station

AD-A281 491

Repair, Evaluation, Maintenance, and Rehabilitation Research Program

Field Testing and Structural Analysis of Vertical Lift Lock Gates

by Brett C. Commander, Jeff X. Schulz, George G. Goble
Bridge Diagnostics, Inc.

Cameron P. Chasten

DTIC
ELECTE
JUL 12 1994
S G D

WES

Approved For Public Release; Distribution Is Unlimited

94-21151

DTIC QUALITY INSPECTED 1

94 7 11 165

REMR

Prepared for Headquarters, U.S. Army Corps of Engineers

The following two letters used as part of the number designating technical reports of research published under the Repair, Evaluation, Maintenance, and rehabilitation (REMR) Research Program identify the problem area under which the report was prepared:

	Problem Area		Problem Area
CS	Concrete and Steel Structures	EM	Electrical and Mechanical
GT	Geotechnical	EI	Environmental Impacts
HY	Hydraulics	OM	Operations Management
CO	Coastal		

The contents of this report are not to be used for advertising, publication, or promotional purposes. Citation of trade names does not constitute an official endorsement or approval of the use of such commercial products.

PRINTED ON RECYCLED PAPER

Repair, Evaluation, Maintenance, and Rehabilitation Research Program

Technical Report REMR-CS-44
June 1994

Field Testing and Structural Analysis of Vertical Lift Lock Gates

by Brett C. Commander, Jeff X. Schulz, George G. Goble

Bridge Diagnostics, Inc.
5398 Manhattan Circle, Suite 280
Boulder, CO 80303

Cameron P. Chasten

U.S. Army Corps of Engineers
Waterways Experiment Station
3909 Halls Ferry Road
Vicksburg, MS 39180-6199

Accesion For
NTIS CRA&I [X]
DTIC TAB [ ]
Unannounced [ ]
Justification .....
By .....
Dist.ibution /
Availability Codes
Dist | Avail and / or Special
A-1

Final report

Approved for public release; distribution is unlimited

Prepared for U.S. Army Corps of Engineers
Washington, DC 20314-1000

Under Work Unit 32641

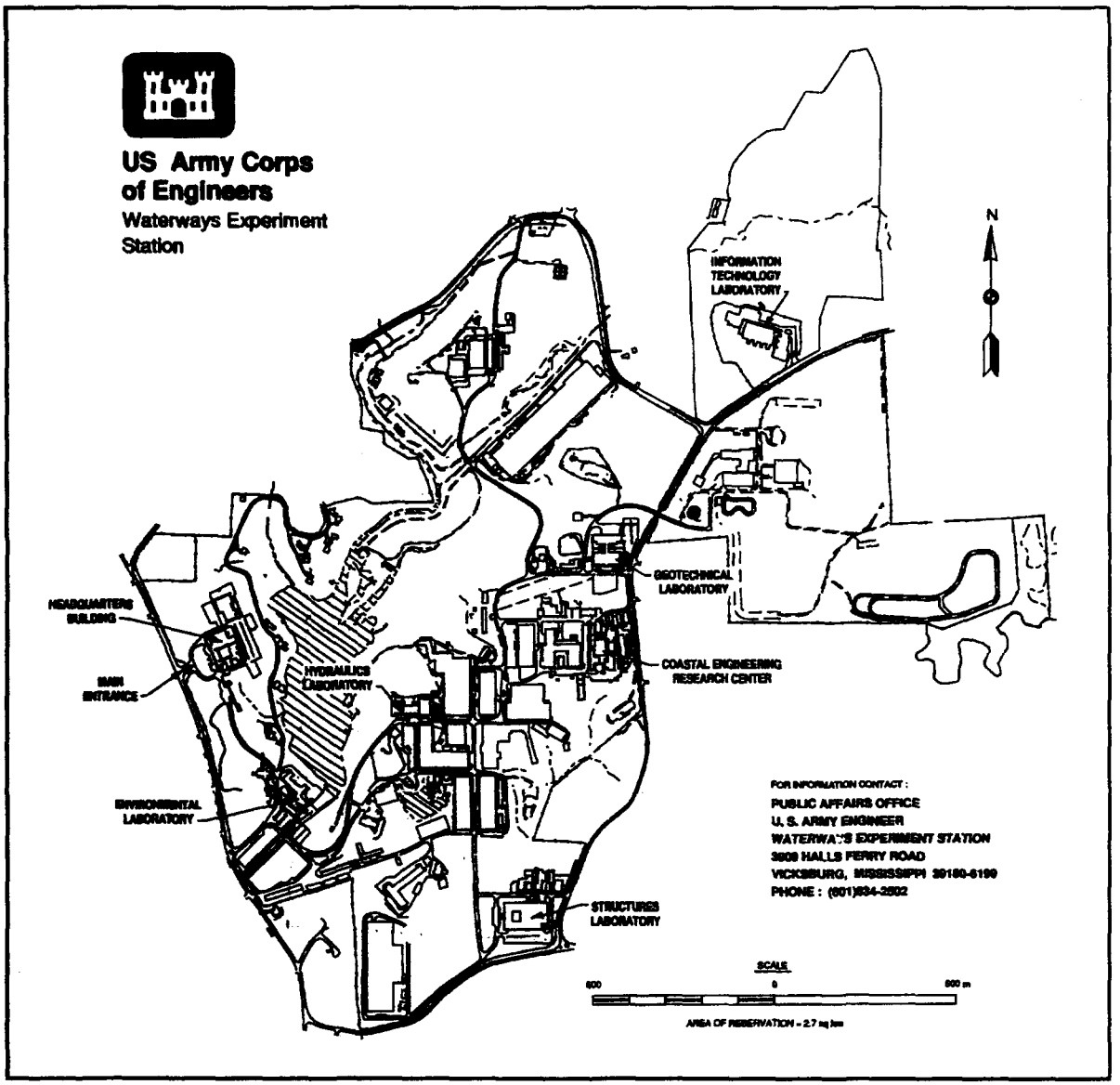

Waterways Experiment Station Cataloging-in-Publication Data

Field testing and structural analysis of vertical lift lock gates / by Brett C. Commander ... [et al.] ; prepared for U.S. Army Corps of Engineers.

81 p. : ill. ; 28 cm. -- (Technical report ; REMR-CS-44)

Includes bibliographic references.

1. Sluice gates -- Testing. 2. Hydraulic gates -- Evaluation. 3. Structural analysis (Engineering) I. Commander, Brett C. II. United States. Army. Corps of Engineers. III. U.S. Army Engineer Waterways Experiment Station. IV. Repair, Evaluation, Maintenance, and Rehabilitation Research Program. V. Title. VI. Series: Technical report (U.S. Army Engineer Waterways Experiment Station) ; REMR-CS-44.

TA7 W34 no.REMR-CS-44

Contents

Preface ix

1—Introduction 1

2—Field Testing 3

Loading and Instrumentation 3
Locks 27 Lift Gate Test Procedures 4
Set 1 tests (SET1-27) 5
Set 2 tests (SET2-27) 11
Field notes 14
Lock 27 field test conclusions 17
Locks and Dam 26 Lift Gate Test Procedures 17
Set 1 test (SET1-26): Test 261A chamber drop 19
Set 2 tests (SET2-26) 20
Field notes 21

3—Structural Analysis and Data Comparison 29

General Modeling Considerations 29
Analytical models 30
Structural models 31
Data Comparison 31
Absolute error 32
Percent error 32
Correlation factor 33
Locks 27 Lift Gate Modeling and Analysis 33
Model discretizaton 34
Loading and boundary conditions 35
Analysis and data comparison 36
Conclusions and recommendations 38
Locks and Dam 26 Lift Gate Modeling and Analysis 39
FE model 39
Loading and boundary conditions 40
Analysis and data comparison 40
Conclusions 43

4—General Conclusions 46

Experimental Studies 47
Setup 47
Additional test position and instrumentation 47
Analysis 48

References 49

Appendix A—Vertical Load Test Experimental Data A1

Appendix B—Head Differential Test Data B1

Locks 27 Strain Data (Test 272B; SET2-27) B2
Locks 27 Strain Data (Test 271C; SET1-27) B6
Locks and Dam 26 Strain Data (Test 262B; SET2-26) B16

List of Figures

Figure 1. Two waterproof strain transducers mounted on downstream girder flange 4

Figure 2. Locks 27 vertical lift gate - downstream face of upstream gate leaf 5

Figure 3. Locks 27 gate leaf configuration (elevations) 6

Figure 4. Transducer locations: Locks 27 - SET1-27 7

Figure 5. Transducer locations: Locks 27 SET1-27 - enlarged view 8

Figure 6. Transducer placement - SET1-27 (Transducers 22, 24, 27) 8

Figure 7. Transducer placement - SET1-27 (Transducrs 11, 14, 19) 8

Figure 8. Transducer placement - SET1-27 (Transducers 13, 23, 26, 28) 9

Figure 9. Transducer placement - SET1-27 (Transducers 21, 25) . 9

Figure 10. Transducer placement - SET1-27 (Transducers 9, 10, 15, 16, 18, 20) 9

Figure 11. Transducer placement - SET1-27 (Transducers 12, 17) . 9

Figure 12. Transducer placement - SET1-27 (Transducers 31, 32) . 10

Figure 13. Transducer placement - SET1-27 (Transducers 29, 30) . 10

Figure 14. Transducer placement - SET1-27 (Transducers 3, 4, 8) . 10

Figure 15. Transducer placement - SET1-27 (Transducers 5, 6, 7) . 10

Figure 16. Transducer locations: Locks 27 SET2-27 11

Figure 17. Transducer placement - SET2-27 (Transducers 16, 18) . 12

Figure 18. Transducer placement - SET2-27 (Transducers 8, 29) . . 12

Figure 19. Transducer placement - SET2-27 (Transducers 13, 26, 28) 12
Figure 20. Transducer placement - SET2-27 (Transducers 15, 22) . . 12
Figure 21. Transducer placement - SET2-27 (Transducers 11, 13, 24) 13
Figure 22. Transducer placement - SET2-27 (Transducers 2, 3, 4, 30) 13
Figure 23. Transducer placement - SET2-27 (Transducers 5, 7) . . . 13
Figure 24. Transducer placement - SET2-27 (Transducers 9, 20) . . . 13
Figure 25. Transducer placement - SET2-27 (Transducers 14, 19, 21, 27) 14
Figure 26. Transducer placement - SET2-27 (Transducers 12, 17, 25, 31) 14
Figure 27. Transducer placement - SET2-27 (Transducers 23, 32) . . 14
Figure 28. Locks and Dam 26 vertical lift gate - downstream face of middle leaf 18
Figure 29. Crack at girder flange-to-diaphragm flange connection . . 18
Figure 30. Locks and Dam 26 lift gate leaf configuration (elevations) 19
Figure 31. Transducers on Locks and Dam 26 lift gate 20
Figure 32. Transducer locations for Locks and Dam 26 SET1-26 . . . 21
Figure 33. Transducer placement - SET1-26 (Transducers 21, 23) . . 22
Figure 34. Transducer placement - SET1-26 (Transducers 13, 15, 24) 22
Figure 35. Transducer placement - SET1-26 (Transducers 9, 11, 14, 16) 22
Figure 36. Transducer placement - SET1-26 (Transducers 10, 12) . . 22
Figure 37. Transducer placement - SET1-26 (Transducers 1, 2) . . . 23
Figure 38. Transducer placement - SET1-26 (Transducer 22) 23
Figure 39. Transducer placement - SET1-26 (Transducer 3) 23
Figure 40. Transducer placement - SET1-26 (Transducers 19, 20) . . 23
Figure 41. Transducer placement - SET1-26 (Transducers 28, 29, 30 24
Figure 42. Transducer placement - SET1-26 (Transducer 17) 24
Figure 43. Transducer placement - SET1-26 (Transducer 18) 24
Figure 44. Transducer placement - SET1-26 (Transducers 25, 26, 27) 24
Figure 45. Transducer placement - SET1-26 (Transducers 31, 32) . . 25
Figure 46. Transducer locations for Locks and Dam 26 SET2-26 . . . 26
Figure 47. Transducer placement - SET2-26 (Transducers 5, 11) . . . 27

Figure 48. Transducer placement - SET2-26 (Transducers 1, 2, 3) . 27
Figure 49. Transducer placement - SET2-26 (Transducers 6, 7, 8) . 27
Figure 50. Transducer placement - SET2-26 (Transducers 9, 10) . . 27
Figure 51. Plan view of finite element mesh for a horizontal girder - Locks 27 34
Figure 52. Finite element mesh of Locks 27 lift gate (hidden lines removed) 34
Figure 53. Static hydrostatic load conditions for Locks 27 lift gate . 35
Figure 54. Dynamic hydrostatic load conditions for Locks 27 lift gate 36
Figure 55. Finite element mesh for Locks and Dam 26 lift gate - middle leaf 40
Figure 56. Hydrostatic loading applied for Locks and Dam 26 analysis 41
Figure 57. Vertical load pressure as a function of head differential . 43
Figure 58. Locks and Dam 26 leaf shear deformation and diaphragm deformation 45
Figure A1. Vertical load strain histories (SET1-27), Channels 22 and 27 . . . . . A2
Figure A2. Vertical Load Strain Histories (SET1-27), Channels 11 and 19 . . . . . A2
Figure A3. Vertical Load Strain Histories (SET1-27), Channels 13, 26, and 28 . . . . . A3
Figure A4. Vertical Load Strain Histories (SET1-27), Channels 10, 18, and 20 . . . . . A3
Figure A5. Vertical Load Strain Histories (SET1-27), Channels 9, 15, and 16 . . . . . A4
Figure A6. Vertical Load Strain Histories (SET1-27), Channels 12 and 17 . . . . . A4
Figure A7. Vertical Load Strain Histories (SET1-27), Channels 29, 30, 31, and 32 . . . . . A5
Figure B1. Locks 27 Strain Histories - Test 272B (SET2-27), Channels 18 and 16 . . . . . B2
Figure B2. Locks 27 strain histories - Test 272B (SET2-27), Channels 8 and 29 . . . . . B2
Figure B3. Locks 27 strain histories - Test 272B (SET2-27), Channels 28, 26, and 13 . . . . . B3

Figure B4. Locks 27 strain histories - Test 272B (SET2-27), Channels 15 and 22 . . . . . B3

Figure B5. Locks 27 strain histories - Test 272B (SET2-27), Channels 3 and 30 . . . . . B4

Figure B6. Locks 27 strain histories - Test 272B (SET2-27), Channels 20 and 9 . . . . . B4

Figure B7. Locks 27 strain histories - Test 272B (SET2-27), Channels 19, 27, 14, and 21 . . . . . B5

Figure B8. Locks 27 strain histories - Test 272B (SET2-27), Channels 12, 17, 31, and 25 . . . . . B5

Figure B9. Locks 27 strain histories - Test 271C (SET1-27), Channels 22 and 27 . . . . . B6

Figure B10. Locks 27 strain histories - Test 271C (SET1-27), Channels 11 and 19 . . . . . B7

Figure B11. Locks 27 strain histories - Test 271C (SET1-27), Channels 28, 26, and 13 . . . . . B7

Figure B12. Locks 27 strain histories - Test 271C (SET1-27), Channels 20, 18, and 10 . . . . . B8

Figure B13. Locks 27 strain histories - Test 271C (SET1-27), Channels 9, 16, and 15 . . . . . B8

Figure B14. Locks 27 strain histories - Test 271C (SET1-27), Channels 12 and 17 . . . . . B9

Figure B15. Locks 27 strain histories - Test 271C (SET1-27), Channel 8 . . . . . B9

Figure B16. Locks 27 strain histories - Test 271C (SET1-27), Channels 6 and 7 . . . . . B10

Figure B17. Locks and Dam 26 strain histories - Test 261A (SET1-26), Channel 21 . . . . . B11

Figure B18. Locks and Dam 26 strain histories - Test 261A (SET1-26), Channels 15, 24, and 13 . . . . . B11

Figure B19. Locks and Dam 26 strain histories - Test 261A (SET1-26), Channels 11, 9, and 14 . . . . . B12

Figure B20. Locks and Dam 26 strain histories - Test 261A (SET1-26), Channels 10 and 12 . . . . . B12

Figure B21. Locks and Dam 26 strain histories - Test 261A (SET1-26), Channels 19 and 20 . . . . . B13

Figure B22. Locks and Dam 26 strain histories - Test 261A (SET1-26), Channels 30, 28, and 29 . . . . . B13

Figure B23. Locks and Dam 26 strain histories - Test 261A (SET1-26), Channels 31 and 32 . . . . . B14

Figure B24. Locks and Dam 26 strain histories - Test 261A (SET1-26), Channels 1 and 4 . . . . . B14

Figure B25. Locks and Dam 26 strain histories - Test 261A (SET1-26), Channels 25, 27, and 26 . . . . . B15

Figure B26. Locks and Dam 26 strain histories - Test 261A (SET1-26), Channel 17 . . . . . B15

Figure B27. Locks and Dam 26 strain histories - Test 262B (SET2-26), Channels 4, 5, and 11 . . . . . B16

Figure B28. Locks and Dam 26 strain histories - Test 262B (SET2-26), Channels 1, 2, and 3 . . . . . B16

Figure B29. Locks and Dam 26 strain histories - Test 262B (SET2-26) (gage slippage on channel 7), Channels 6, 7, and 8 . . . . B17

Figure B30. Locks and Dam 26 strain histories - Test 262B (SET2-26), Channels 9, 10, and 12 . . . . . B17

Preface

The work described in this report was sponsored by the U.S. Army Engineer District (USAED), St. Louis, and Headquarters, U.S. Army Corps of Engineers (HQUSACE), as part of the Concrete and Steel Structures Problem Area of the Repair, Evaluation, Maintenance, and Rehabilitation (REMR) Research Program. The work was performed under the REMR Work Unit 32641, "Evaluation and Repair of Hydraulic Steel Structures (HSS)," for which Mr. Cameron P. Chasten, Information Technology Laboratory (ITL), U.S. Army Engineer Waterways Experiment Station (WES), was Principal Investigator. Mr. Don Dressler was the HQUSACE Technical Monitor.

Mr. William N. Rushing (CERD-C) was the REMR Coordinator at the Directorate of Research and Development, HQUSACE; Mr. James E. Crews (CECW-O) and Dr. Tony C. Liu (CECW-EG) served as the REMR Overview Committee; Mr. William F. McCleese, Structures Laboratory (SL), WES, was the REMR Program Manager; and Mr. James E. McDonald, SL, WES, was the Problem Area Leader.

The work was performed by Bridge Diagnostics Incorporated (BDI) under U.S. Army Corps of Engineers Contract Number DACW39-92-C-0064. The report was prepared by Messrs. Brett C. Commander and Jeff X. Schulz, and Dr. George G. Goble, BDI; and Mr. Chasten, under the general supervision of Mr. H. Wayne Jones, Chief, Scientific and Engineering Applications Center (S&EAC), Computer-Aided Engineering Division, ITL, WES, and Dr. N. Radhakrishnan, Director, ITL. Acknowledgment is expressed to Messrs. Thomas Ruf, Engineering Division, and Robert Kelsey, Operations Division, USAED, St. Louis, for organizing and assisting in field testing performed at the Mississippi River Locks 27 and Locks and Dam 26.

At the time of publication of this report, Director of WES was Dr. Robert W. Whalin. Commander was COL Bruce K. Howard, EN.

1 Introduction

There are over 160 commercially active locks (including over 200 lock chambers) on the United States inland and intracoastal waterway systems. The age of these locks ranges from 1 to over 150 years. Approximately 40 percent of the locks are over 50 years old and the median age of all lock chambers is approximately 35 years (Headquarters, U.S. Army Corps of Engineers (HQUSACE) 1988). There is a need for development of structural evaluation tools that can provide assessment of the strength and safety of these aging structures.

A primary goal of the Repair, Evaluation, Maintenance, and Rehabilitation (REMR) project "Evaluation and Repair of Hydraulic Steel Structures (HSS)" is to develop structural evaluation guidance for assessment of aging steel lock gates. Lock gates include miter gates, lift gates, sector gates, and tainter gates. This report describes experimental and analytical studies that were conducted for two vertical-lift lock gates. EM 1110-2-2703 and EM 1110-2-2701 (HQUSACE 1962, 1984) describe the use, design, and layout of vertical lift gates.

Due to complex geometry and loading conditions, analysis and design of vertical lift gates include many simplifying assumptions. Although good approximations can be made in the development of analytical models, it is not possible to make exact simulations of the loading, structural geometry, and boundary (support) conditions of a structure. Therefore, it is difficult to develop an *exact* model of even a new structure. For existing structures, construction tolerances, deterioration of seals, and wear at support points are factors that further alter loading and structural conditions. To ensure that a safe structural design is produced, assumptions on loading and structural characteristics can generally be conservative. However, for a structural evaluation, the primary goal is to assess the current condition of a structure. So that a reliable assessment can be made, it is desirable to identify the unknown quantities (loading, boundary conditions, etc.) with sufficient accuracy.

Experimental systems can measure the actual response of a structure subjected to various loading. However, with most systems only a few selected points on a structure can be monitored. An optimum evaluation system would incorporate both analytical and experimental techniques. An

analytical model of such a system can be systematically modified until it simulates structural behavior observed under experimental conditions. This type of evaluation system is currently under development in this study. A similar study for miter lock gates has been conducted (Commander et al. 1992a, 1992b).

The objectives of this study are to measure the behavior of vertical lift lock gates experimentally and to develop modeling and analysis procedures that may provide a basis for the evaluation of existing gates and design of new gates. In this study, lift gates at Mississippi River Locks 27 near Granite City, IL, and Locks and Dam 26 (Melvin Price) near Alton, IL, were investigated. The upstream lock gate of the auxiliary lock at Locks 27 and the upstream lock gate of the main lock at Locks and Dam 26 were instrumented and tested under various loading conditions in June 1992. Analytical models were developed and analyses were performed for each.

The lift gate of the auxiliary lock at Locks 27 was selected for study on the following basis. This gate is identical in construction to the lift gate in the main lock chamber. The gate of the main lock will be replaced since several of its structural members have cracked. Since the auxiliary lock lift gate is in good condition, the experimental data may provide insight on the development of improved modeling and analysis procedures which will benefit the design of a replacement gate in the main lock. Furthermore, the acquired data may suggest possible causes of cracking in the main lock gate. The lift gate at Locks and Dam 26 is ideal for the verification of the testing and analysis procedures since it is a new structure in good condition.

This report describes the testing, analytical modeling, and analysis procedures of each lift gate. Chapter 2 describes the instrumentation and testing for the experimental studies. The analytical studies and comparisons of analytical and experimental data are discussed in Chapter 3. Chapter 4 gives a summary of the study and provides recommendations on future experimental and analytical studies for vertical lift gates. Appendices A and B include graphical comparisons of the analytical predictions and the experimental responses.

2 Field Testing

Loading and Instrumentation

One leaf of each vertical lift gate was monitored during field testing to measure the in-service structural behavior. A data acquisition system (DAS) recorded strain measurements as various loads were applied to the structure. For each test, two general loading conditions were applied.

a. Vertical load. Vertical load due to self-weight was applied by lifting the gate from the bottom sill.

b. Hydrostatic head differential load. Filling or emptying the lock chamber produced varying head differential (difference in upper pool elevation and lock chamber water elevation). This condition imposed both lateral and vertical pressure loads to the gate leaves.

Instrumentation consisted of a DAS, electronic cables, and submergible steel strain transducers. The transducers measure strain over an effective gage length of 3 in. (7.62 cm). Each test included approximately 30 transducers that were mounted on various structural members (girder flanges, skin plate, bracing, etc.). Where transducers were to be attached, hand-held grinders were used to remove the paint. C-clamps connected transducers to the edges of member flanges, and small steel tabs with bolts connected the transducers to locations not accessible for C-clamps. The steel tabs were glued to structural steel with cyanoacrylate glue. For each transducer, approximately 100 ft (30.48 m) of cable connected the transducer to the DAS. Transducer cables were routed along the girders and through girder drain holes from the transducers to the DAS. Figure 1 shows two of the waterproof strain transducers C-clamped to a girder flange. During installation and removal of the instrumentation, the locks were closed and the gates were raised clear of the water.

Strain transducers are mounted much faster and easier than conventional foil strain gages. Generally, two persons can mount a set of over 30 transducers in less than 1 day (Commander et al. 1992b). For these tests, significant time was lost as the gates were raised and lowered for instrumentation setup and tow lockage. The upstream leaf of the Locks 27 lift

Figure 1. Two waterproof strain transducers mounted on downstream girder flange

gate operates at approximately 1 ft (0.3048 m)/min and must be raised approximately 50 ft (15.24 m) to clear the upper pool elevation. Although not all experimental data were compared to analytical data (Chapter 3), the following sections describe each test in detail. Data for all tests are available through CEWES-IM-DS.

Locks 27 Lift Gate Test Procedures

The vertical lift gate of the auxiliary lock at Locks 27 has two leaves. The upstream (lower) leaf was tested since it is subject to larger service loads and its counterpart in the main lock chamber has exhibited considerable cracking (U.S. Army Engineer District, St. Louis (USACE) 1990). Each leaf is composed of six horizontal girders, three vertical diaphragms, and many downstream bracing members. Figure 2 shows the downstream face of the upstream leaf.

Two sets of tests were performed. In the first set (SET1-27), the gate was instrumented extensively in a localized area. The transducers were attached at locations similar to where cracking had occurred in the main lock chamber gate. The second set (SET2-27) consisted of a more general layout of transducers to observe the structural response of the main structural members. Instrumentation and testing of the leaf required

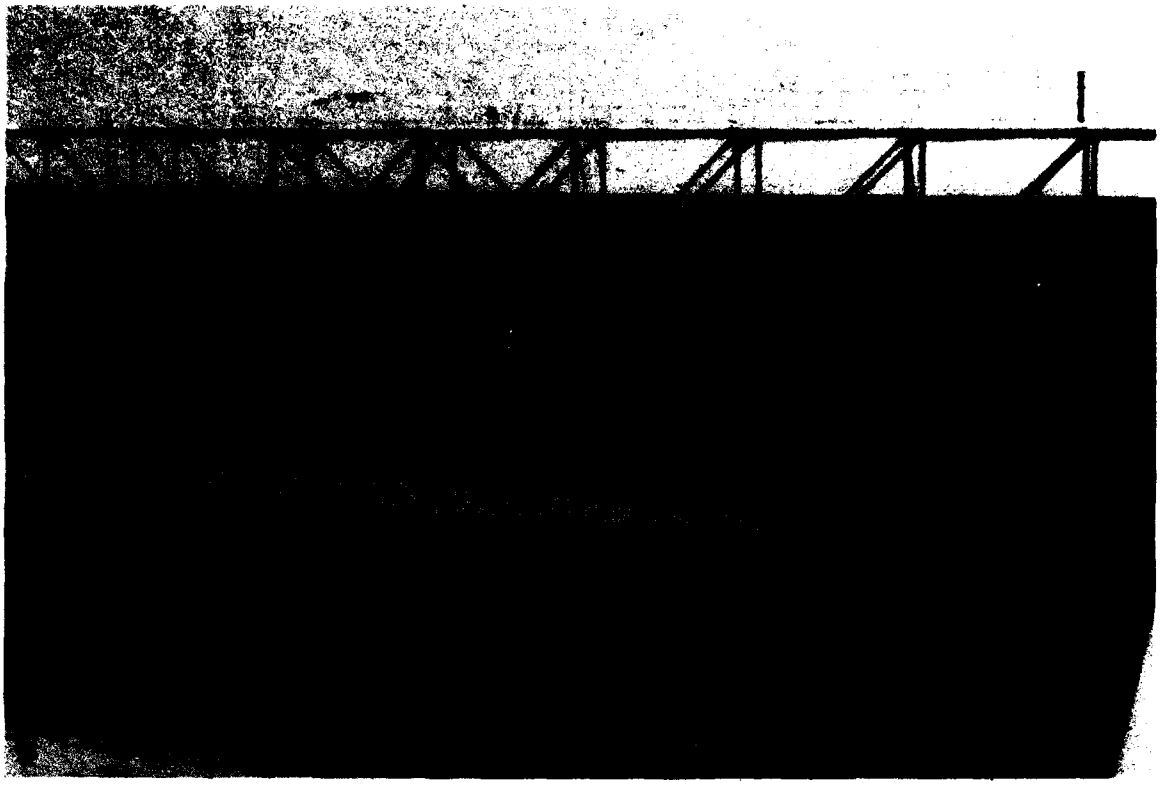

Figure 2. Locks 27 vertical lift gate - downstream face of upstream gate leaf

approximately 30 hours. A work flat provided access to the gate for instrumentation.

Vertical load and head differential load were applied during each set of tests. For the vertical load tests, the instrumented leaf was positioned on the bottom sill (so that all dead load was transferred to the sill) and then lifted a distance of approximately 2 ft (0.61 m). The DAS recorded strains as the leaf was lifted from the bottom sill. For the head differential tests, the instrumented leaf was positioned to form a damming surface for the lock chamber. Monitoring of strain data started as the lock chamber culvert valves were opened and continued as the chamber was filled or emptied. Figure 3 illustrates the pool and gate leaf elevations for the head differential tests.

Set 1 tests (SET1-27)

Vertical load tests. Figures 4 through 15 illustrate the location of the 30 strain transducers mounted on the structure. The corresponding DAS channel number identifies each transducer for convenience of reporting results. Four tests (described in following paragraphs) were conducted in 1 day. The upper pool elevation (el) was 399.88 ft (121.9 m) and the lower pool elevation was 386.9 ft (117.93 m).

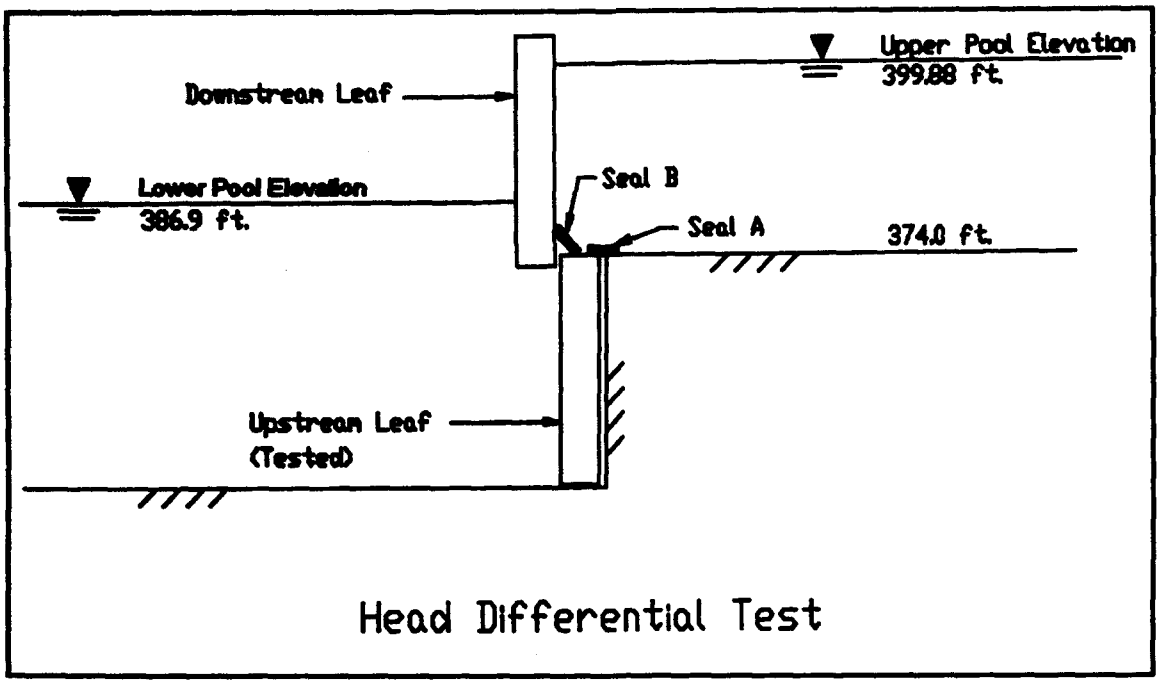

Figure 3. Locks 27 gate leaf configuration (elevations)

a. Test 271A. This test consisted of vertical loading due to dead weight. The upstream leaf was lowered to the bottom sill so the dead weight (reduced slightly due to buoyancy) was supported. To establish a datum, all strain transducers were zeroed (balanced) with the gate resting on the sill. At this position, the weight is carried by the sill and not the structural members. The DAS recorded data continuously at 32 Hertz (Hz) as the gate was lifted approximately 2 ft (0.6096 m) and returned to the sill.

At the start of Test 271A (when the datum was established), the lifting chain partially supported the gate. Therefore, the recorded strain measurements did not include the total vertical load due to the weight of the leaf. To assure that the upstream leaf rested on the sill in a subsequent test (Test 271D), the lifting chains were adjusted at the completion of Test 271A.

b. Test 271D. Following the head differential tests, Test 271D was conducted in the same manner as Test 271A. However, it is assumed that the lifting chain was adjusted so no load was carried by the chain at the start of the test.

Head differential tests. In preparation of these tests, the lock operator lowered the upstream leaf (the monitored leaf) to the sill and raised the downstream leaf as shown in Figure 3 (transducers were balanced in this position). The DAS recorded data continuously at 32 Hz as the lock chamber was emptied (Test 271B) or filled (Test 271C) to vary the head differential load on the lift gate. As the chamber was filled or emptied, times at

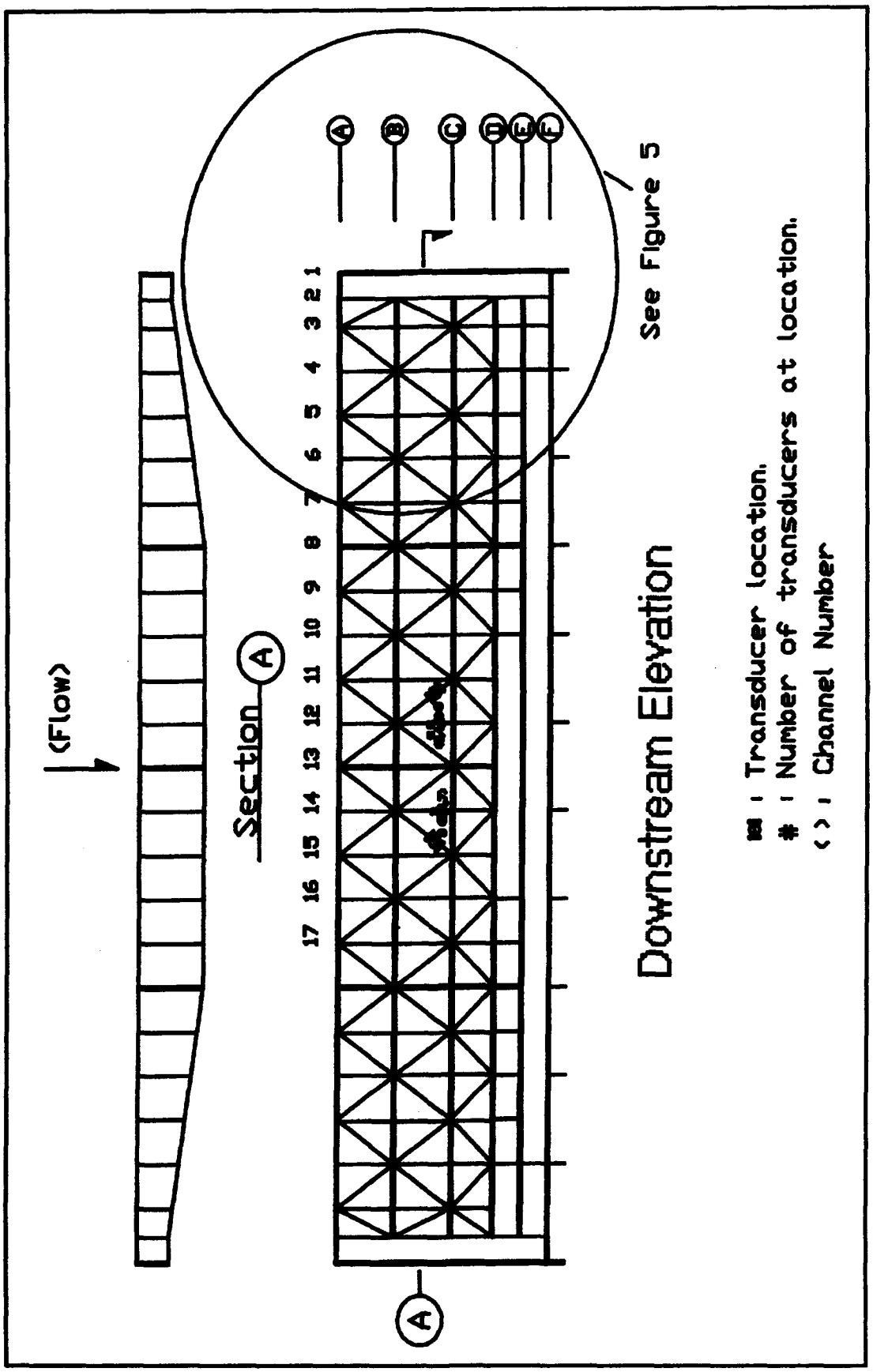

Figure 4. Transducer locations: Locks 27 - SET1-27

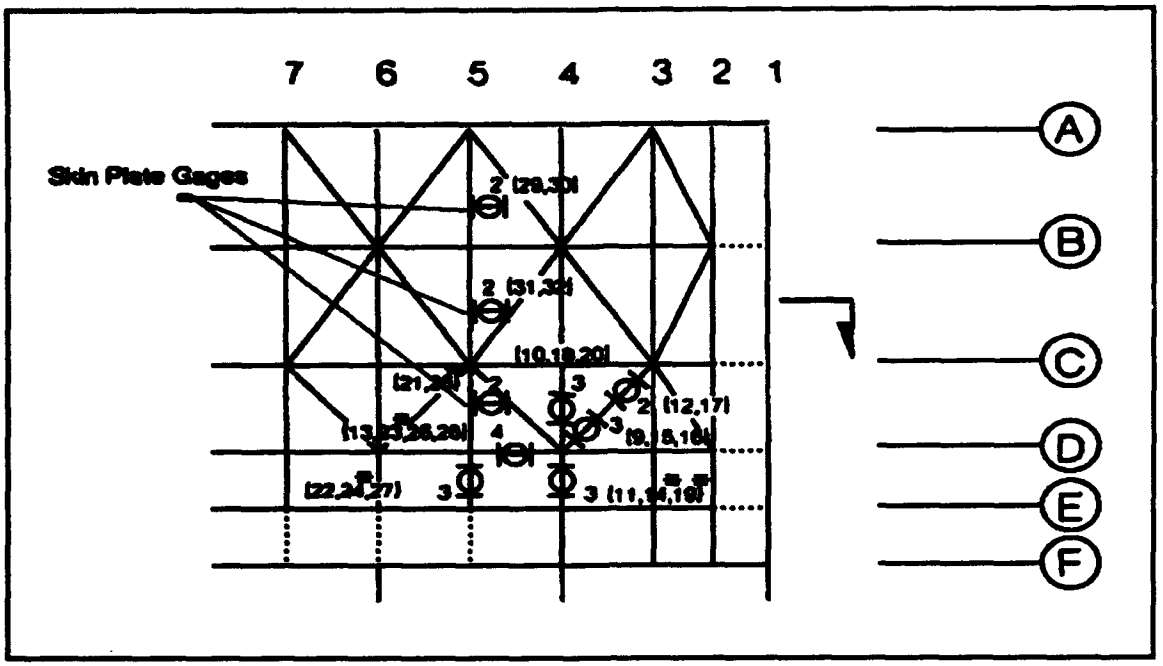

Figure 5. Transducer locations: Locks 27 SET1-27 - enlarged view

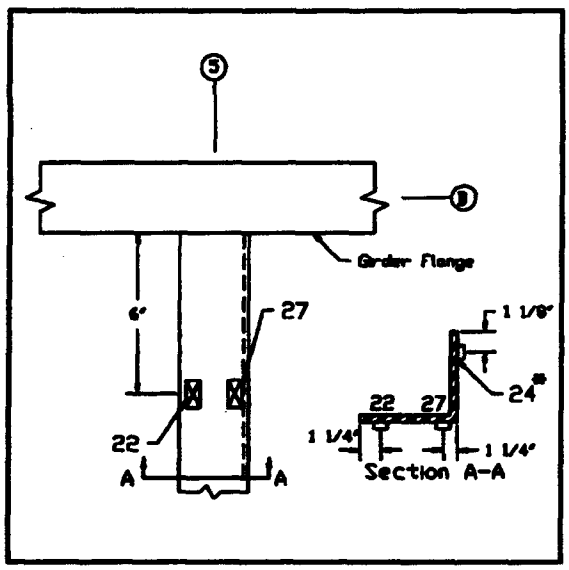

Figure 6. Transducer placement - SET1-27 (Transducers 22, 24, 27)

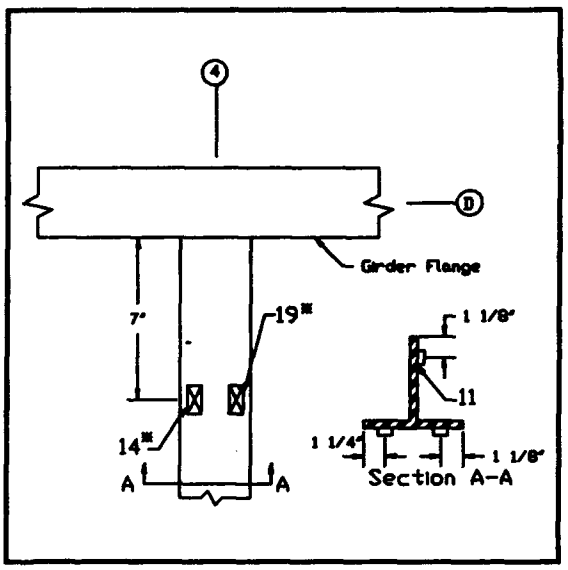

Figure 7. Transducer placement - SET1-27 (Transducers 11, 14, 19)

each 1-ft (0.3048 m) interval of chamber pool variation were recorded electronically with the strain data. This was necessary to correlate strain data with head differential load.

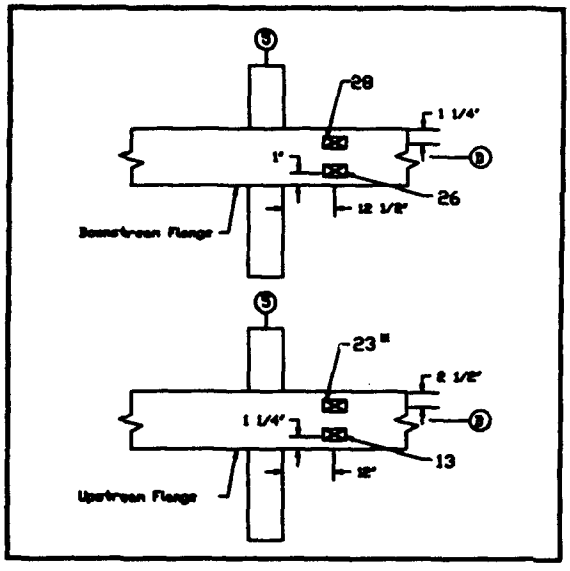

Figure 8. Transducer placement - SET1-27 (Transducers 13, 23, 26, 28)

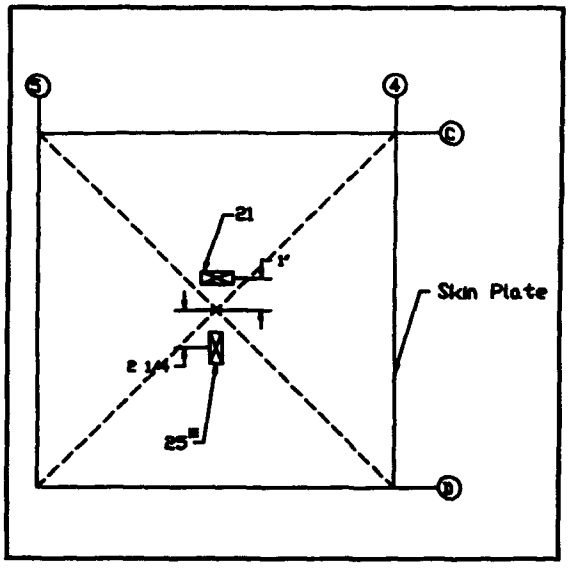

Figure 9. Transducer placement - SET1-27 (Transducers 21, 25)

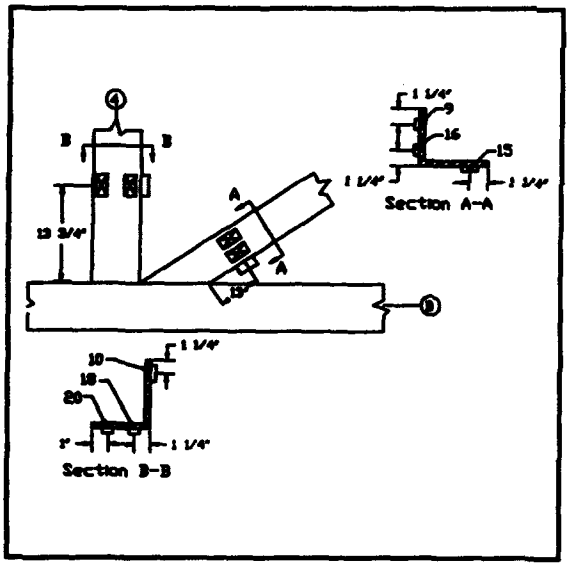

Figure 10. Transducer placement - SET1-27 (Transducers 9, 10, 15, 16, 18, 20)

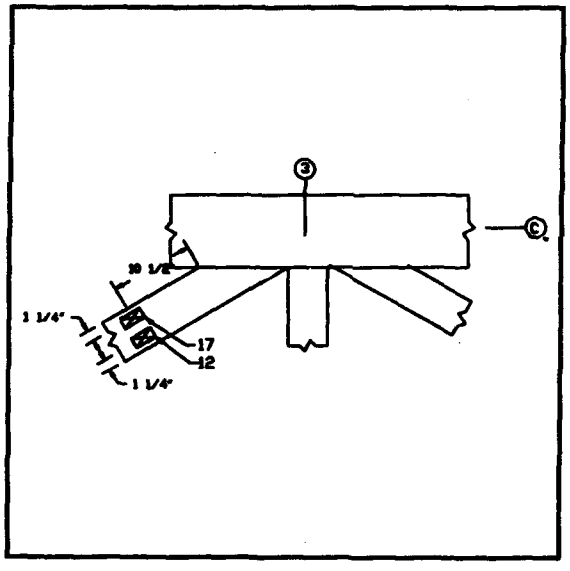

Figure 11. Transducer placement - SET1-27 (Transducers 12, 17)

a. Test 271B: chamber drop. The data were established with the lock chamber full and no differential head (chamber water elevation equal to the upper pool elevation). The DAS recorded data as the chamber water level dropped from upper pool to lower pool elevation. 1-ft (0.3048 m) intervals of chamber pool elevation were identified by an elevation marker located on the lock wall. For approximately the first 6 ft (1.83 m) of chamber drop, the marker was not visible and the position could not be identified accurately. However, the last 6 ft (1.83 m) were identified.

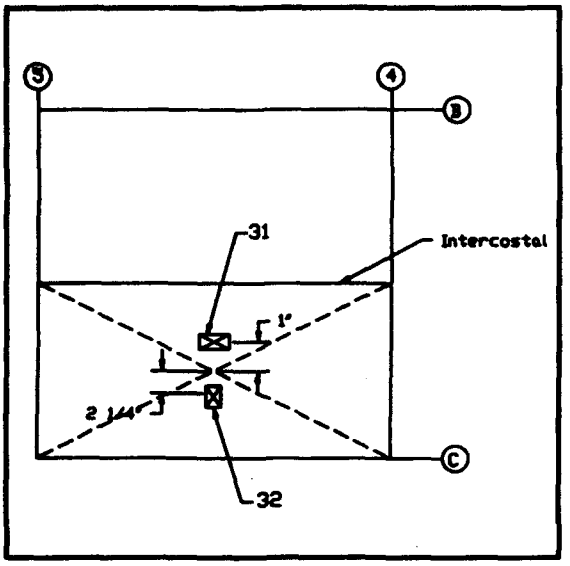

Figure 12. Transducer placement - SET1-27 (Transducers 31, 32)

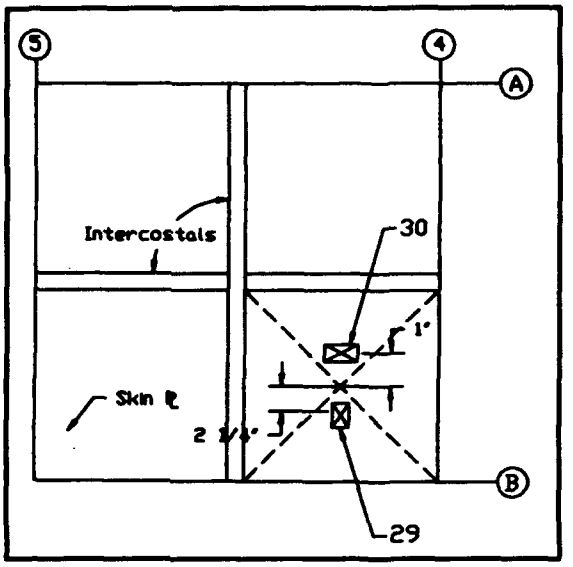

Figure 13. Transducer placement - SET1-27 (Transducers 29, 30)

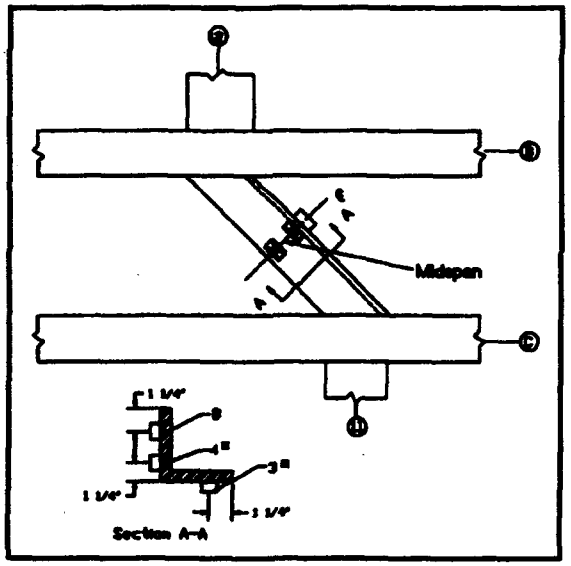

Figure 14. Transducer placement - SET1-27 (Transducers 3, 4, 8)

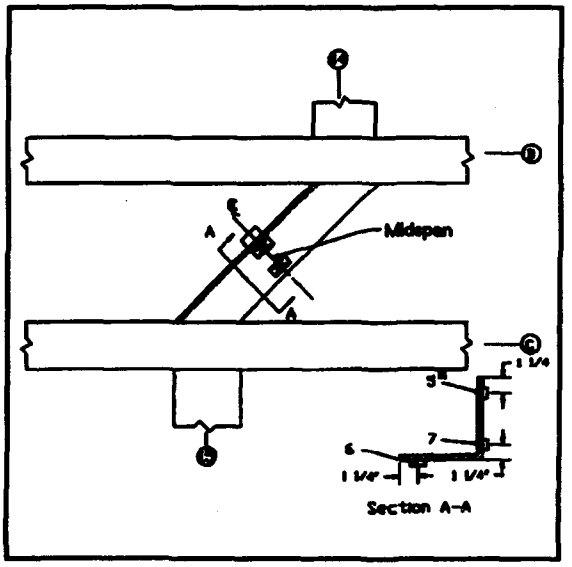

Figure 15. Transducer placement - SET1-27 (Transducers 5, 6, 7)

b. Test 271C: chamber fill. In this test, the DAS recorded data as the chamber filled. The data were established with the lock chamber empty; the initial condition consisted of a 12-ft, 9-in. (3.9 m) differential head. Since the lock wall gage was not always visible, the lockmaster identified 1-ft (0.3048 m) intervals of chamber pool elevation using a pressure gage installed in the control room. (This was done for all subsequent tests.)

Set 2 tests (SET2-27)

At the completion of the SET1-27 series of tests, the upstream gate leaf was prepared for the second series of tests (SET2-27) in which three tests were performed. Figures 16 through 27 show the locations of the 28 strain transducers mounted on the leaf. (Two of the original 30 transducers malfunctioned.) Each transducer is identified by the DAS channel number. Upper pool and lower pool elevations were 400.25 (122 m) and 387.26 ft (118 m), respectively.

a. **Vertical load test: Test 272A.** This test was similar to Test 271A and Test 271D. The data for the strain measurements were established with the leaf resting on the sill. The DAS recorded data

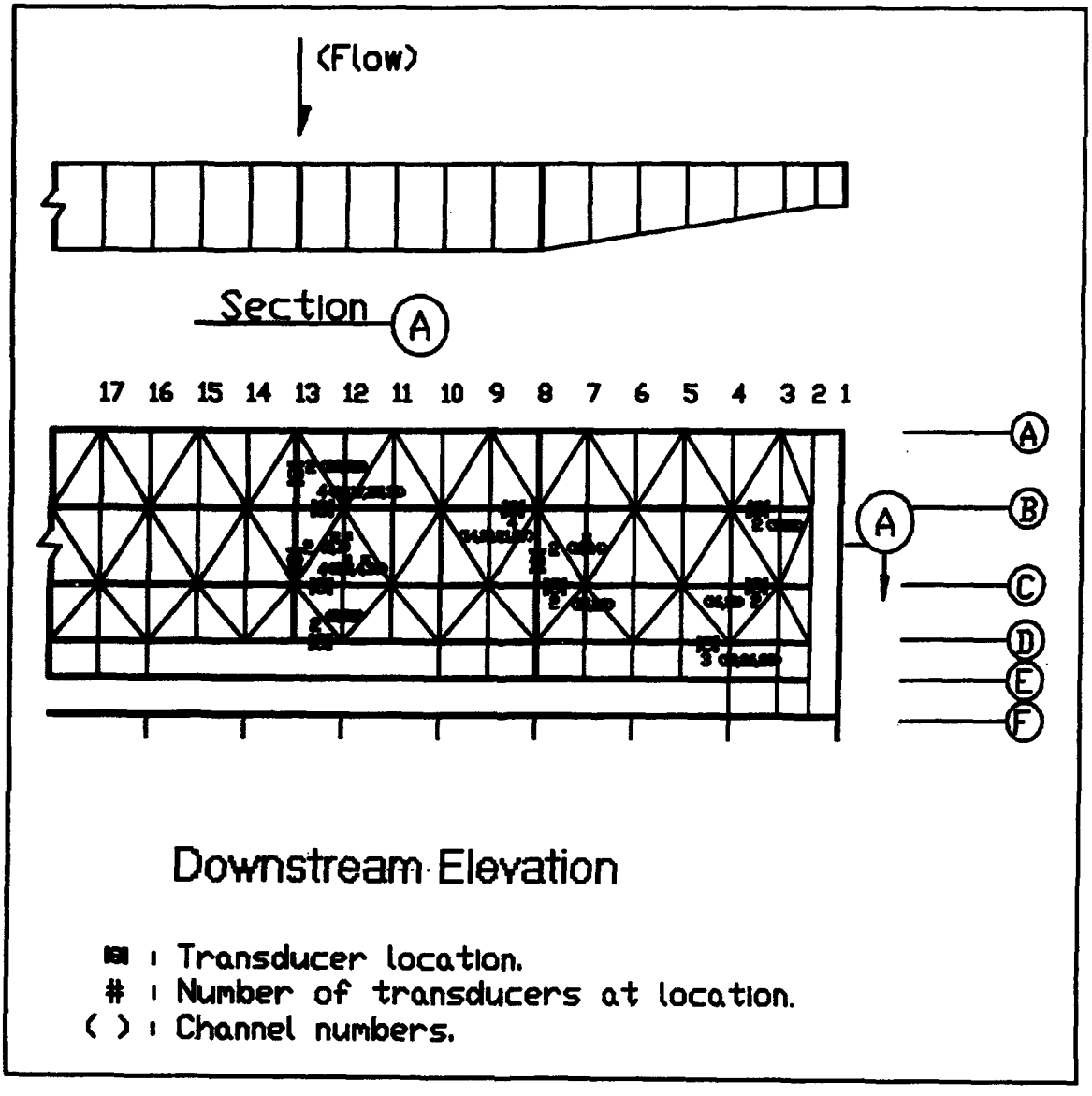

Figure 16. Transducer locations: Locks 27 SET2-27

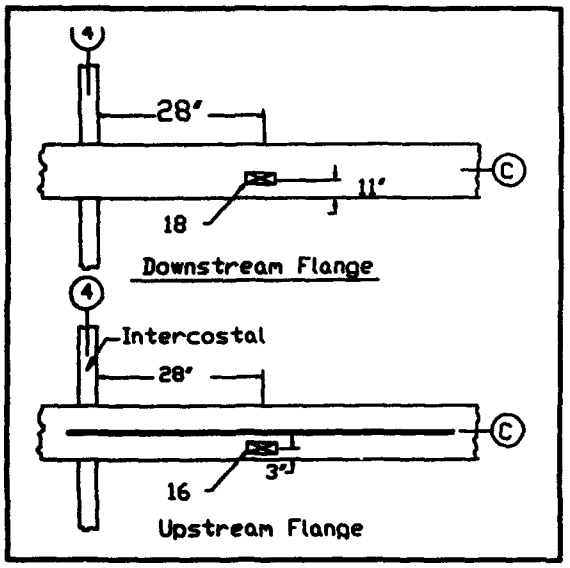

Figure 17. Transducer placement - SET2-27 (Transducers 16, 18)

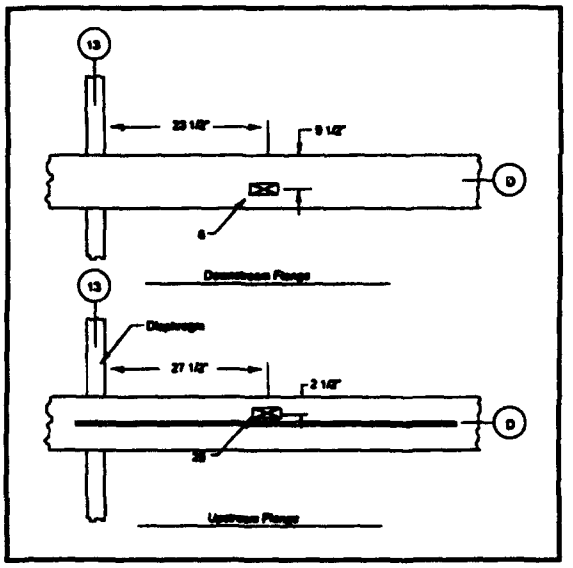

Figure 18. Transducer placement - SET2-27 (Transducers 8, 29)

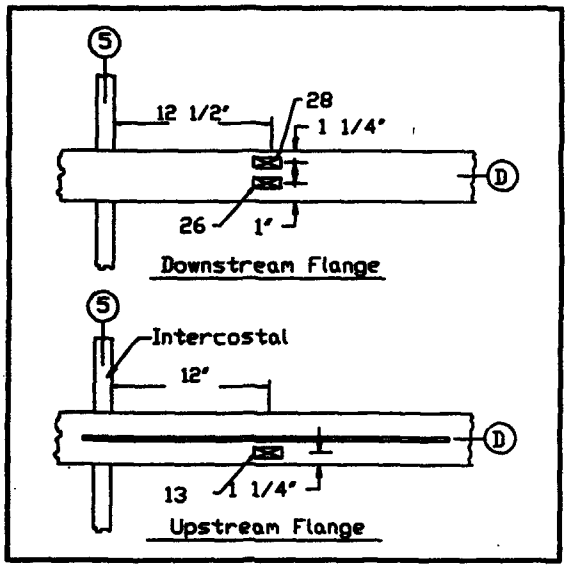

Figure 19. Transducer placement - SET2-27 (Transducers 13, 26, 28)

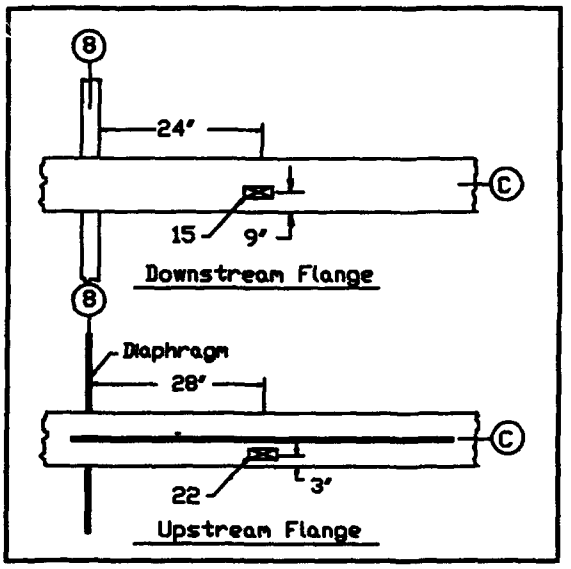

Figure 20. Transducer placement - SET2-27 (Transducers 15, 22)

continuously as the leaf was raised from resting position to approximately 1 ft (0.3048 m) above the sill.

b. **Head differential tests.** After Test 272A, the upstream leaf was positioned on the sill, and the downstream leaf was raised. Testing was conducted as described for the Set1-27 tests.

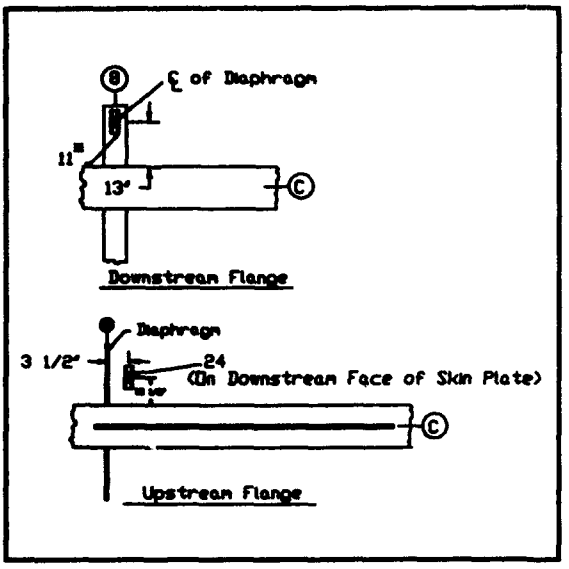

Figure 21. Transducer placement - SET2-27 (Transducers 11, 13, 24)

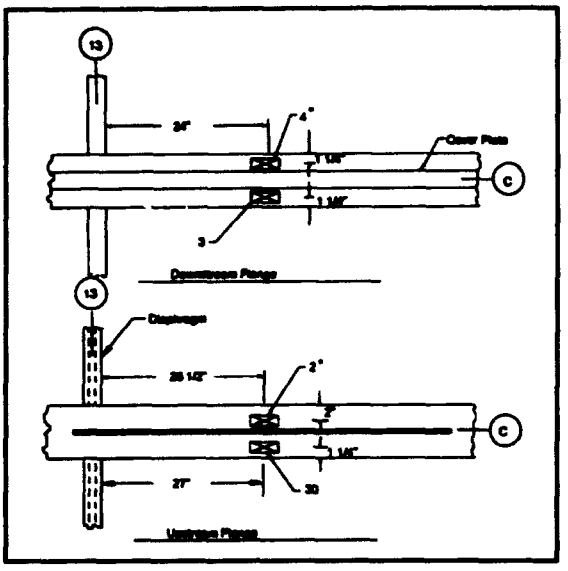

Figure 22. Transducer placement - SET2-27 (Transducers 2, 3, 4, 30)

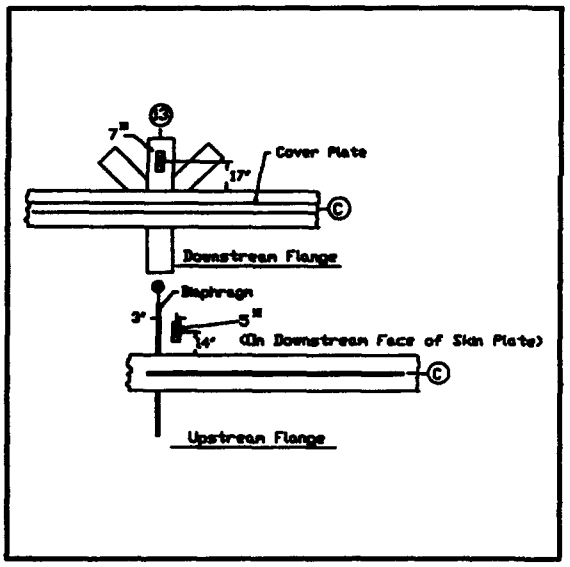

Figure 23. Transducer placement - SET2-27 (Transducers 5, 7)

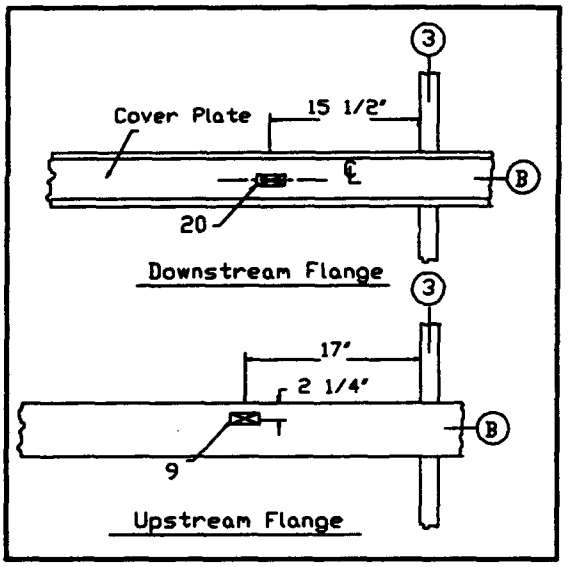

Figure 24. Transducer placement - SET2-27 (Transducers 9, 20)

(1) *Test 272B: chamber drop.* This test was similar to Test 271B. The DAS recorded data continuously as the differential head was varied from 0 to approximately 12 ft (3.66 m).

(2) *Test 272C: chamber fill.* Test 272C was similar to Test 271C. The data were set with 12 ft (3.66 m) of differential head (the chamber level was slightly higher than the low-pool elevation due to leakage around the lift gate seals). The DAS recorded

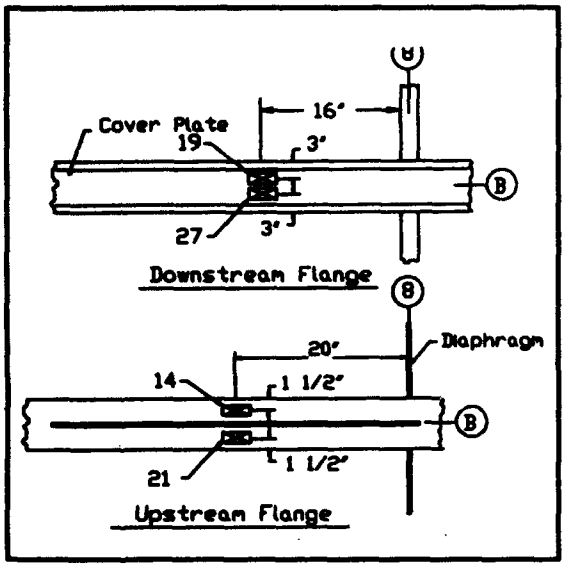

Figure 25. Transducer placement - SET2-27 (Transducers 14, 19, 21, 27)

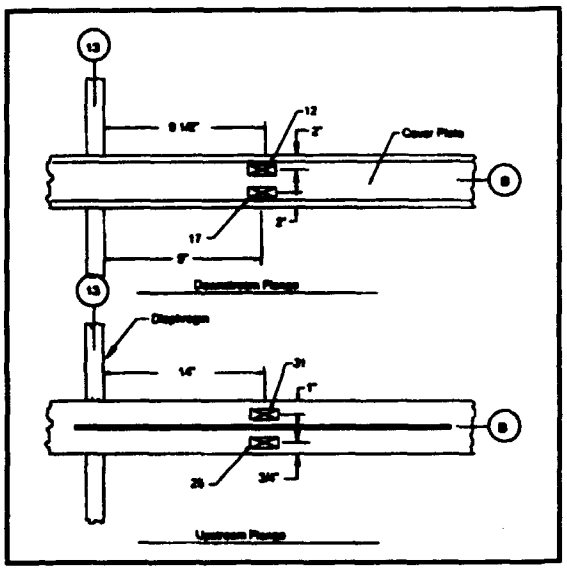

Figure 26. Transducer placement - SET2-27 (Transducers 12, 17, 25, 31)

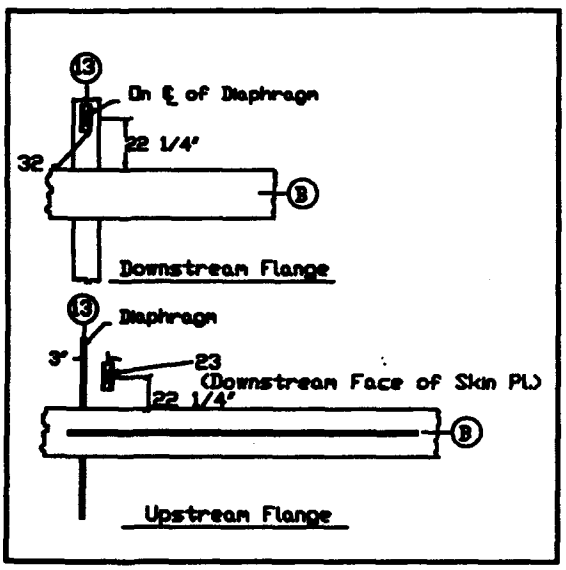

Figure 27. Transducer placement - SET2-27 (Transducers 23, 32)

data continuously as the chamber pool level was raised to the upper pool elevation.

Field Notes

a. Several transducers malfunctioned during testing due to electrical problems or slippage from inadequate clamping. The data from these transducers were not compared with the analytical data.

Transducers that malfunctioned for tests in SET1-27 correspond to DAS channel numbers 3, 4, 5, 14, 19, 23, 24, and 25 (Channel 19 malfunctioned during Test 271D only). Transducers numbered 1, 2, 4, 5, 7, 10, and 11 were questionable for tests of SET2-27. Each unreliable transducer is identified with an asterisk in Figures 4 through 27.

b. Due to the submergence and vertical movement of the leaf, it was required that the transducer cables be attached to the leaf and grouped together. To save time in future testing of lift gates, several transducers should be grouped together before installation.

c. The clamping and gluing methods (used for attaching the strain transducers to the structural members) worked quite well for making underwater measurements.

d. The following summaries provide field data file names (DAS channel numbering/ strain data), the data for each test, and a description of the data record.

(1) *Test 271A Summary.*

Data File:	SET1-27.CHN / TEST271A.DAT
Balance:	Leaf assumed on sill.
Data Record:	Start with leaf assumed on sill; record as leaf raised approximately 2 ft (0.6096 m) and lowered; stop at time leaf was lowered to sill.
Notes:	Channels 3 and 4 obtained erratic values (the transducers may have malfunctioned).

(2) *Test 271D Summary.*

Data File:	SET1-27.CHN / TEST271D.DAT
Balance:	Leaf on sill.
Data Record:	Start with leaf on sill; record as leaf raised approximately 2 ft (0.6096 m) and lowered; stop at time leaf was lowered to sill.
Notes:	On observation of strain records during testing, Channel 23 was not responding correctly. Channels 14 and 19 malfunctioned as the gate was being lowered.

(3) *Test 271B Summary.*

Data File:	SET1-27.CHN / TEST271B.DAT
Balance:	Zero head, leaf on sill.
Data Record:	Start at zero head; random position indicator marks exist in the data file for approximately the first 6 ft (1.83 m) of chamber drop; the last six marks are accurate and correspond to head

differentials of 7-, 8-, 9-, 10-, 11-, and 12-ft (3.66 m) head. The last mark was recorded at a head of 12 ft (3.66 m); the final head differential was approximately 12.5 ft (3.81 m); stop recording.

Notes: The differential between upper and lower pools does not equal 12.5 ft. The chamber level was slightly higher than lower pool due to leakage around the lift gate. The final head differential was measured using instruments used by the lock operator.

(4) *Test 271C Summary.*

Data File: SET1-27.CHN / TEST271C.DAT
Balance: 12-ft 9-in. (3.9 m) head, leaf on sill.
Data Record: Start at 12-ft 9-in. (3.9 m) head; indicator marks at 12-, 11-, 10-, 9-, 8-, 7-, 6-, 5-, 4-, 3-, 2-, 1-, and 0-ft (3.66-, 3.35-, 3.048-, 2.74-, 2.44-, 2.13-, 1.83-, 1.52-, 1.22-, 0.914-, 0.6096-, 0.3048-, and 0-m) head; stop recording.

(5) *Test 272A Summary.*

Data File: SET2-27.CHN / TEST272A.DAT
Balance: Leaf on sill.
Data Record: Start with leaf on sill, stop at the time the leaf was raised approximately 1 ft (0.3048 m).

(6) *Test 272B Summary.*

Data File: SET2-27.CHN / TEST272B.DAT
Balance: Zero head; leaf on sill.
Data Record: Start at zero head; indicator marks at 1-, 2-, 3-, 4-, 5-, 6-, 7-, 8-, 9-, 10-, and 11-ft (0.3048-, 0.6096-, 0.914-, 1.22-, 1.52-, 1.83-, 2.13-, 2.44-, 2.74-, 3.048-, and 3.35-m) head; stop (head differential at approximately 12 ft (3.66 m) at stop time).

(7) *Test 272C Summary.*

Data File: SET2-27.CHN / TEST272C.DAT
Balance: 12-ft (3.66-m) head; leaf on sill.
Data Record: Start at 12-ft (3.66-m) head; indicator marks at 11-, 10-, 9-, 8-, 7-, 6-, 5-, 4-, 3-, 2-, and 1-ft (3.35-, 3.048-, 2.74-, 2.44-, 2.13-, 1.83-, 1.52-, 1.22-, 0.914-, 0.6096-, and 0.3048-m) head; stop at approximately zero head.

Lock 27 Field Test Conclusions

Based on the experimental data, various conclusions can be made concerning the position of the gate leaf and the effectiveness of the gate seals. This information is extremely important in the development of an analytical model.

a. The strain data indicated that the leaf was at least partially resting on the bottom sill at the beginning of the vertical load tests. Appendix A (Figures A1 through A7) provides strain history plots for Test 271A. The plots show abrupt changes in strain initially (as the gate leaf was lifted from the sill), constant strain levels as the gate continued to be lifted and lowered, and a sudden return to near-zero strain levels as the gate leaf was returned to the sill. It is a fair assumption that the gate leaf was resting on the sill during the head differential tests as well.

b. Bending behavior of the horizontal girders was determined from the strain data taken during the head differential tests. Strain values for locations on upstream girder flanges were in compression. The direction of bending (or displacements) is such that the hydraulic pressure must have been greater on the upstream face of the gate than on the downstream face. This observation shows that the seal between the leaf and the upstream sill (Seal A in Figure 3) was not functioning properly. It was found later that Seal A had been removed a number of years ago to alleviate vibration problems (private communication).

Locks and Dam 26 Lift Gate Test Procedures

The upstream lift gate at Locks and Dam 26 consists of three leaves. The middle leaf was tested since it is subject to the largest service loads. Additionally, a crack had previously occurred on a girder flange (the crack had been repaired prior to the test). The middle leaf consists of 4 horizontal girders braced on the downstream side with diagonal members, and 12 vertical diaphragms as shown in Figure 28. The gate is new and the construction is much simpler than that of the Locks 27 lift gates. Instrumentation and testing of the Locks and Dam 26 lift gate leaf was completed over a 2-day time span. The lock could be closed for only 4 hours at a time, however, instrumentation and testing were completed within these constraints. The nappe of the downstream leaf provided access to the middle leaf.

Similar to Locks 27 studies, testing included two sets of transducers. In the first set (SET1-26), transducers were located to obtain the general structural response characteristics (bending in the girders and diaphragms and axial forces in the diagonal members). After the SET1-26 tests were completed, a crack was discovered in a girder flange. Figure 29 shows the

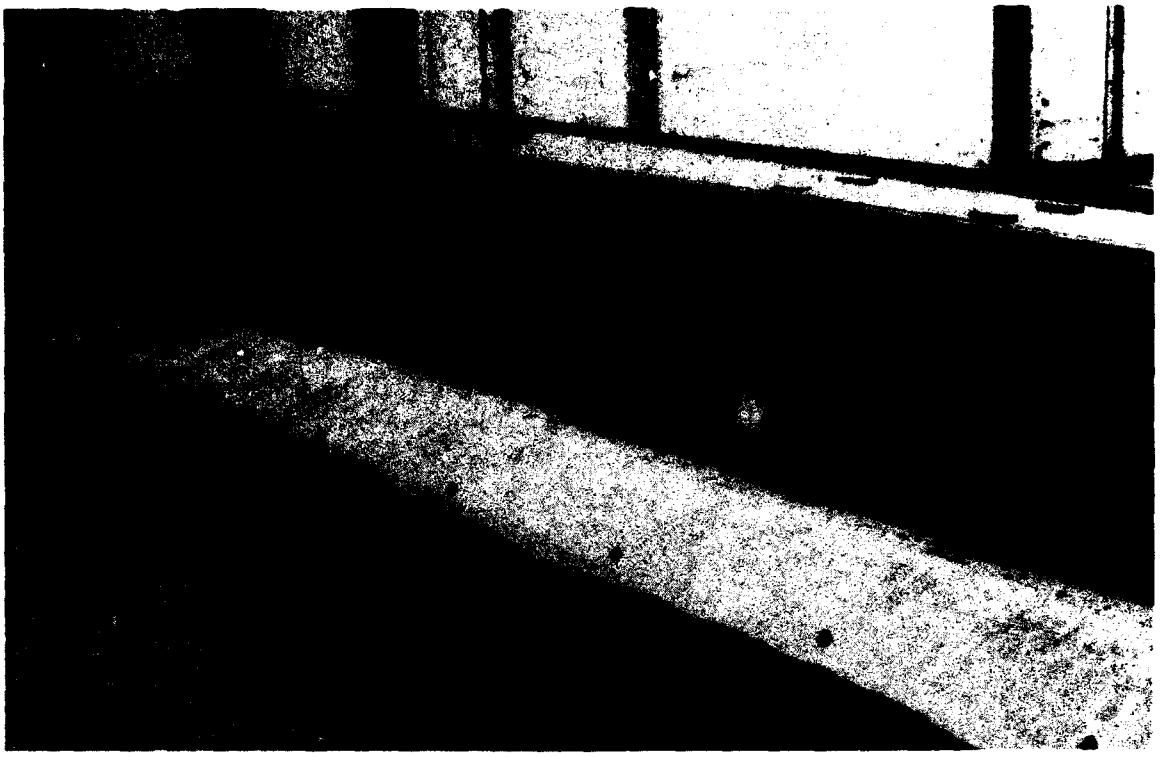

Figure 28. Locks and Dam 26 vertical lift gate - downstream face of middle leaf

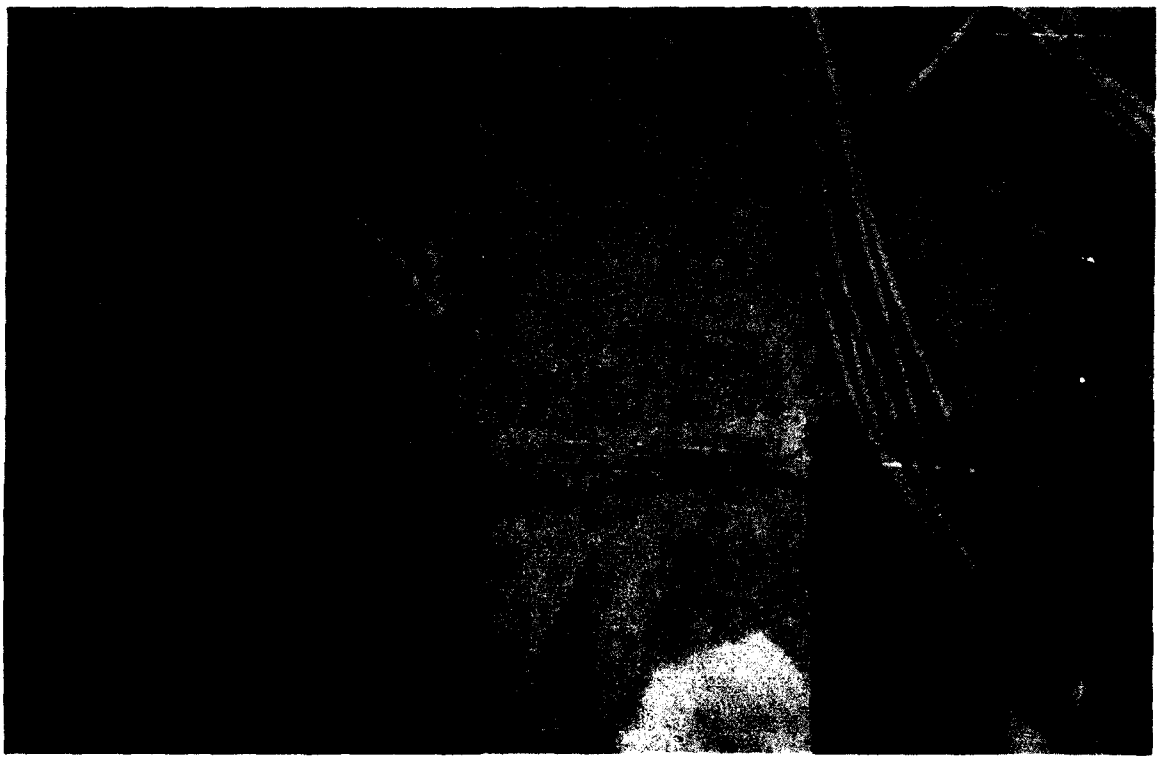

Figure 29. Crack at girder flange-to-diaphragm flange connection

crack starting at the weld that joins the vertical diaphragm flange plate to the girder flange. To examine the effect of the crack, tests were performed with a second set (SET2-26) of transducers positioned in a localized area around the cracked diaphragm.

A total of four tests, including one vertical load test and three head differential tests, were conducted. The vertical load test was similar to those of the Locks 27 lift gate. For the head differential tests, the leafs were positioned as shown in Figure 30. The upper pool elevation was 419.0 ft (127.7 m), the lower pool elevation was 399.8 ft (121.9 m), and the elevation of the top girder of the middle leaf was 408.6 ft (124.5 m). A scale located on the lock wall was used to monitor the pool level as it varied. Typically, the pool elevation time was recorded at 1-ft (0.3048 m) intervals with the strain data.

Set 1 test (SET1-26): Test 261A chamber drop

SET1-26 included 28 transducers; four channels (5-8) were inoperable at the time of the test. Several of the transducers for this setup are shown in Figure 31. Figures 32 through 45 show the locations of the transducers and the corresponding DAS channel numbers. A crew of four persons instrumented and tested the leaf in approximately 5 hr.

A head differential test (Test 261A) was the only test conducted with this transducer configuration. Strain data were recorded as the chamber water level dropped from the upper pool elevation (datum position) to the lower pool elevation. Data recording began as the lock valves were

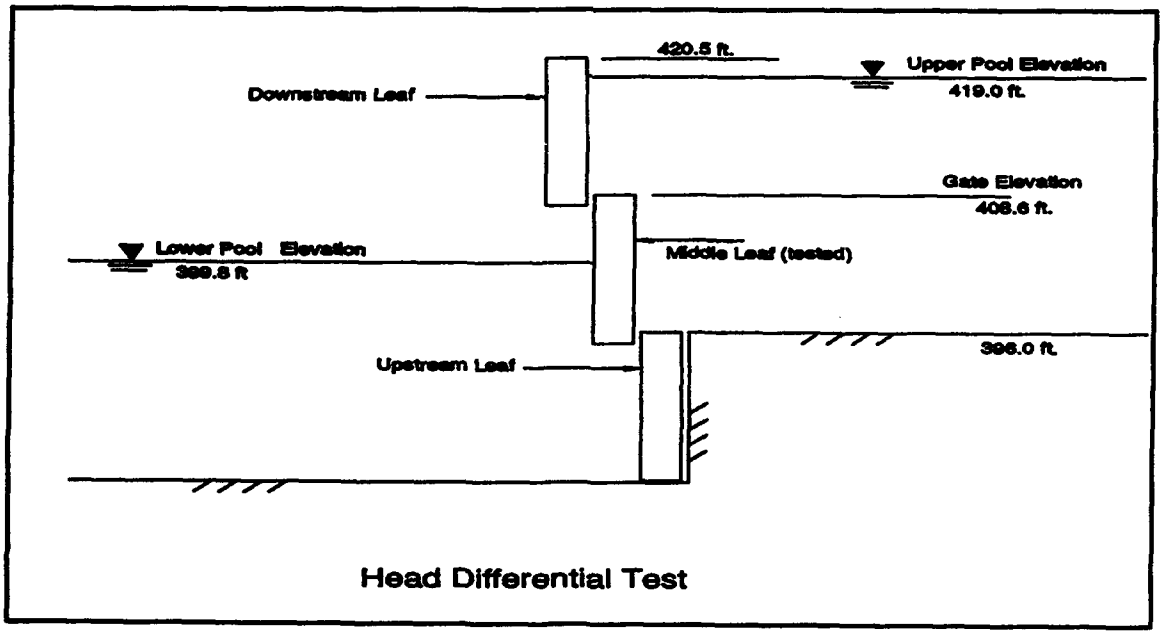

Figure 30. Locks and Dam 26 lift gate leaf configuration (elevations)

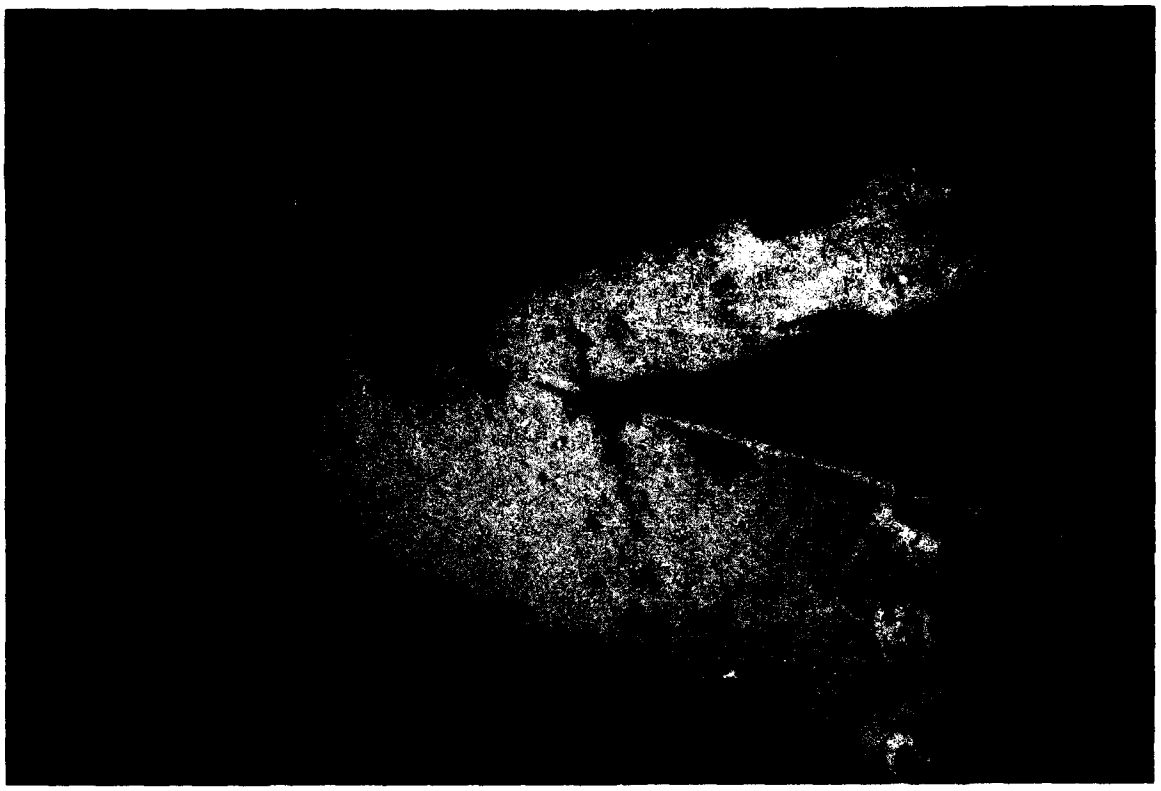

Figure 31. Transducers on Locks and Dam 26 lift gate

opened to drain the chamber. Chamber pool elevation times were recorded at 1-ft (0.3048 m) intervals starting at el 418.0 ft (127.4 m).

Set 2 tests (SET2-26)

SET2-26 tests included 12 transducers that were located around the cracked diaphragm as shown in Figures 46 through 50. One vertical load test and two head differential tests were performed. The instrumentation and testing for SET 2-26 was completed in less than 4 hr.

a. **Vertical Load Test: Test 262A.** This test was similar to the vertical load tests at Lock 27 (Test 271A and Test 271D). The gate leaf was lowered as near to the bottom sill as it would go. At this position the data were set (transducers were balanced). The DAS recorded strain data continuously at 32 Hz as the leaf was lifted approximately 1 ft (0.3048 m) and then lowered to the sill.

b. **Head Differential Tests.** The head differential tests were conducted similar to those of the Locks 27 tests and Test 261A.

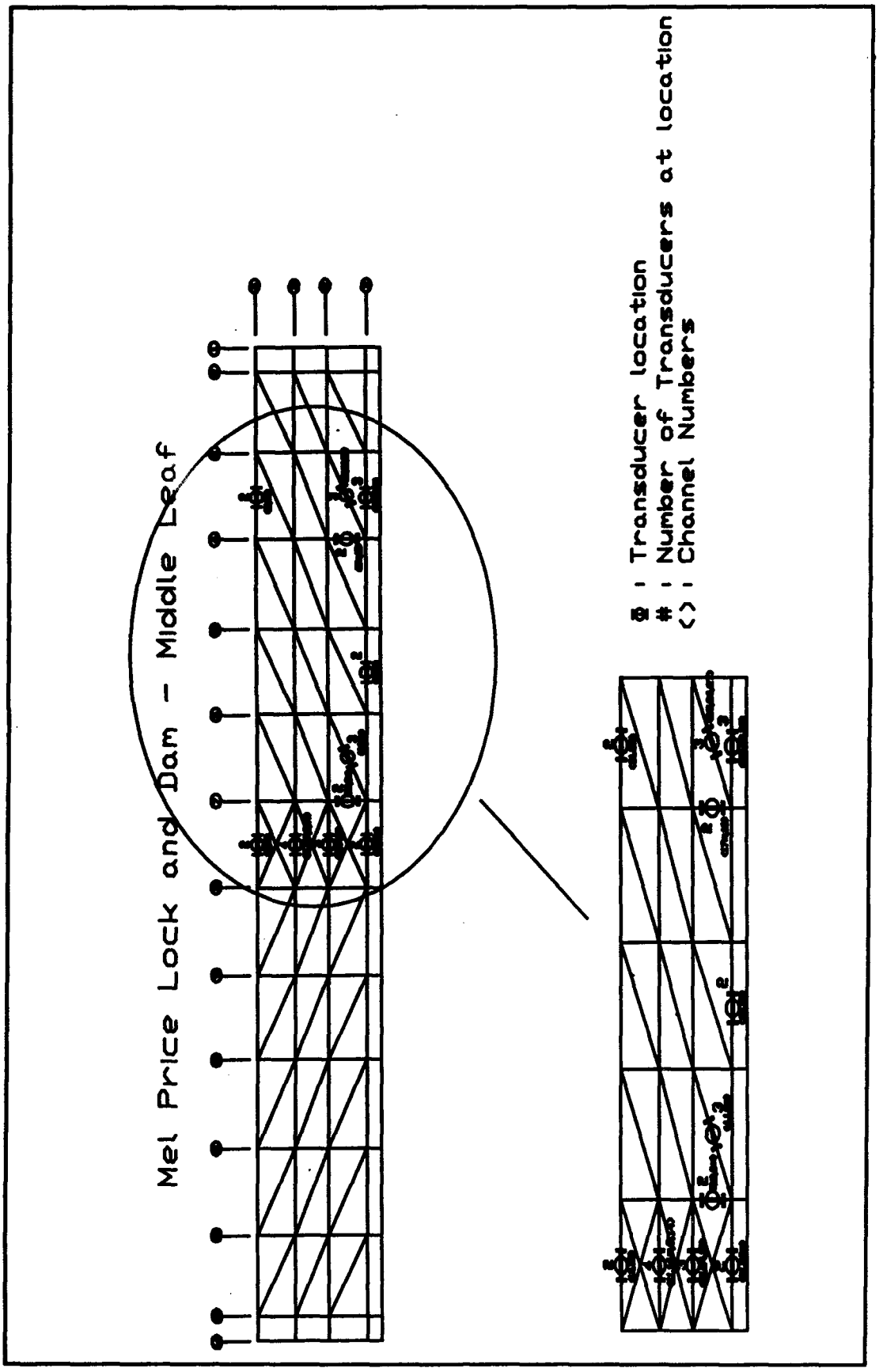

Figure 32. Transducer locations for Locks and Dam 26 SET1-26

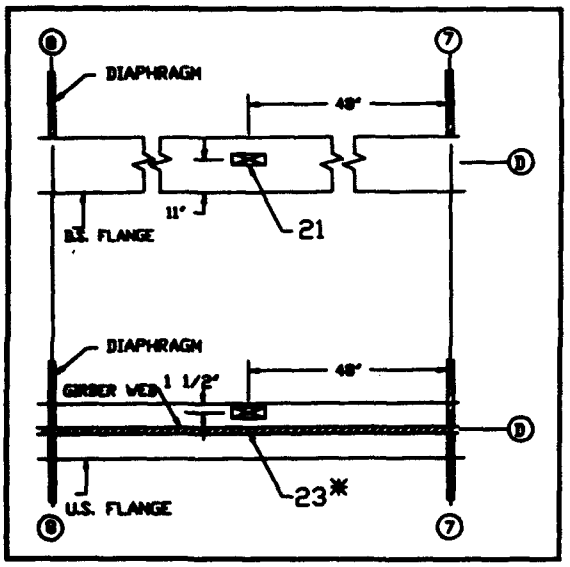

Figure 33. Transducer placement - SET1-26 (Transducers 21, 23)

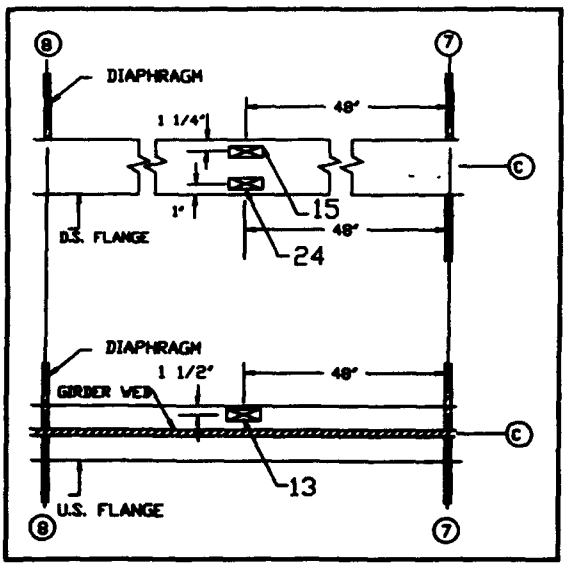

Figure 34. Transducer placement - SET1-26 (Transducers 13, 15, 24)

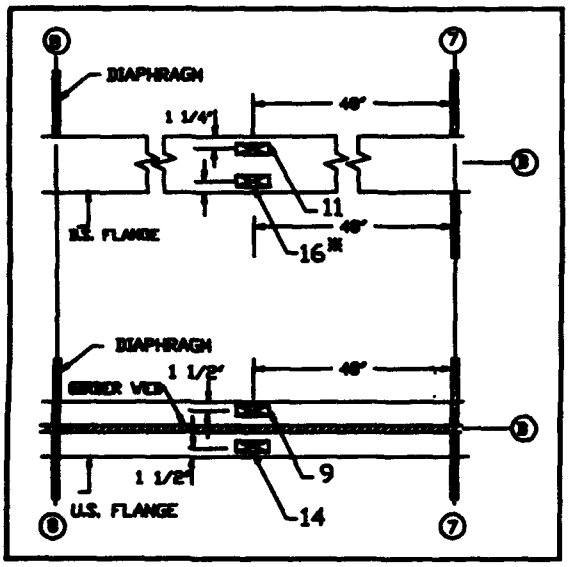

Figure 35. Transducer placement - SET1-26 (Transducers 9, 11, 14, 16)

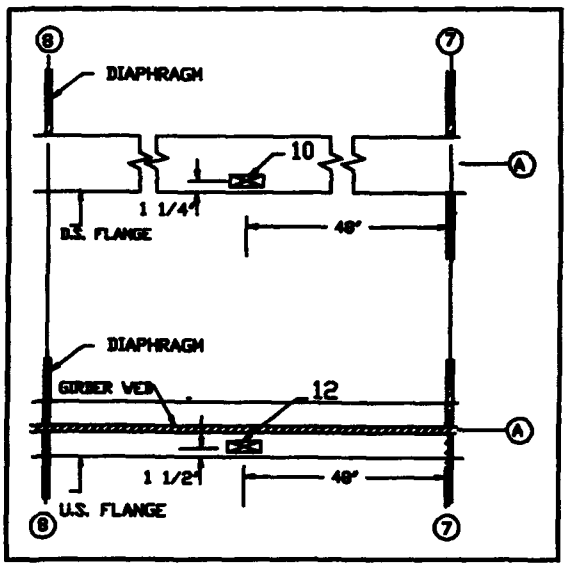

Figure 36. Transducer placement - SET1-26 (Transducers 10, 12)

(1) *Test 262B: chamber drop.* This test was conducted under similar conditions as Test 261A. Strain data were recorded as the chamber water level dropped from the upper pool elevation (datum position) the lower pool elevation.

(2) *Test 262C: chamber fill.* The datum for transducers was set when the chamber pool elevation was equal to the low pool elevation (maximum head). The DAS recorded strain data from the time that the lock valves were opened to fill the chamber to

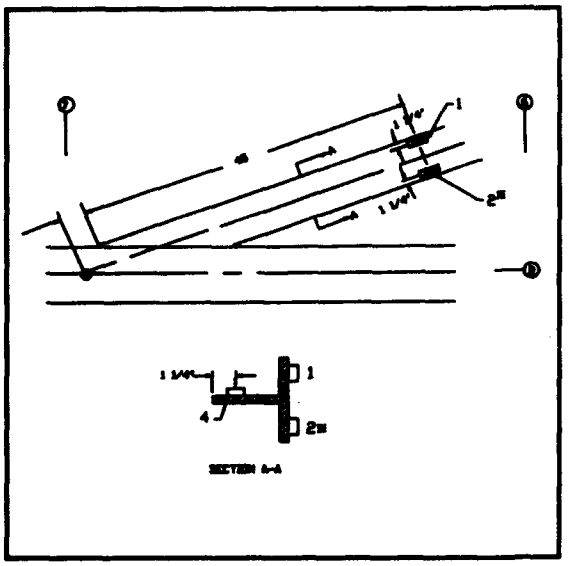

Figure 37. Transducer placement - SET1-26 (Transducers 1, 2)

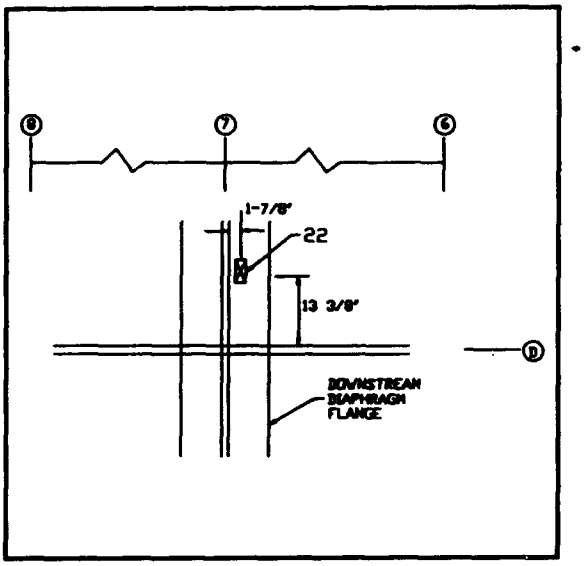

Figure 38. Transducer placement - SET1-26 (Transducer 22)

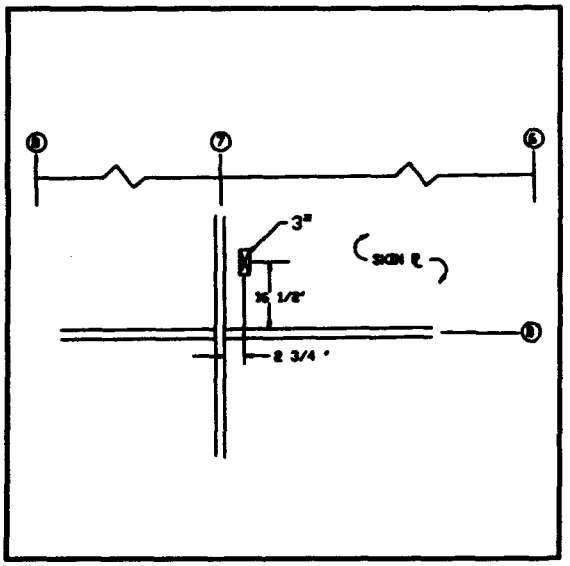

Figure 39. Transducer placement - SET1-26 (Transducer 3)

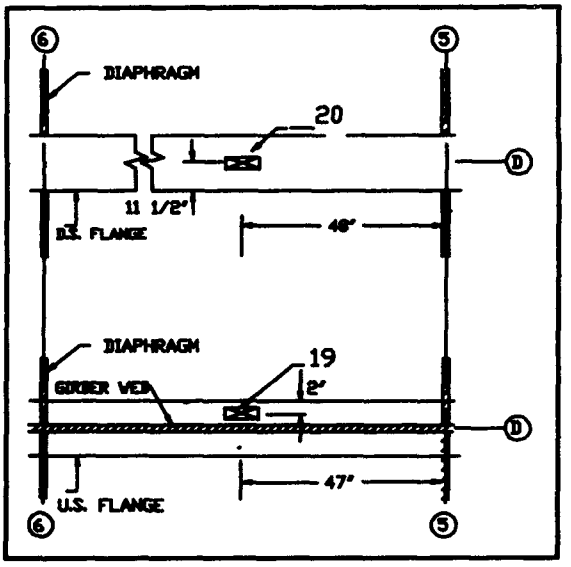

Figure 40. Transducer placement - SET1-26 (Transducers 19, 20)

the time when the chamber pool level reached the upper pool elevation. Pool elevation times were recorded at 1-ft (0.3048 m) intervals.

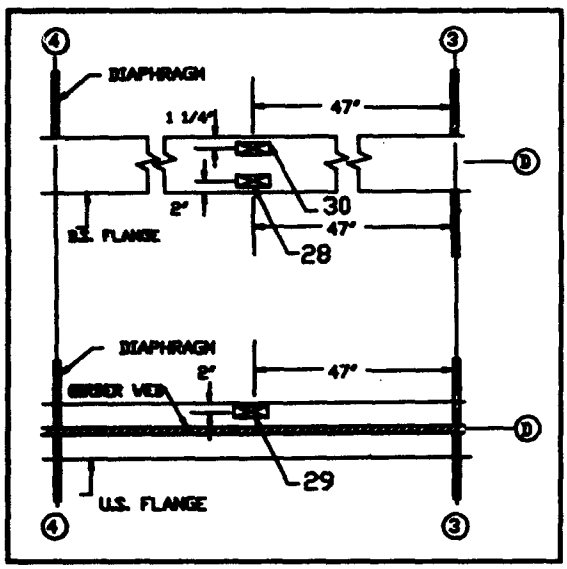

Figure 41. Transducer placement - SET1-26 (Transducers 28, 29, 30)

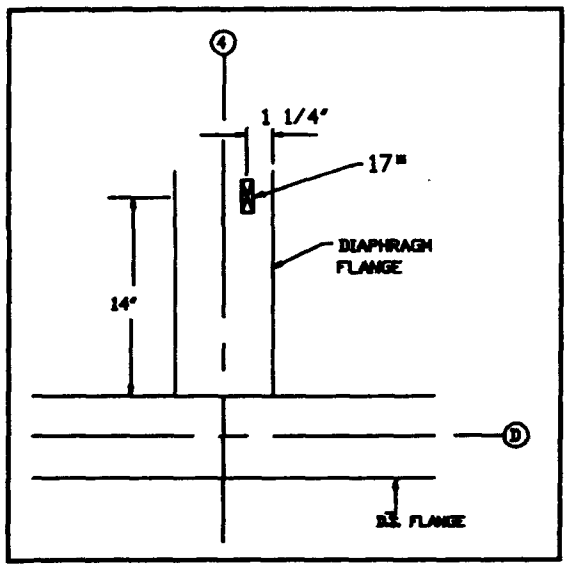

Figure 42. Transducer placement - SET1-26 (Transducer 17)

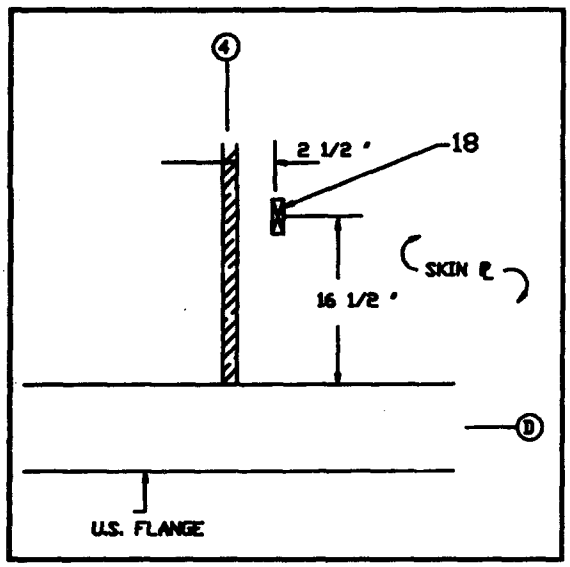

Figure 43. Transducer placement - SET1-26 (Transducer 18)

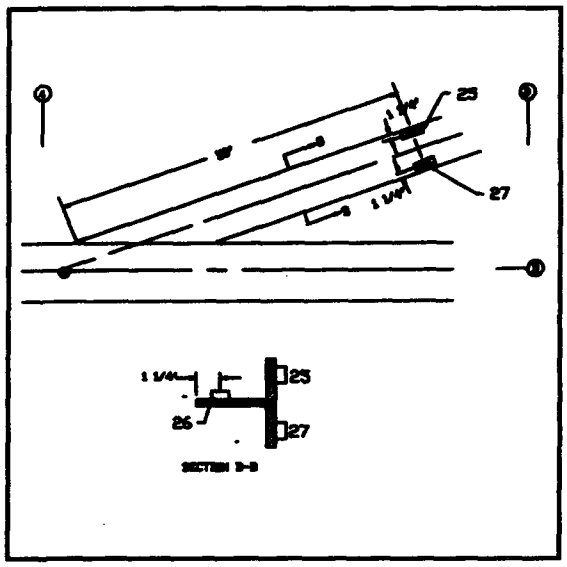

Figure 44. Transducer placement - SET1-26 (Transducers 25, 26, 27)

Field notes

a. DAS channels 2, 3, 16, 17, 23 malfunctioned during the first test, Test 261A. The 12 transducers for SET2-26 tests functioned properly.

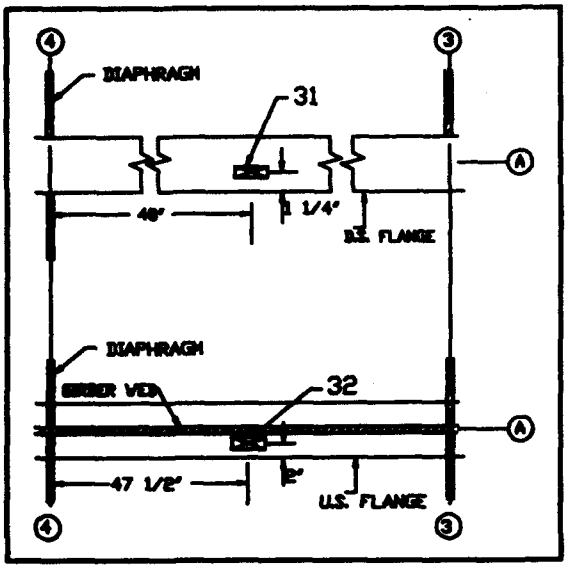

Figure 45. Transducer Placement - SET1-26 (Transducers 31, 32)

b. The results of the vertical load test (Test 262A) were inconclusive since the leaf could not be lowered completely to the sill. No strain differential occurred during the vertical load test, indicating that the leaf was not resting on the sill initially.

c. The following test summaries are provided similar to those for the Locks 27 Lift Gate.

(1) *Test 261A Summary.*

Data File:	SET1-26.CHN / TEST261A.DAT
Balance:	Zero head
Data Record:	Start at zero head; elevation marks at 1-ft (0.3048-m) intervals.

(2) *Test 262A Summary.*

Data File:	SET2-26.CHN / TEST262A.DAT
Balance:	Leaf on bottom sill.
Data Record:	Start with leaf on sill; record as leaf raised approximately 1 ft (0.3048 m) and lowered; stop at time leaf was lowered to sill.
NOTES:	Due to binding or debris, the gate leaf was likely not resting on the sill at the start of the test.

(3) *Test 262B Summary.*

File Name:	SET2-26.CHN / TEST262B.DAT
Balance:	Zero head
Data Record:	Zero head to maximum head. Pool elevations

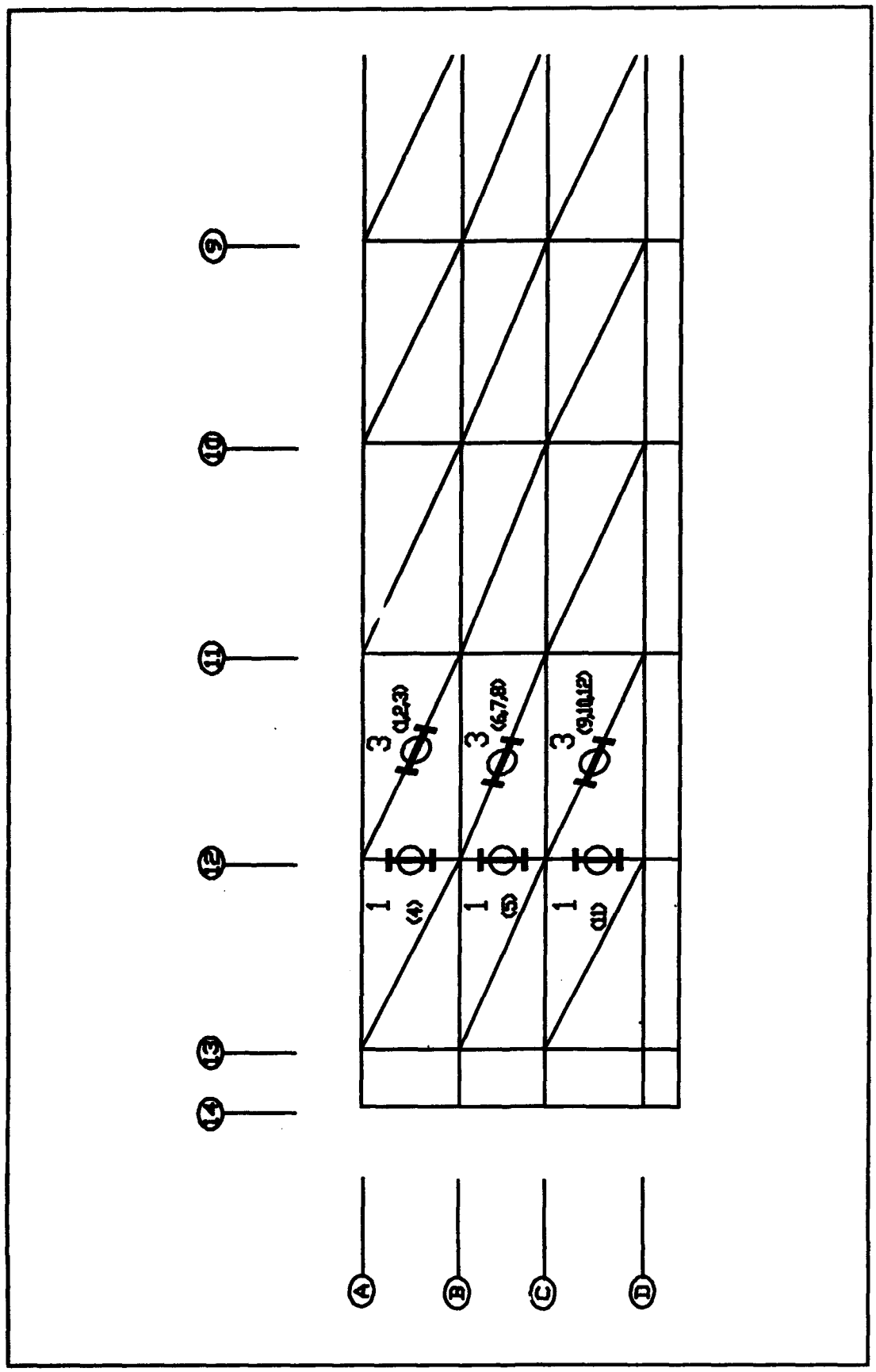

Figure 46. Transducer locations for Locks and Dam 26 SET2-26

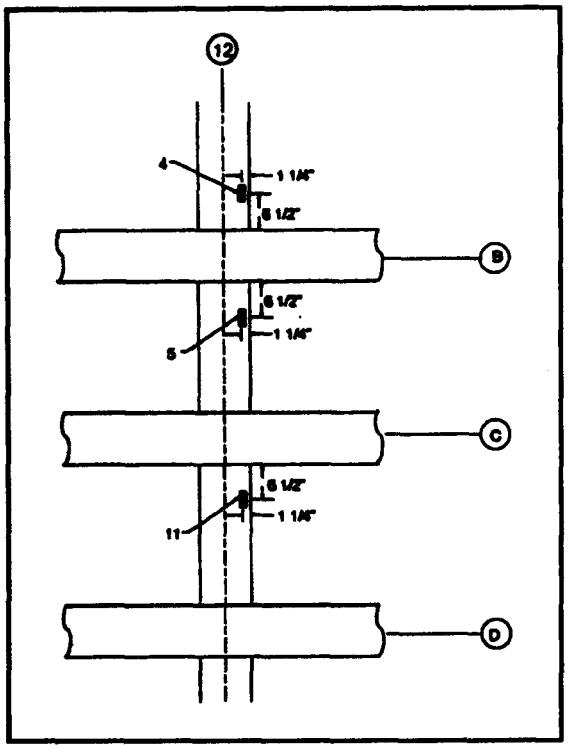

Figure 47. Transducer placement - SET2-26 (Transducers 5, 11)

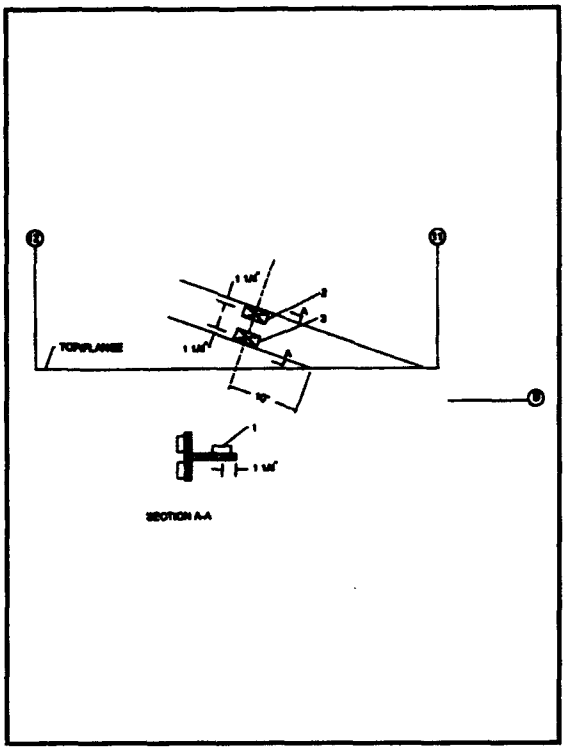

Figure 48. Transducer placement - SET2-26 (Transducers 1, 2, 3)

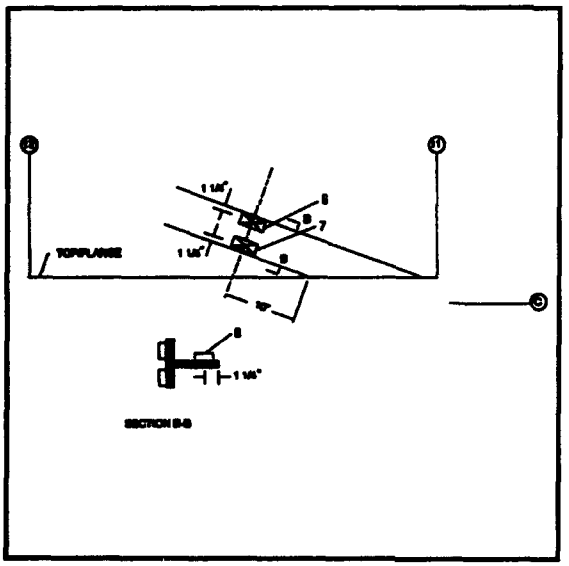

Figure 49. Transducer placement - SET2-26 (Transducers 6, 7, 8)

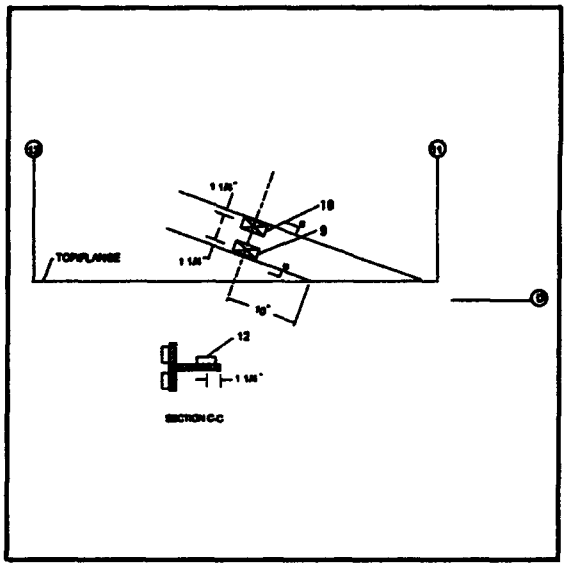

Figure 50. Transducer placement - SET2-26 (Transducers 9, 10)

times recorded at 1-ft (0.3048 m) intervals beginning at 418.0 ft (127.4 m).

(4) *Test 262C Summary.*

File Name:	SET2-26.CHN / TEST262C.DAT
Balance:	Maximum head
Data Record:	Maximum head to zero head. Pool elevations times recorded at 1-ft (0.3048 m) intervals beginning at 401.0 ft (122.2 m).

3 Structural Analysis and Data Comparison

General Modeling Considerations

The lift gates of this study (Figures 2 and 28) are complex stiffened-plate structures that are subjected to significant vertical and horizontal loads. Head differential pressure produces vertical forces on the top girder and retainer plate and horizontal forces on the skin plate. Vertical forces due to structural weight are applied to the structure when gate leaves are lifted. A skin plate, located on the upstream face of the structure, forms the damming surface and provides resistance to horizontal loads. The skin plate is stiffened by horizontal girders and vertical diaphragms. Bracing members, located on the downstream side of the lift gate, provide lateral stability to girders for horizontal loading and provide a framing system to resist vertical loads.

To simulate structural behavior, a two-dimensional (2-D) model in the plane of the leaf might be considered. However, uniform behavior of the structure through its depth (distance from upstream to downstream faces) would be assumed. The depth of a gate leaf significantly affects the structural loads and load transfer characteristics. Resistance to vertical load of the upstream (skin plate) and downstream (bracing) faces is not equal. Therefore, under vertical loads, out-of-plane behavior exists due to the occurrence of uneven vertical deflections through the depth. The magnitude of this effect is highly dependent on the depth of the leaf. Furthermore, horizontal and vertical forces act concurrently. The depth of the gate must be represented if these effects are to be realistically modeled.

Primary goals of this study include: 1) to develop modeling procedures that may be used in evaluation and design of lift gates, and 2) to study local behavior of downstream bracing members (these members are prone to cracking). Due to the structural complexity and desired results (study of bracing behavior), a three-dimensional (3-D) finite element model of the gate leaves was considered necessary. Loading and boundary conditions (BC) representative of test conditions were simulated in development of each model.

Analytical models

Techniques and assumptions regarding development of the analytical models are outlined.

a. The geometry of the finite element mesh is defined by a 3-D (X, Y, Z) coordinate system. The Z coordinates define the position in the upstream/downstream direction, and the X and Y coordinates define the horizontal and vertical location, respectively. The Z coordinate for nodes on the upstream face are located at the center of the skin plate thickness. For nodes on the downstream face, the Z coordinates are located at the girder web-to-flange (downstream) interface. X and Y coordinates for nodal points on both the upstream and downstream faces of the leaf are located: 1) at the girder web-to-diaphragm web intersections, and 2) at the intersection between center lines of downstream vertical bracing members and girder webs.

b. Hybrid plate-membrane elements simulate the skin plate and the webs of girders and diaphragms. The elements are four-node quadrilaterals composed of two triangles. Each element is a combination of a membrane element and a plate element, and is capable of resisting in-plane forces and bending about both in-plane axes.

c. Eccentric space frame elements (Commander et al. 1992b) model girder flanges, diaphragm flanges, and bracing members. These elements include 6 degrees of freedom per node (three displacements and three rotations). The frame elements have only a length dimension but include stiffness terms for each degree of freedom. An eccentricity term offsets the element neutral axis from its node points (a value of zero eccentricity is acceptable).

d. Eccentricity terms are used to define the distance between the nodal points and the flange and brace element neutral axes. Eccentricity terms for the upstream girder flange elements equal one-half the thickness of the skin plate plus one-half the thickness of the flange plate (the upstream nodes are located at the center of the skin plate). Therefore, each flange element neutral axis is placed at a realistic location without defining additional nodal points. The eccentricity of the neutral axis (in the through depth direction of the leaf) for each bracing element is defined with respect to the web-flange interfaces of the girders.

e. Boundary conditions are applied to the structural model by fixing (eliminating) degrees of freedom at specified nodal points. The BC can be applied to any of the global degrees of freedom (three displacements and three rotations) at any node. Boundary conditions vary depending on the position of the gate leaf. During the head differential tests, the Locks 27 lift gate leaf presumably rested on the sill and the Locks and Dam 26 lift gate middle leaf was suspended by the lifting cables. For either case, BC are applied in the

upstream direction to the nodes along the vertical end girders on the downstream face of the model only. Vertical BC are applied at nodes nearest the hoist locations (for the Locks and Dam 26 case) and along the bottom of the gate when it was assumed that the leaf was resting on the bottom sill (for the Locks 27 case).

f. Since both gates are welded structures, all connections (including flange-to-web interfaces, girder and diaphragm flange intersections, and bracing-to-flange attachments) are assumed to be rigid.

Structural models

Structural models were developed and analyses were performed to simulate the head differential tests only. (For the vertical load tests, it was not certain if the gate leaves were resting on the sill.) Loading conditions that were assumed to represent those in the field were applied to the model. The general-purpose finite element program Structural Analysis and Correlation (SAC) performed the analyses. SAC has been used in bridge studies (Goble, Schulz, and Commander 1990) and is currently under development for the analysis and evaluation of miter lock gates (Commander et al. 1992a, 1992b). In the current study, the following modifications have been made to improve SAC:

a. The quadrilateral plate-membrane element has been modified to simulate rectangular and nonrectangular shapes. For the miter gate studies, this element could represent only rectangular shapes.

b. The algorithm that calculates nodal loads for plate elements subject to pressure loading was improved. The modified algorithm calculates nodal load distribution for the new nonrectangular shapes of the plate elements.

c. SAC now includes vertical hydrostatic loading that is not present in miter gates.

Data Comparison

Subsequent to analysis, the analytical and experimental strain data were compared to evaluate the accuracy of the computer models. Using the structural models, strain magnitudes were computed at locations representing those where the transducers were attached during the field tests. SAC computes strain in frame elements considering axial deformations and flexure about the two cross-sectional axes. To perform these calculations, SAC requires input data to define the position of the transducer. This data includes the distance along length of the element and the location of the transducer with respect to the two principal axes of the element cross section. Strains that are computed for quadrilateral elements

include effects of membrane (in-plane) displacements and flexure about the two in-plane axes. Quantities that are used for data comparisons include absolute error, percent error, and a correlation factor. Each of these comparisons is discussed.

Absolute error

The absolute error E_{abs} provides a simple measure of model accuracy that is most useful in comparing one model to another. The difference in analytical and experimental strain is computed at each transducer location for every load case considered. The absolute error is the sum of the absolute values of the differences.

$$E_{abs} = \sum_{i=1}^{n} \left| \varepsilon_{f_i} - \varepsilon_{c_i} \right| \tag{1}$$

where

ε_{fi} = Field strain measurement of a single transducer for a given head differential load

ε_{ci} = Computed strain corresponding to ε_{fi}

n = The number of transducers times the number of applied load cases (total number of different strain readings)

Percent error

The percent error E_{per} provides a better conceptual evaluation of a model than the absolute error. The summation of the differences (between analytical and experimental results) squared is divided by the summation of the field strains squared. The percentage error is computed by the following equation:

$$E_{per} = \frac{\sum_{i=1}^{n} (\varepsilon_{f_i} - \varepsilon_{c_i})^2}{\sum_{i=1}^{n} \varepsilon_{f_i}^2} \times 100 \tag{2}$$

The terms of Equation 2 are squared so they are always positive and strain values with the larger magnitudes have a larger effect on the error term.

Correlation factor

The correlation factor (*CF*) is a measure of how strongly two variables are linearly related. The *CF* can range from -1.0 to 1.0. A *CF* of 1.0 indicates that there is a perfect linear correlation between the two variables in a positive sense (as one variable increases, the other increases). A perfectly opposite correlation (as one variable increases, the other decreases) would result in a *CF* of -1.0. If the variables are uncorrelated (there is no linear relationship between the two sets of data), a *CF* of 0.0 is obtained. The *CF* is useful in comparing analytical and experimental (field) data. The *CF* provides a measure of how closely the shape of the experimental and analytical strain-versus-head differential curves match. For a good model, the analtyical and experimental data should be linearly related in a positive sense (the *CF* should be approximately equal to 1.0). The *CF* is computed using the following equation:

$$CF = \frac{\frac{1}{n}\sum_{i=1}^{n}(\varepsilon_{fi} - \bar{\varepsilon}_f)(\varepsilon_{ci} - \bar{\varepsilon}_c)}{\sigma_{ef}\sigma_{ec}} \tag{3}$$

where

ε_{fi}, ε_{ci}, and n are as described above,

$\bar{\varepsilon}_f$ = Mean value of the measured strains

$\bar{\varepsilon}_c$ = Mean value of the computed strains

σ_{ef} = Sample standard deviation of the measured strains

σ_{ec} = Sample standard deviation of the computed strains

Locks 27 Lift Gate Modeling and Analysis

The Locks 27 lift gate is a large and very complex structure that is difficult to model. This structure includes a significant number of connections (requires assumptions on fixity) and many bracing elements that have different orientations and cross-sectional shapes (each must be uniquely defined). Hydrostatic loads are unknown since the existing seals on the upstream leaf (the tested leaf) are old and the top seal has been removed. Several analyses with different assumptions on loading and model BC were developed for the Locks 27 lift gate. To determine the most appropriate analyses, analytical results were compared to SET2-27 (most general transducer layout) head differential test data of Test 272B. Modeling and results for each analysis are described in the following sections.

Model discretizaton

The skin plate, girder and diaphragm webs, girder and diaphragm flanges, bracing members, and connections are modeled as described previously. Figure 51 shows the finite element discretization for a horizontal girder and the entire mesh of the leaf model is shown in Figure 52. The model includes 404 nodal points (2,424 degrees of freedom), 1,141 elements, and 64 different element groups (different element cross sections). To maintain a model of manageable size, the girder and diaphragm web elements extend through the depth of the leaf in single layer. The mesh is relatively course and, for some load conditions, the model may not predict accurate stress levels in the web plates. However, accurate predictions of

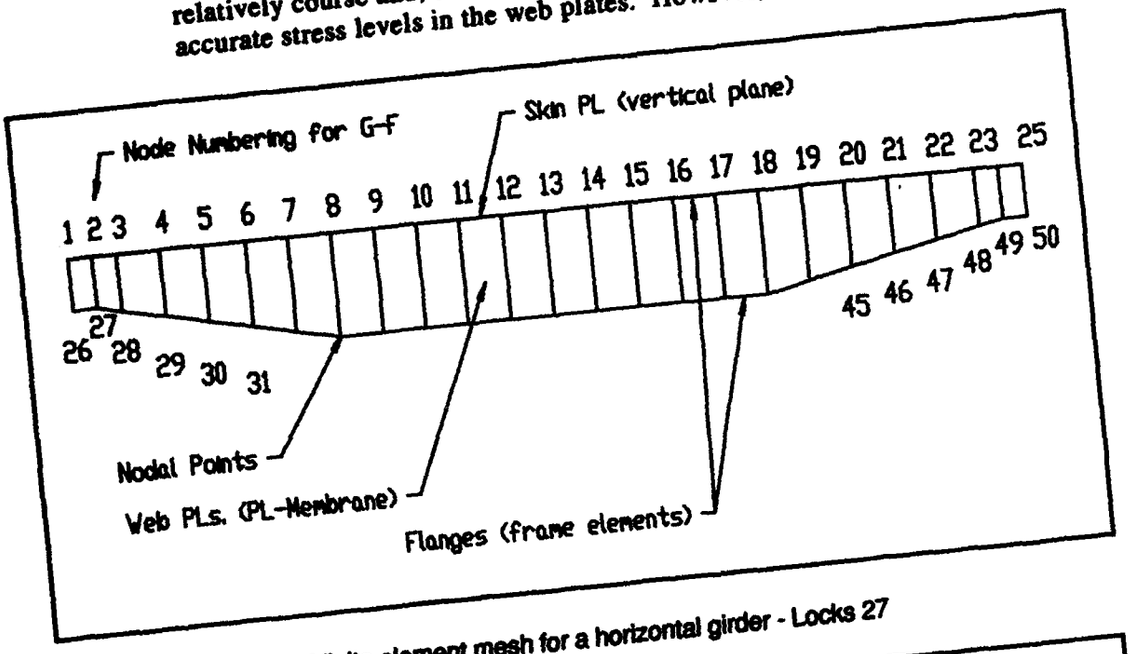

Figure 51. Plan view of finite element mesh for a horizontal girder - Locks 27

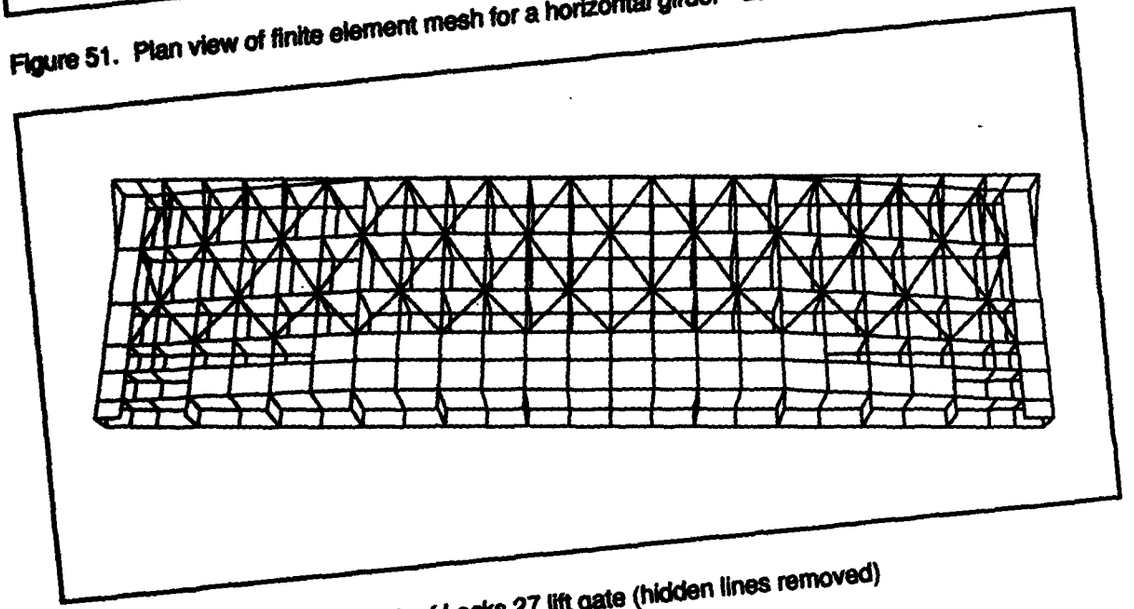

Figure 52. Finite element mesh of Locks 27 lift gate (hidden lines removed)

the displacement and overall load transfer behavior should be obtained. A personal computer would likely not have the memory capacity required to analyze a more refined model. With the chosen discretization, the analysis for the Locks 27 model required approximately eight megabytes (Mb) of random access memory. The models for each analysis included the same finite element mesh.

Loading and boundary conditions

Figure 53 illustrates two cases of horizontal pressure distributions for a lift gate subject to static head differential loading. The first case applies when Seal A (the seal between the upstream sill and the upstream leaf) is disfunctional or does not exist, and the second case is applicable when Seal A is perfect. (Vertical loading exists but is not relevant since the leaf is on the bottom sill.) For this study the first case applies, since the Locks 27 lift gate (auxiliary lock) does not have a seal between the upstream sill and the upstream leaf. A different (dynamic) pressure distribution may exist if the water is flowing under the leaf (Analysis 2 discussion).

To simulate the support of the lock wall, the nodal degrees of freedom in the upstream (through depth) direction for the nodes along the vertical end girders were fixed (i.e. nodes 26 and 50 of Figure 51). BC were applied only on the downstream nodes where the end girders bear against the lock wall slot. Field measurements indicated that the leaf rested on the bottom sill (Chapter 2). Therefore, vertical degrees of freedom at the bottom nodes of elements that represent the bearing plates were fixed. BC were applied at only the downstream nodes of these elements. With both upstream and downstream nodes fixed, the analysis would show uplift reactions if the bottom girder twisted slightly.

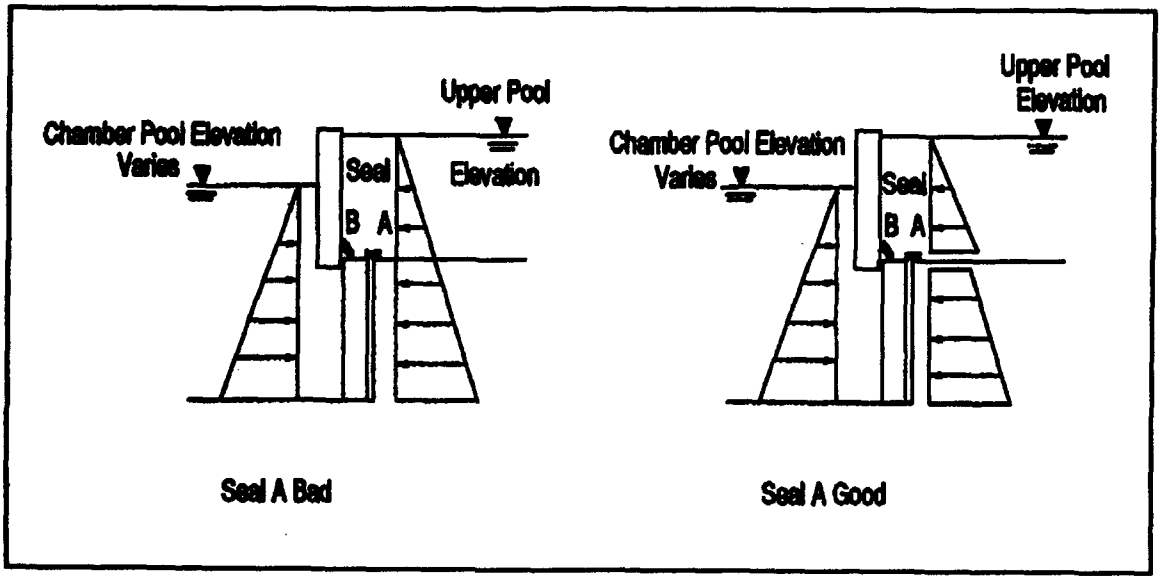

Figure 53. Static hydrostatic load conditions for Locks 27 lift gate

Analysis and data comparison

Analysis 1. The model for this analysis included BC previously described and simulated loads corresponding to the first pressure distribution shown in Figure 53. The comparison between analysis results and experimental data was poor. Although the calculated *CF* was acceptable (*CF* = 0.9), the magnitudes of the computed strains were on average about 150 percent larger than the corresponding measured strains. This error is attributed to inaccurate representation of loading and BC (supports).

a. Loading. For Analysis 1, static head differential loading was assumed. However, if there are no seals at the bottom of the leaf and at position A of Figure 53, water can flow under the leaf (Figure 54). With a flow velocity, the pressure head on the upstream face of the leaf (shown in Figure 53) and the resultant force in the downstream direction is reduced. Given a large enough flow velocity, the pressure could be reduced to zero at the bottom of the leaf.

b. Boundary conditions. Test results showed that the leaf rested (at least partially) on the sill (Chapter 2). This was considered in the development of the first model by including fixed vertical BC at the bottom nodes. However, no restraint was imposed in the horizontal (upstream) direction. Considering the structural weight and the downward pressure applied to the top girder, it is likely that a considerable amount of horizontal friction resistance exists between the sill and the bearing plates.

Analysis 2. The mesh and BC for the model of this analysis were identical to those for the model of Analysis 1. However, to study the effect of flowing water, loads were simulated using the assumed pressure

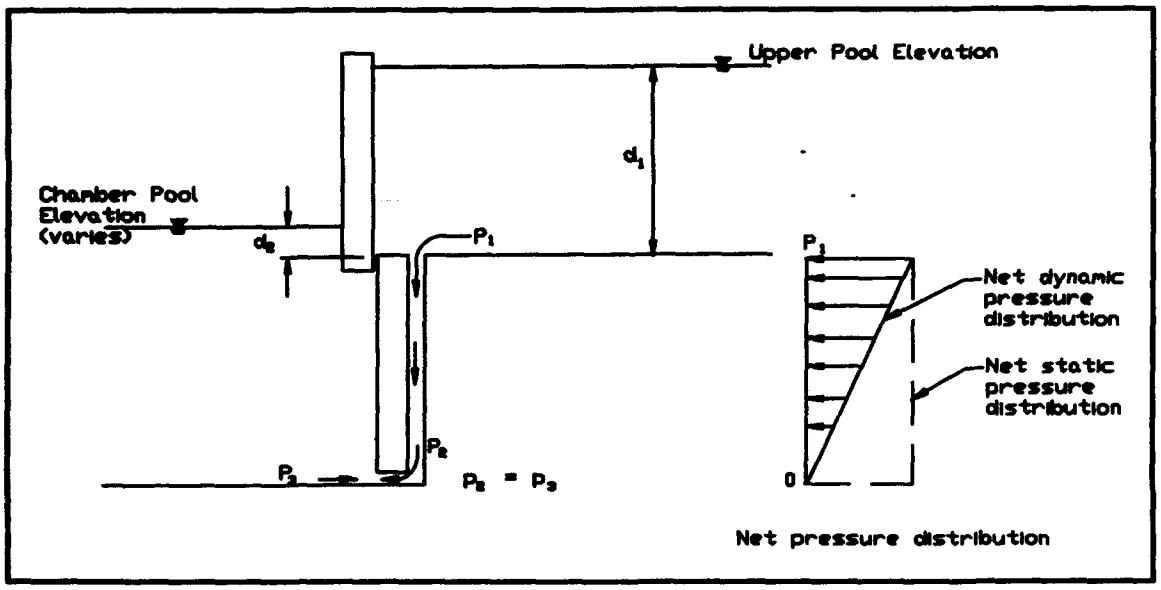

Figure 54. Dynamic hydrostatic load conditions for Locks 27 lift gate

distribution shown in Figure 54. This distribution was developed by assuming that the pressure varies linearly from the hydrostatic head pressure at the top, $P_1 = \gamma(d_1 - d_2)$, to zero at the bottom, where γ is the unit weight of water and d_1 and d_2 are defined by Figure 54. The total horizontal force for this distribution is less than one-half of that for the static distribution.

The comparison of analytical and experimental data for this case is much better than that for Analysis 1. Analysis including the new load model resulted in the following comparison quantities: $E_{abs} = 4829$ microstrain ($\mu\varepsilon$), $E_{per} = 19.2$ percent, and $CF = 0.9357$. These results are based on the comparisons of 18 strain channels and 6 different load cases (chamber pool elevations). The average transducer error is equal to E_{abs} divided by the number of strain channels used in the comparison and the number of load cases applied in the analysis. The average transducer error for this case is 44.7 $\mu\varepsilon$. The strain magnitudes improved significantly compared to those computed for Analysis 1. However, the amount girder flexure computed from the analysis was consistently greater (by approximately 50 percent) than that computed from the field measurements. The greatest difference was in the lower girders (girders C and D of Figure 4). Since the flexure in the girders was still overestimated, the frictional resistance along the bottom sill was assumed to have a significant effect on the behavior.

Analysis 3. Analysis 3 was conducted to examine the effects of the frictional resistance at the bottom sill. The model of Analysis 2 was modified by fixing the horizontal (upstream direction) degrees of freedom for the bottom downstream nodes. All other loading and BC were identical to those included in Analysis 2. Analysis 3 predicted strain magnitudes that were significantly reduced from those predicted in previous analyses. In fact, the analytical strains were considerably less than the measured strains.

Analysis 4. Extreme cases for horizontal BC along the sill were applied in Analysis 2 (free) and Analysis 3 (fixed). The computed results from these cases enveloped the measured strain magnitudes. Apparently, the actual support conditions (in the upstream direction) along the bottom sill are not fixed or free. To simulate the actual support conditions, elastic spring elements of unknown stiffness were connected between the bottom nodes of the gate leaf and fixed nodes located in the plane of the sill. The spring elements replaced the fixed horizontal BC and were oriented to simulate elastic restraint in the horizontal (upstream) direction. An optimization procedure in SAC (Commander et al. 1992a) was employed to compute the unknown stiffness. The optimization procedure is simply an iterative process in which unknown terms can be varied within a specified range of values until results are of acceptable accuracy. The accuracy of the model (optimization objective function) is based on the E_{abs} value of Equation 1.

In the optimization process, each spring element had the same stiffness with a specified range between 0.0 and 100.0 kips/in. (175.13 kN/cm). Iterative analyses were performed and the best correlation was obtained with a spring stiffness equal to 48.1 kips/in. (84.24 kN/cm). When compared to the Test 272B experimental results, the analysis incorporating the optimum spring stiffness produced strains for which $E_{abs} = 3661$ με, $E_{per} = 10.9$ percent, and $CF = 0.9438$, all of which are acceptable results. These results are based on the same 18 transducer locations and 6 load cases that were used in the previous comparisons. The average transducer error for this case is 33.9 με.

Strain-history comparisons between field data of Test 272B (SET2-27) and the Analysis 4 model results are presented in Appendix B, Figures B1 through B8. Strain results of different transducers at a given member cross section are shown on the same plot. The difference in strain obtained at different locations on a given cross section indicates the amount of flexure, and the average strain provides a measure of axial force. The actual values of flexural or axial force are not given, but qualitative comparison can be made for the analytical and experimental data. The graphical comparisons are generally very good (Figures B1 through B8).

Data for Test 271C (SET1-27) are shown in Appendix B, Figures B9 through B16. These plots show the results for the downstream bracing members and one girder. For the bracing members in general, the predicted axial behavior compares with the experimental results rather well, but the flexural behavior is not well represented. Possible explanations for this are described in the discussion of SET1-26 results.

Conclusions and recommendations

Based on the results of these analyses, the actual loading is best represented by the load distribution shown in Figure 54 and some frictional resistance does exist at the sill. However, for Analysis 4 of this study, the iterative process for computing the optimum BC (spring stiffness) might be considered to be an academic exercise. The resistance at the sill is not the only unknown parameter. Although the load model of Figure 54 is the most accurate case considered, it is based on many assumptions and may not be entirely correct. Furthermore, a linear frictional resistance model that acts uniformly across the width of the lock chamber is not totally realistic. The normal forces (therefore, friction resistance) due to gravity loads may not be uniform across the lock chamber. Even if they are, the displacement would be constrained until frictional resistance was overcome at some value of head differential. Slipping would occur until a new equilibrium position was reached and the resistance would change. However, the evaluation of the support restraint did test the optimization process and showed that analysis correlations could be improved by the automated procedure.

Since neither the load model or BC can be defined with a high degree of certainty, any further speculation concerning the accuracy of the analytical model would be somewhat trivial. However, results from these studies can be used in planning of future studies. When obtaining test data, it is desired to eliminate as many unknowns as possible. The following are recommendations for future experimental studies:

a. The use of pressure transducers should be considered. Pressure transducers could be attached to the upstream face of the skin plate to obtaining data for development of a realistic load model.

b. The uncertainty in the BC along the bottom sill could be eliminated simply by testing the leaf when it is raised a short distance from the sill. To determine the effect of the frictional resistance, the leaf should also be tested in its lowest position (resting on the sill). A comparison of data obtained with the gate in the two positions would provide significant information. The data would show whether or not the sill was providing significant horizontal resistance. If horizontal resistance is significant, the data would provide information that could be used to develop an appropriate resistance model.

Locks and Dam 26 Lift Gate Modeling and Analysis

The general configuration of girders, diaphragms, and bracing members for the Locks and Dam 26 lift gate leaf is similar to that of the Locks 27 leaf. However, the Locks and Dam 26 lift gate leaf is considerably smaller, the construction is simpler, and there are significantly fewer unique cross sections (there is more repetition in member section types). Based on field observations, the seals between the leafs and lock walls do not leak significantly, so hydrostatic loading is well known. At the bottom of the leaf, frictional resistance does not exist because the leaf is suspended. Due to these conditions, the modeling and analysis for the Locks and Dam 26 lift gate leaf was much simpler compared to the Locks 27 case. The following sections describe the development of the analytical model, analyses, and comparison of analytical and experimental data.

FE model

The model for the middle leaf was developed using the same general modeling considerations used for the Locks 27 models. The general configuration of the mesh and representation of various members were the same. However, compared to the Locks 27 case, model development took a fraction of the time and the size of the model was smaller. Figure 55 shows the finite element model of the middle leaf. The model consists of

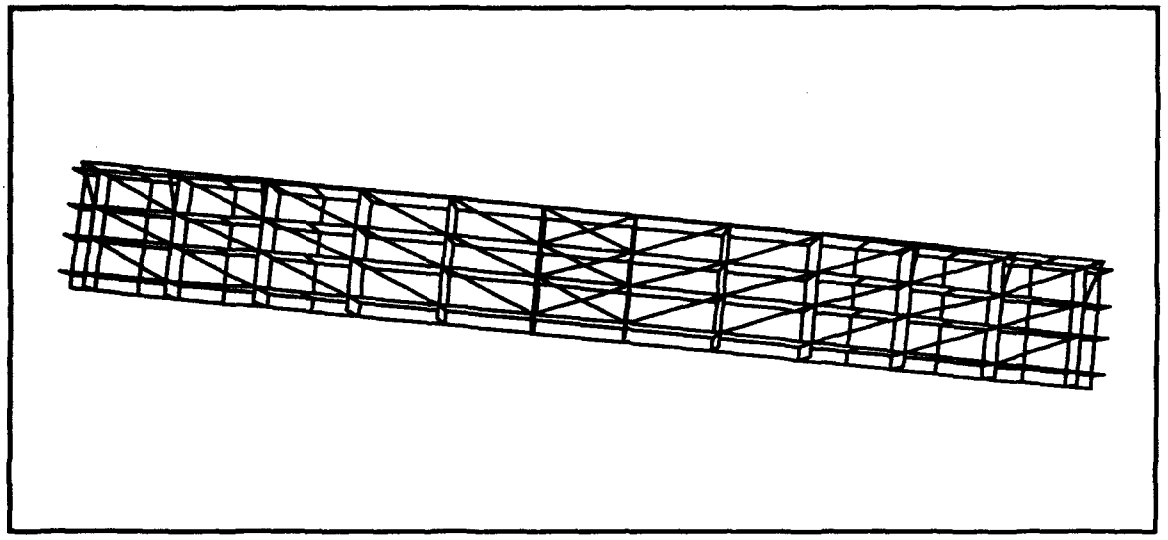

Figure 55. Finite element mesh for Locks and Dam 26 lift gate - middle leaf

261 nodes (1,566 degrees of freedom), 512 elements, and 32 element groups.

Loading and boundary conditions

For the head differential tests, the middle leaf was supported by the lifting cables and positioned above the bottom sill. This condition eliminated several unknowns, regarding BC and hydrostatic pressure distribution, that existed for the Locks 27 lift gate. With functional seals, the pressure distribution shown in Figure 56 exists. Loads based on this distribution were simulated in the analyses.

The middle leaf was suspended and the adjacent leaves do not provide significant resistance in the horizontal, or upstream, direction (horizontal displacements of adjacent leaves would be approximately the same as those of the middle leaf). Therefore, no BC were applied to the bottom (or top) nodes of the model. To simulate the support of the lock wall, the horizontal degrees of freedom for nodes along the vertical end girders (downstream nodes) were fixed (similar to nodes 26 and 50 of Figure 51). Vertical constraints were applied to the nodes nearest the hoist connections.

Analysis and data comparison

Analyses were conducted with loads simulating 3.0-ft (0.914-m) increments of head differential using a single model with the BC and loading as described above. No significant problems were experienced in the analyses, and the required computer capacity and run time was much less than

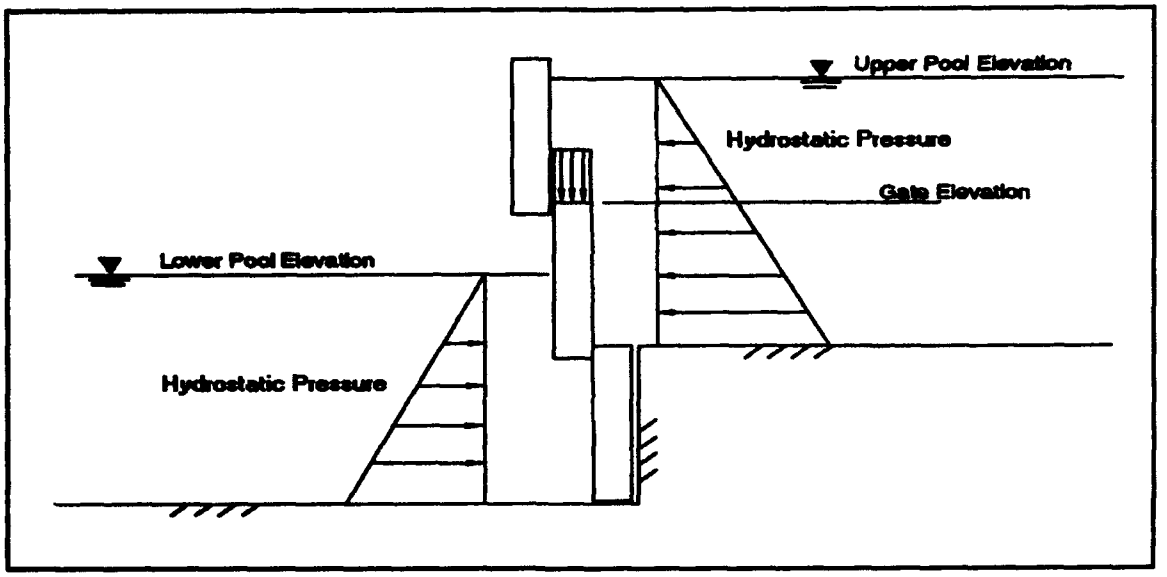

Figure 56. Hydrostatic loading applied for Locks and Dam 26 analysis

that of the Locks 27 models. To verify the analyses, analytical data were compared to head differential test data of both SET1-26 and SET2-26.

SET1-26. For the initial data comparisons, computed strains were compared with the experimental data of Test 261A (chamber drop test). The SET1-26 data were used to evaluate the overall behavior of the model since the transducer configuration was the more general layout. The comparisons resulted in $E_{per} = 6.6$ percent, $CF = 0.9715$, and an average error of 40.3 με. The measured strains reached levels of 500 microstrain, therefore, an average error of only 40 με is acceptable. Strain-history plots comparing the analysis and SET1-26 data are presented in Appendix B, Figures B17 through B26. Each plot includes data for a number of locations at a given member cross section.

Figures B17 through B23 show the analytical (COMP) and experimental (FIELD) girder strains at various girder cross sections. Each one of these comparisons is quite good. The flexural response (indicated by the difference in upstream and downstream flange strain) of the girders was generally over predicted by the analysis. However, the differences are slight and the computed strain values are acceptably accurate. Figures B24 and B25 show strain comparisons for two of the bracing members. The results show that the predicted axial behavior (indicated by the average of cross-sectional strains) in the bracing elements is reasonably accurate. However, the flexural response of the bracing members determined using the field strains are not well represented by the analysis results. (Figure B26 shows the erratic readings obtained with the channel 17 transducer where slippage of the transducer occurred.)

With a model of this scale, it is not possible to capture the flexural behavior of the bracing members due to the following considerations:

a. The connection details are represented by a single point at member intersections. The intersection between members in the actual structure consists of a finite dimension (relatively large compared to the cross-sectional dimensions and lengths of the members).

b. The bracing members are typically welded to the girder flanges along the flange of the angle or tee section, and the web is free. Therefore, it is likely that a substantial amount of shear lag is present at the ends of the bracing members. It is not possible to model shear lag without a significantly more detailed analysis.

c. The presence of member warping or out-of-straightness due to fabrication tolerances or residual stresses can significantly affect the strain readings when an axial force is applied. For example, if tension is applied to a bent bracing member, strain readings will indicate flexural behavior as the member is straightened, even if no end moments are present. (No visible out-of-straightness was observed during field testing.)

SET2-26. To study the effect of the cracked diaphragm, the analytical strains were compared to the measured strains of the SET2-26 (Figures 46 through 50) chamber drop test (Test 262B). Strain-history comparisons for Test 262B are provided in Appendix B, Figures B27 through B30. Similar to SET1-26 results, the comparisons for axial behavior of the bracing elements are acceptable, while the comparisons for flexural behavior are poor. Review of the diaphragm flange strain data yields some interesting insight regarding head differential vertical loading. The structural response due to vertical loading provides an explanation for the occurrence of cracking in the flange plate.

a. *Vertical loading*. The top girder web of a submerged lift gate leaf forms a horizontal damming surface. The magnitude of the head differential vertical load is dependent on the difference between the pressures acting on the upper and lower surfaces of the girder web. Pressure due to the hydrostatic head of the upper pool acts on the upper surface and when the chamber pool elevation is above the top girder, pressure due to the hydrostatic head of the chamber pool acts on the lower surface. When the chamber pool level is below the top girder, the pressure on the lower surface is zero. As the chamber pool is dropped from the upper pool elevation to the top girder elevation, the vertical load increases proportionally with the head differential. As the chamber pool continues to drop, the vertical load is dependent only on the upper pool elevation. A graph of the vertical load pressure with respect to head differential for this test is shown in Figure 57. The loading consists of a linearly increasing force up to a head differential of approximately 11 ft (3.35 m) (difference between upper pool and top girder elevations) and is then constant for the remaining chamber drop.

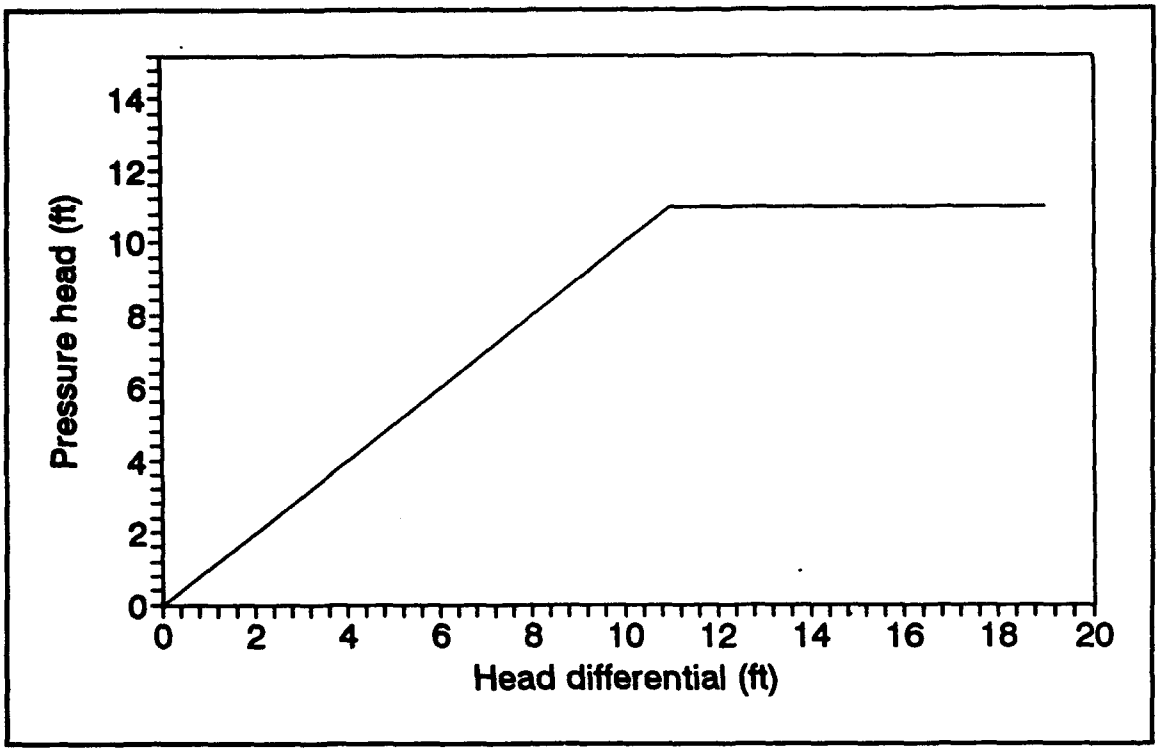

Figure 57. Vertical load pressure as a function of head differential

b. Structural response. All of the strain histories obtained from the diaphragms and diagonal braces have the same shape as the vertical loading shown in Figure 57. Although the head differential horizontal load continues to increase as the chamber pool drops below the top girder (approximately 11-ft (3.35-m) head differential), the strains remain relatively constant for head differential greater than 11 ft (3.35 m). This indicates that these elements are primarily affected by the vertical loading only. Therefore, it is reasonable to assume that the crack at the girder and diaphragm flange interface may be caused by deflections induced by the vertical loading.

Conclusions

The SET1-26 results show that the model of this analysis provides a reasonable representation of the leaf. The general behavior was well represented as indicated by the girder responses and the overall error comparisons. However, with a model of this scale it was not possible to simulate the flexural behavior of the bracing members. The Test 262B results provide significant information on vertical load response of lift gates. The following paragraphs discuss the structural behavior and provide an explanation on the occurrence of diaphragm flange cracking.

Under vertical loading, deflection induced stresses may have contributed to the formation of the crack at the girder and diaphragm flange interface. If sufficient horizontal shear resistance were present between each girder, the entire leaf would act as a large beam under distributed vertical load. The gate leaf would bend in the plane of the leaf about its neutral axis with the upper girders subject to compression and the lower girders subject to tension. This type of response is described by the Euler-Bernoulli beam response in which plane sections remain plane and perpendicular to the neutral axis. Given this type of response, the diaphragm members would remain straight and would rotate to remain perpendicular to the girders. However, as indicated by recorded strains data, the deformation of the gate leaf was more representative of shear deformation in which vertical planes tend to remain vertical.

Strains recorded at the edges of the diaphragm flange varied in sign (compression and tension) depending on the position of the transducer along the length of the diaphragm. The signs of the measured strains (as well as the position of the crack) indicated that a considerable amount of lateral bending was induced in the flange plate and that each diaphragm was forced to deflect in an S-shape. This type of deflection is consistent with shear deformation as indicated by Figure 58. The figure shows transducer locations and the respective strain directions (C = compression and T = tension). Based on the measured strains, it is apparent that the crack in the flange was at least partially caused by high tension and shear stresses at the diaphragm flange-girder flange interface. This is a result of the diaphragm displacement resulting from the shear deformation of the gate leaf. The high depth-to-length ratio of the gate leaf and insufficient shear resistance provided by the diagonal braces allow significant shear deformation to occur as opposed to normal flexure deformation. Under distributed vertical load:

a. Horizontal girders deflect vertically and bend in the plane of the leaf about their weak axes, much like a simply supported beam subject to uniform load. Under vertical distributed loading, the slope (change in vertical deflection per unit length) of the girder flange varies from maximum at the ends to zero at midspan since the vertical shear in the leaf is greatest near the ends.

b. The welded connections between the girders and diaphragms do not allow any relative rotation between the diaphragm flange and the girder flange. The diaphragm flanges are considerably smaller and more flexible than the girder flanges. Therefore, the ends of the diaphragms are forced to rotate with the slope of the girder flange.

c. The diaphragms are forced to deflect in double curvature (S-shape) to maintain continuity with the girder flanges at each end of the diaphragm. This deformation results in large tensile (and compressive) stresses at the ends of the of the diaphragm flanges (Figure 58) and large shear stresses along the length.

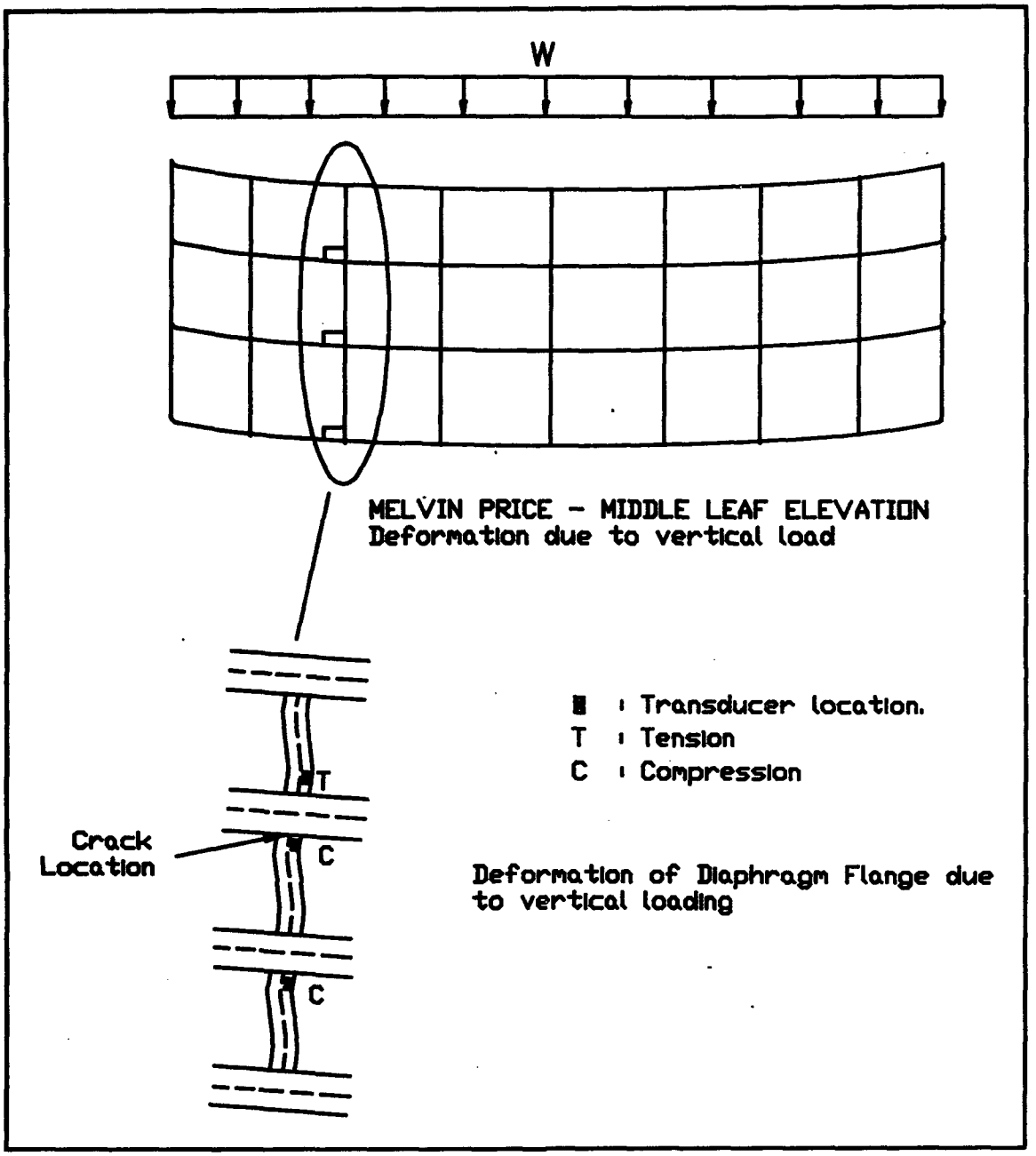

Figure 58. Locks and Dam 26 leaf shear deformation and diaphragm deformation

Although welding-induced residual tensile stresses and stress concentration may have had a significant influence on the crack formation, the conditions described previously would promote the type of cracking that was observed. The crack initiated at the weld between the diaphragm flange and the girder flange and was oriented in a direction perpendicular to tensile stresses in the diaphragm flange (that would occur for the displacement described). The cracked diaphragm was near the end of the leaf where the girder flange slope is greatest. It is likely that similar cracking will occur at tension locations near the ends of diaphragm at similar locations (near both ends of the leaf).

4 General Conclusions

The objectives of this study were to measure the behavior of vertical lift lock gates experimentally and to develop modeling and analysis procedures for design and evaluation of vertical lift gates. An evaluation system that incorporates a realistic analytical approach and experimental data provides a considerable amount of information that is not generally available. Experimentally measured strain data provide direct information on the structural response and a means of determining the accuracy of the analysis. A representative analysis can then provide the information required for design and evaluation. The ability to obtain a substantial amount of structural response data from a vertical lift gate with minimal impact on lock traffic was demonstrated with good success at both lock sites. Based on experimental strain data obtained during the field tests, it was determined that the finite element models of the vertical lift gates provided reasonably accurate predictions of the general behavior. The combination of experimental and analytical data provided quantitative information on lift gate behavior and loading conditions.

Data comparisons performed for the Lock 27 lift gate leaf were used to establish appropriate load conditions and BC. Based on comparison of analytical and experimental data, it was concluded that the dynamic load model (Figure 54) is most appropriate. In an attempt to evaluate the effect of the horizontal friction determined to be present along the bottom sill of Locks 27, a parameter optimization algorithm was utilized. Unknown BC were simulated with elastic supports and a stiffness constant was computed automatically by the optimization process. The model optimization technique resulted in approximately a 10-percent improvement in E_{per} comparing measured and computed strains. Through the Locks and Dam 26 study, it was verified that the downstream bracing members are primarily affected by vertical loading, and a probable cause for the cracking of a diaphragm flange was obtained. The following sections provide recommendations for future experimental and analytical studies.

Experimental Studies

During instrumentation of each structure, the primary concerns were how to efficiently place cables through the structure so that gate leaf operation would not be inhibited, and whether or not the method of attaching the transducers with tabs and cyanoacrylate glue would be suitable for underwater use. A considerable amount of experience that will aid in improving field procedures for future testing was gained during the field tests at Locks 27 and Locks and Dam 26.

Setup

a. As opposed to installing each transducer cable separately (as was done in the Locks 27 tests), groups of cables that connect to transducers in the same area on the structure should be wrapped together in groups (as was done during the Locks and Dam 26 test). This greatly reduces the time required for instrumentation setup and removal.

b. Prior to running these tests, there was significant concern on the use of underwater strain transducers and their method of attachment. The waterproof strain transducers performed properly with the exception of a few that became inoperative during testing. Considering the cost of the waterproof transducers, it may be beneficial to improve the durability of the transducers. The tests proved that the method of attaching the submergible transducers with tabs and cyanoacrylate glue works quite well. The tabs remained intact under relatively extreme conditions (all transducers were submerged and some of the transducers and the cables were subject to water rushing through leaking seals and drain holes).

Additional test position and instrumentation

Many uncertainties in loading and support conditions of vertical lift gates exist, and these uncertainties could be quantified through additional testing and analytical procedures. When ambiguous loading or BC exist, testing procedures should be designed to determine as many unknowns as possible. For example, the Locks 27 data comparisons confirmed that a significant amount of horizontal resistance (upstream direction) existed at the bottom sill and that the initial load assumptions were incorrect. The effects at the bottom sill could have been evaluated more efficiently by conducting additional head differential tests with the leaf lifted above the sill. The comparison of field data (for the leaf on the sill and above the sill) would indicate the amount of frictional resistance at the bearing locations. In future tests, pressure transducers could be attached to the skin plate at various elevations to provide accurate data on the actual pressure

distribution. A realistic load model could then be developed, based on measured pressures at various depths along the skin plate.

Analysis

For the models of this study, the flexure of the main structural members and the axial behavior of the smaller bracing elements were well represented. However, the models did not have sufficient detail to accurately reproduce the observed flexural response of the bracing members. Flexure does occur due to various secondary effects such as eccentricity of the connection details, shear lag, and any existing out-of-straightness in the bracing members. If a more realistic representation of the bending in the smaller members is necessary, the analysis program should be modified to include the effect of connection size and geometry. In cases where the connection details are relatively large compared to the member length, such as the diaphragm flanges of the Locks and Dam 26 lift gate, connection modeling may be beneficial.

A significant goal of this project is to develop a testing and analysis system for vertical lift gates that can be used for evaluation purposes on a routine basis. The information obtained during this study will aid in improving the efficiency of future studies. The following are considerations for future analytical work.

a. The analyses of this study provided reasonable comparisons with the field data, but the time required to generate the models and the analysis time for each were rather extensive. An automated model generation program (preprocessor) tailored for vertical lift gates would be beneficial to perform this type of analysis on a routine basis. Such a program would automatically develop the finite element mesh given the basic geometry of a gate leaf. Due to the variety of lift gate configurations, it would be difficult to develop a general program. However, development of software that simplifies the mesh generation process is feasible.

b. If only general behavior (flexure of girders and diaphragms) is to be modeled, then a grid analysis approach may be appropriate for routine analysis. The Locks 27 analysis requirements exceeded the limits of the typical personal computer. With a 3-D analysis procedure, personal computer limitations are likely to be a constraint for the analysis of large structures. It may be beneficial to investigate the use of simpler analysis procedures using the existing field data acquired during this study. The 3-D approach will likely be required for detailed cases such as representation of strains in bracing members.

References

Commander, B. C., Schulz, J. X., Goble, G. G., and Chasten, C. C. (1992a). "Computer-aided, field-verified structural evaluation; Report 1, Development of computer modeling techniques for miter lock gates," Technical Report ITL-92-12, U. S. Army Engineer Waterways Experiment Station, Vicksburg, MS.

_____. (1992b). "Computer-aided, field-verified structural evaluation; Report 2, Field test and analysis correlation at John Hollis Bankhead Lock and Dam," Technical Report ITL-92-12, U. S. Army Engineer Waterways Experiment Station, Vicksburg, MS.

Goble, G. G., Schulz, J. X., Commander, B. C. (1990). "Simple load capacity tests for bridges to determine safe posting levels: Final report," submitted to the Pennsylvania Department of Transportation by the Department of Civil and Architectural Engineering, University of Colorado, Boulder, CO.

Headquarters, U.S. Army Corps of Engineers. (1962). "Engineering and design, vertical lift crest gates," Engineer Manual 1110-2-2701, Washington, D.C.

_____. (1984). "Engineering and design, lock gates and operating equipment," Engineer Manual 1110-2-2703, Washington, D.C.

_____. (1988). "The 1988 Inland Waterway Review," Institute for Water Resources, Ft. Belvoir, VA.

U.S. Army Engineer District, St. Louis. (1990). "Locks No. 27 Mississippi River, report on: lift gate study," St. Louis, MO.

Appendix A
Vertical Load Test Experimental Data

This appendix includes graphical plots of the experimental data obtained at Locks 27 for Test 271A (vertical load test). Strain values for various transducers (identified by the DAS channel number in the plot legends) are presented as a function of testing time. The transducer locations are shown in Figures 4 through 15 in the main text. Each strain history shows the same characteristics. An abrubt change in strain occurs at the beginning of the test (as the gate leaf was lifted from the sill), a constant strain level is maintained for most of the testing time (as the gate continued to be lifted and lowered), and at the end of the test the plots show a sudden return to near-zero strain (as the gate leaf was returned to the sill). The occurrence of strain at each location is attributed to the effect of structural weight being transferred from the sill to the lifting chains. While resting on the sill, member strains due to structural weight should be near zero. Since each strain value returns to near zero, this indicates that the gate was at least partially resting on the bottom sill at the beginning of the vertical load test.

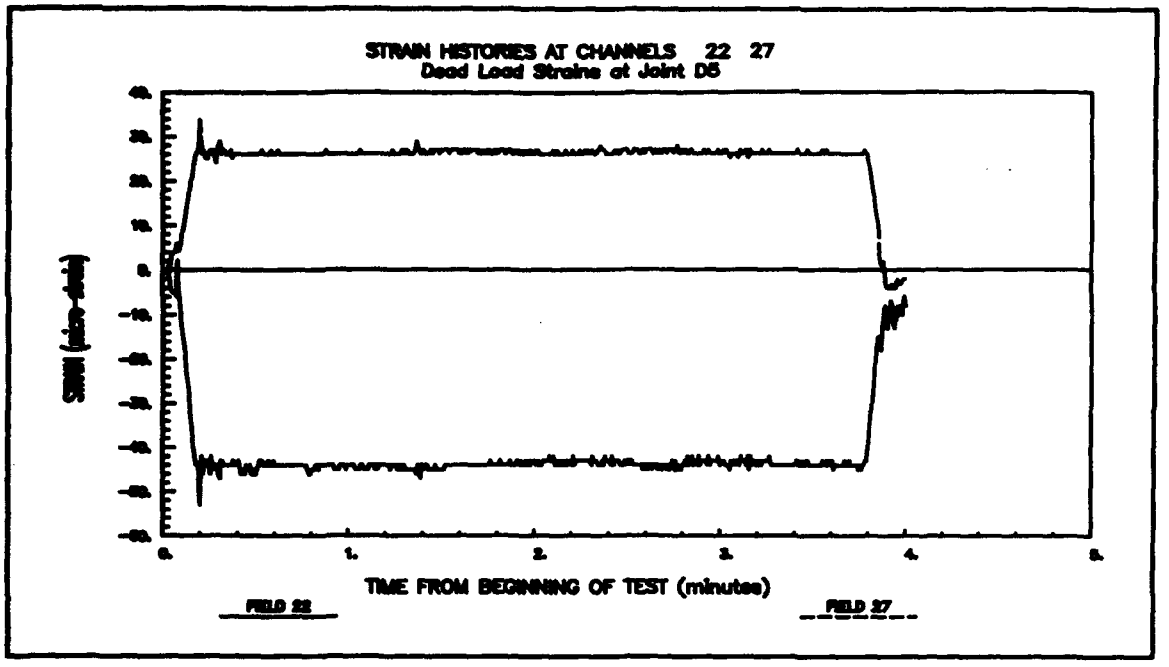

Figure A1. Vertical load strain histories (SET1-27), Channels 22 and 27

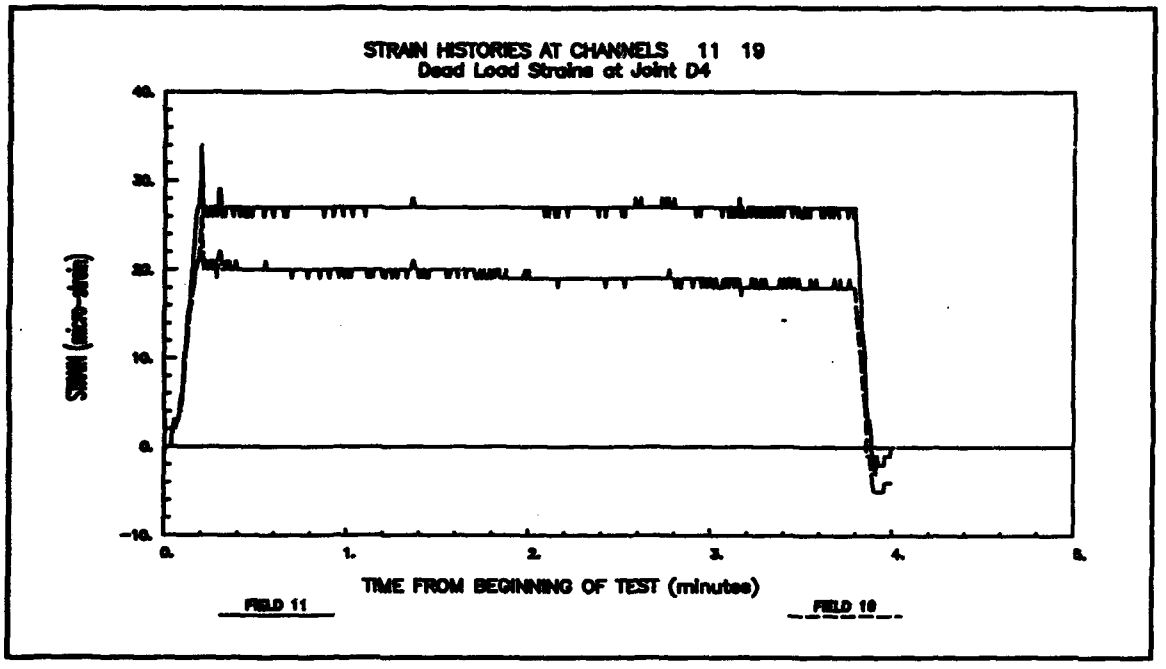

Figure A2. Vertical load strain histories (SET1-27), Channels 11 and 19

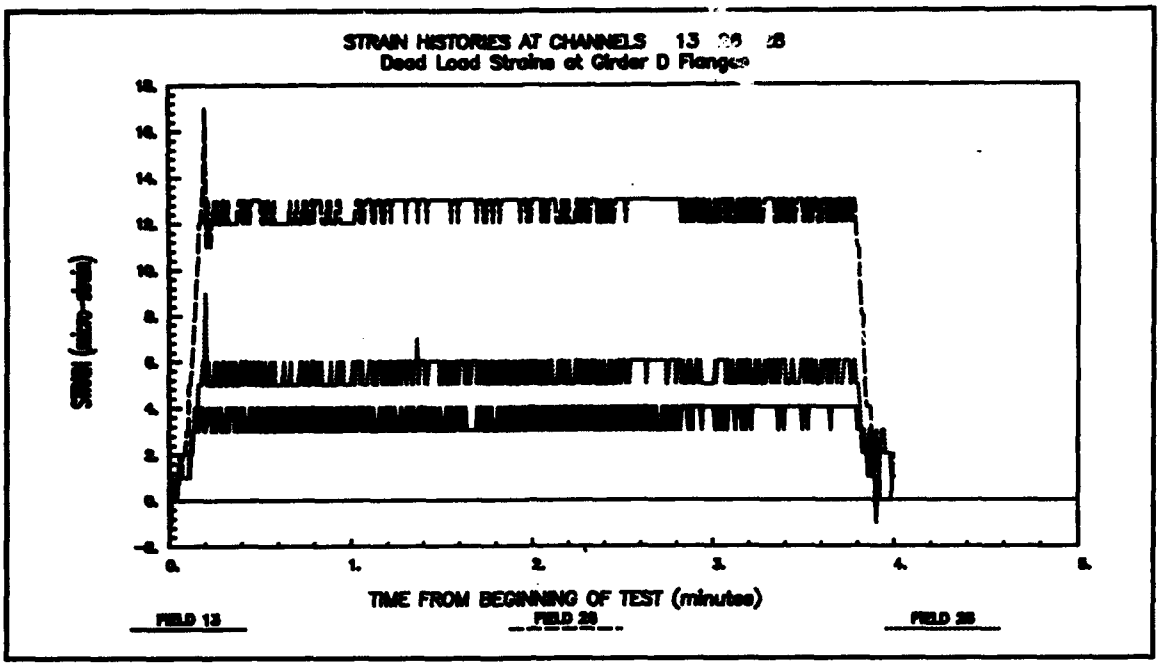

Figure A3. Vertical load strain histories (SET1-27), Channels 13, 26, and 28

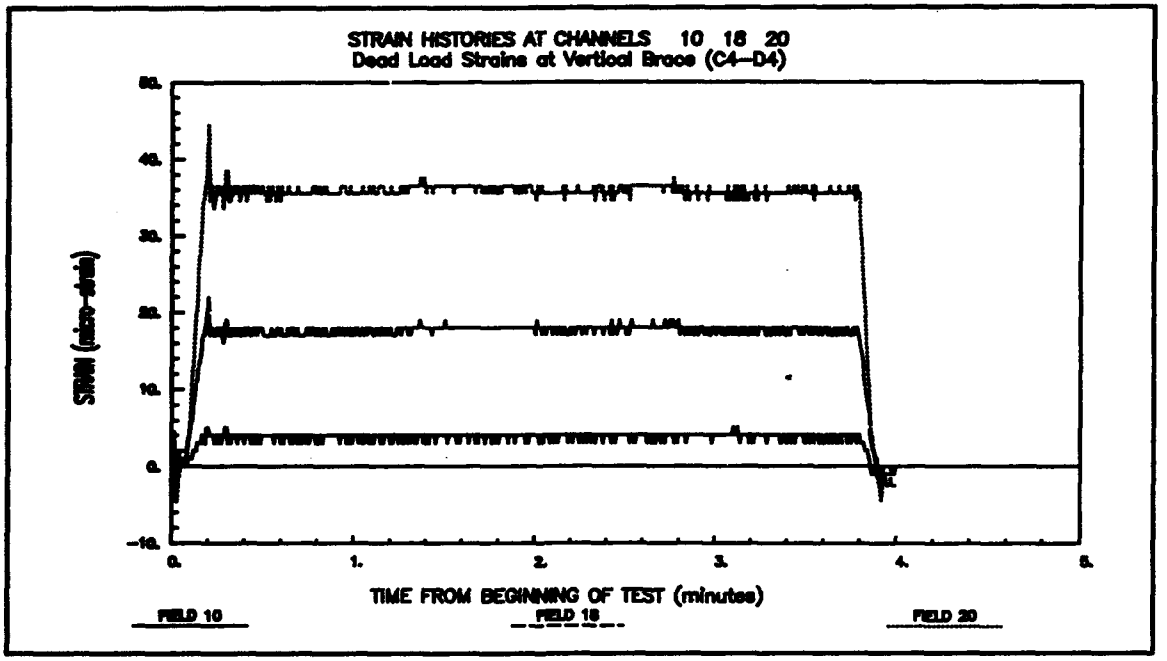

Figure A4. Vertical load strain histories (SET1-27), Channels 10, 18, and 20

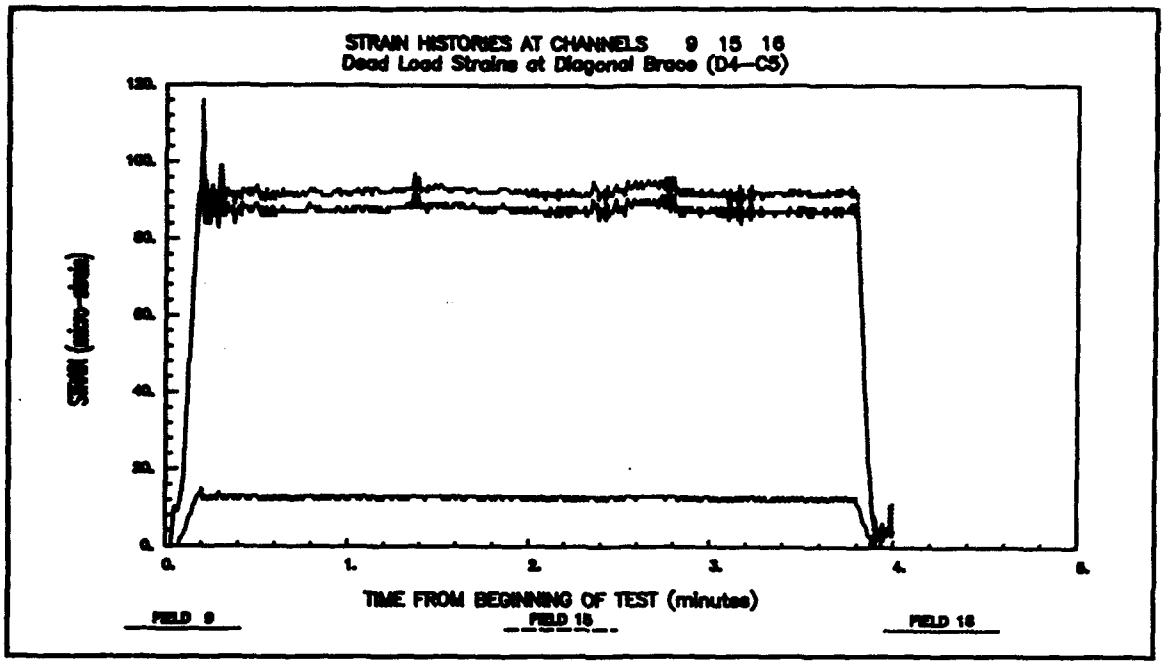

Figure A5. Vertical load strain histories (SET1-27), Channels 9, 15, and 16

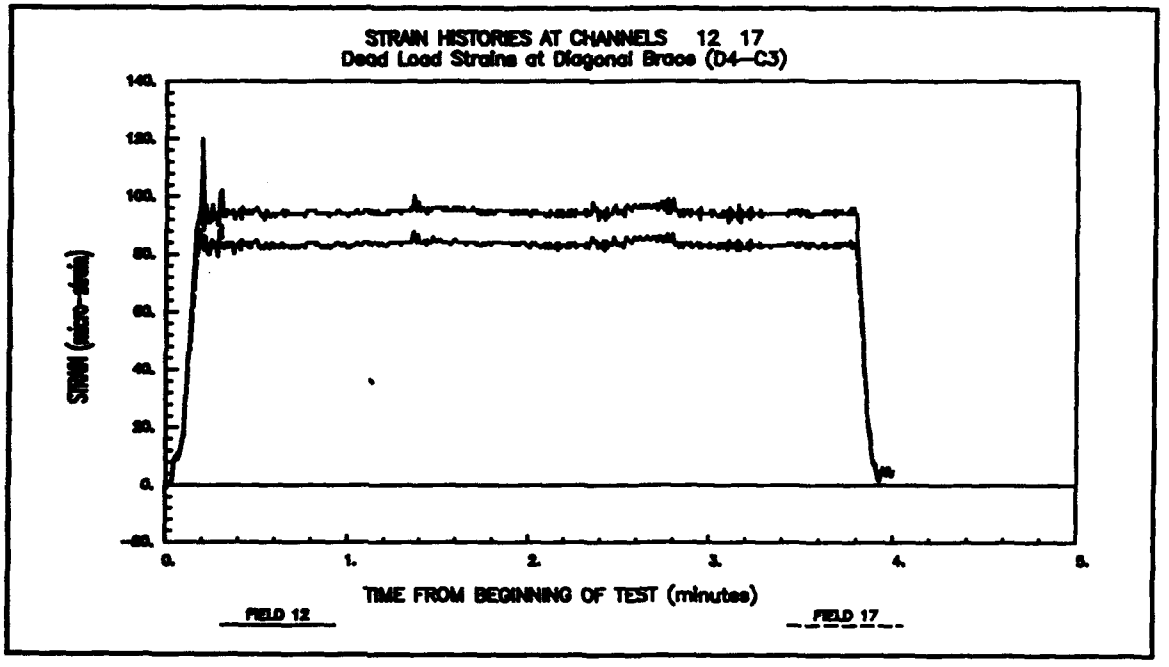

Figure A6. Vertical load strain histories (SET1-27), Channels 12 and 17

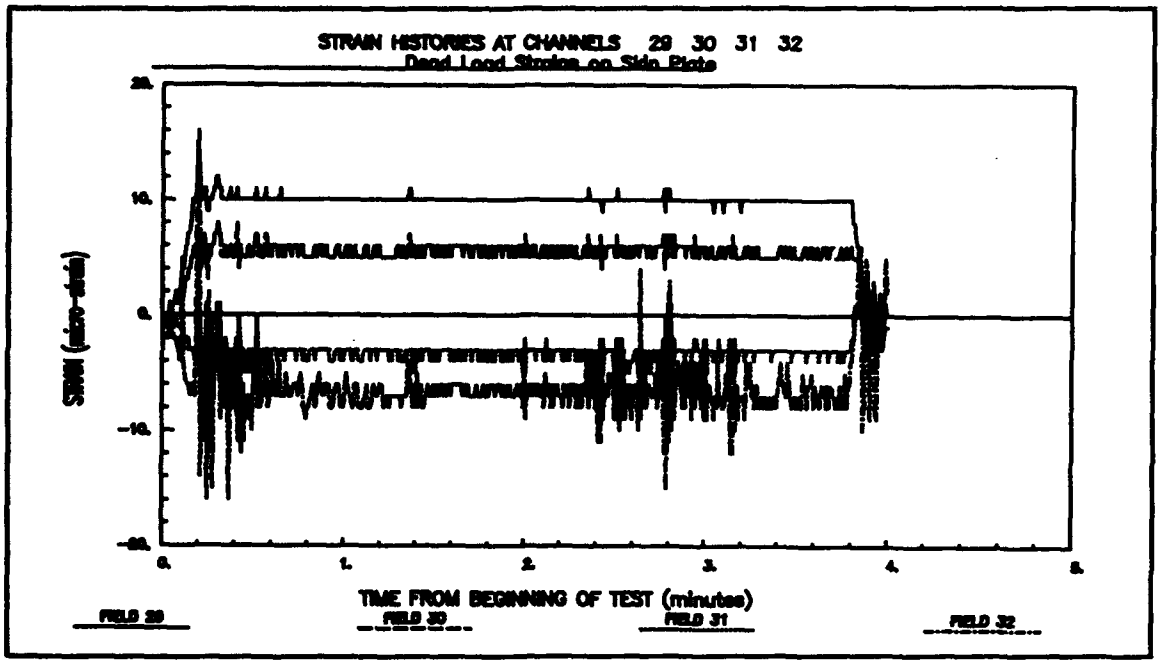

Figure A7. Vertical load strain histories (SET1-27), Channels 29, 30, 31, and 32

Appendix B
Head Differential Test Data

This appendix includes graphical plots of experimental and analytical data for head differential Tests 272B, 271C, 261A, and 262B. The graphical representations of the strain data provide a visual means of examining the structural response of the lift gates that is useful in evaluating the structural behavior and quality of the analyses. Strain measurements and the analytical data for various DAS channel numbers are plotted as a function of head differential. Channel numbers correspond to the transducer locations shown in the main text in Figures 4 through 15 for SET1-27, Figures 16 through 27 for SET2-27, Figures 31 through 44 for SET1-26, and Figures 45 through 49 for SET2-26. Experimental data for each channel are plotted using different types of continuous lines, and computed strains corresponding to each channel are plotted by different marks. The plot legends show which line type and marker type is associated with a particular data channel. The experimental and computed data is referred to in the legend by the terms *FIELD* and *COMP*, respectively, followed by the associated data channel numbers.

Locks 27 Strain Data (Test 272B; SET2-27)

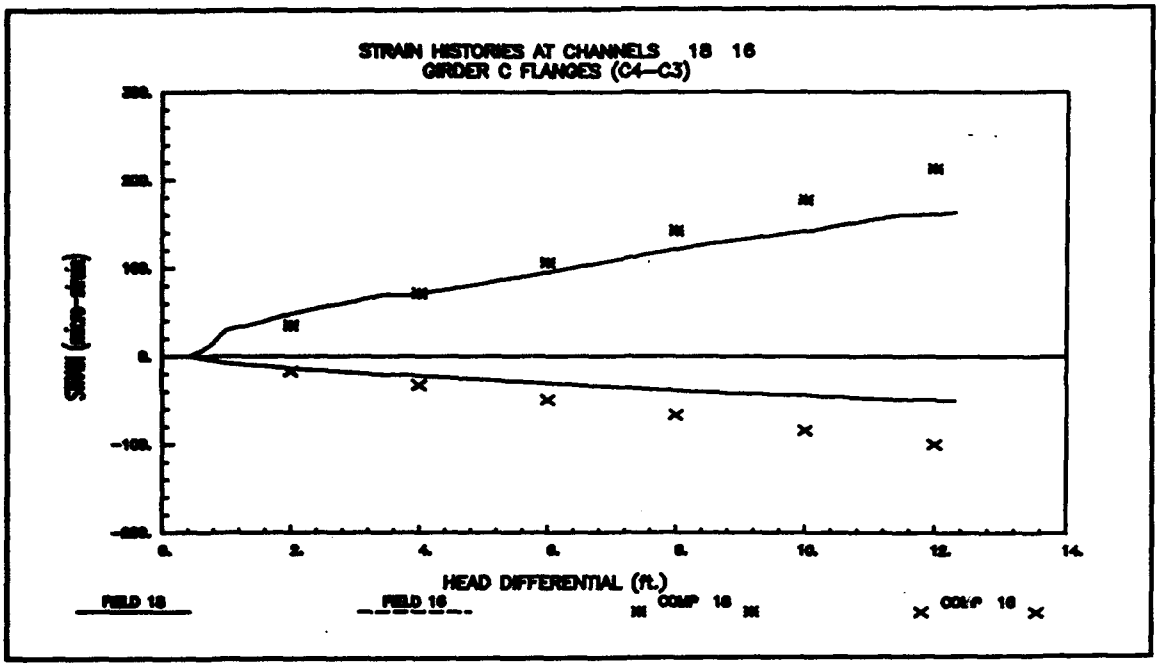

Figure B1. Locks 27 strain histories - Test 272B (SET2-27), Channels 18 and 16

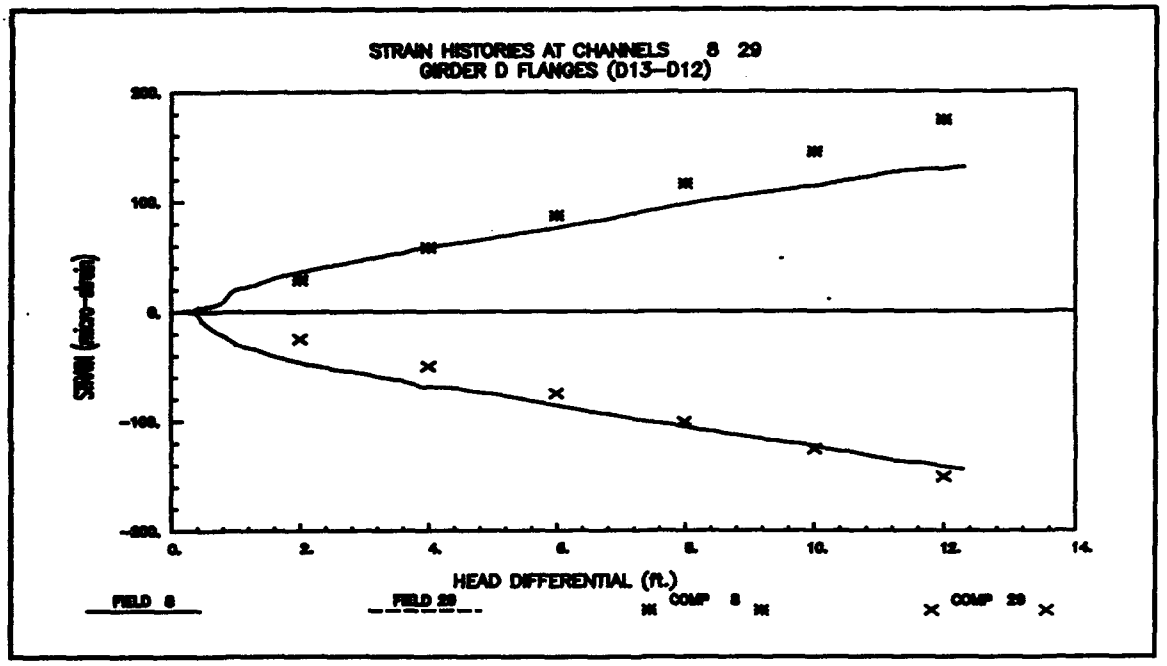

Figure B2. Locks 27 strain histories - Test 272B (SET2-27), Channels 8 and 29

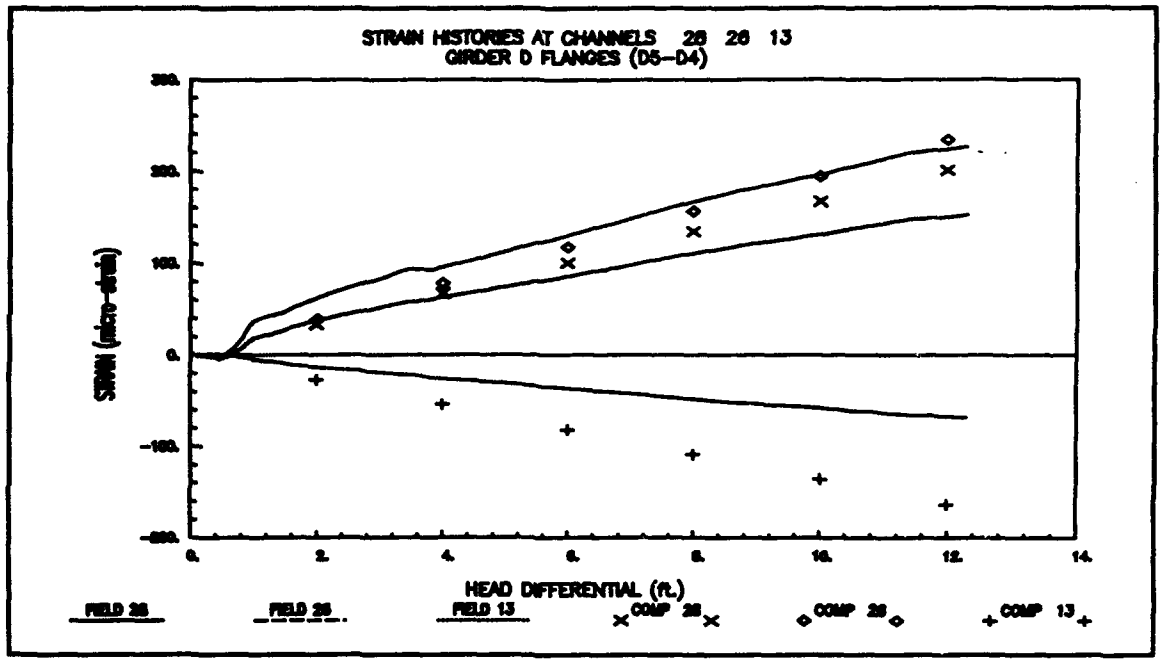

Figure B3. Locks 27 strain histories - Test 272B (SET2-27), Channels 28, 26, and 13

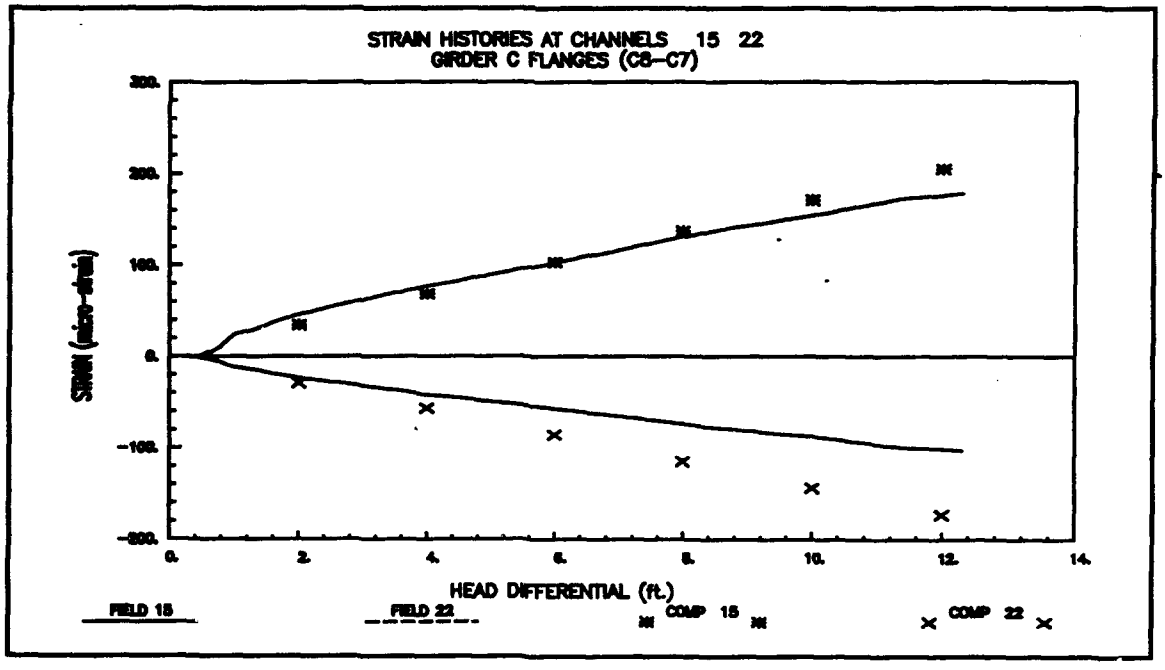

Figure B4. Locks 27 strain histories - Test 272B (SET2-27), Channels 15 and 22

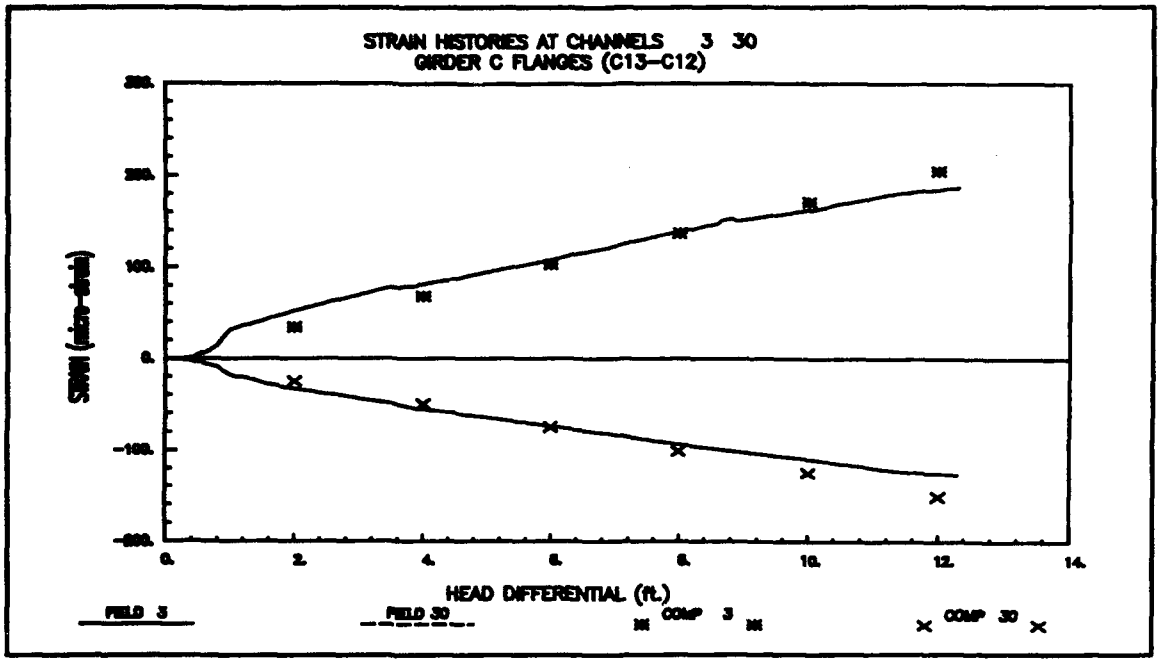

Figure B5. Locks 27 strain histories - Test 272B (SET2-27), Channels 3 and 30

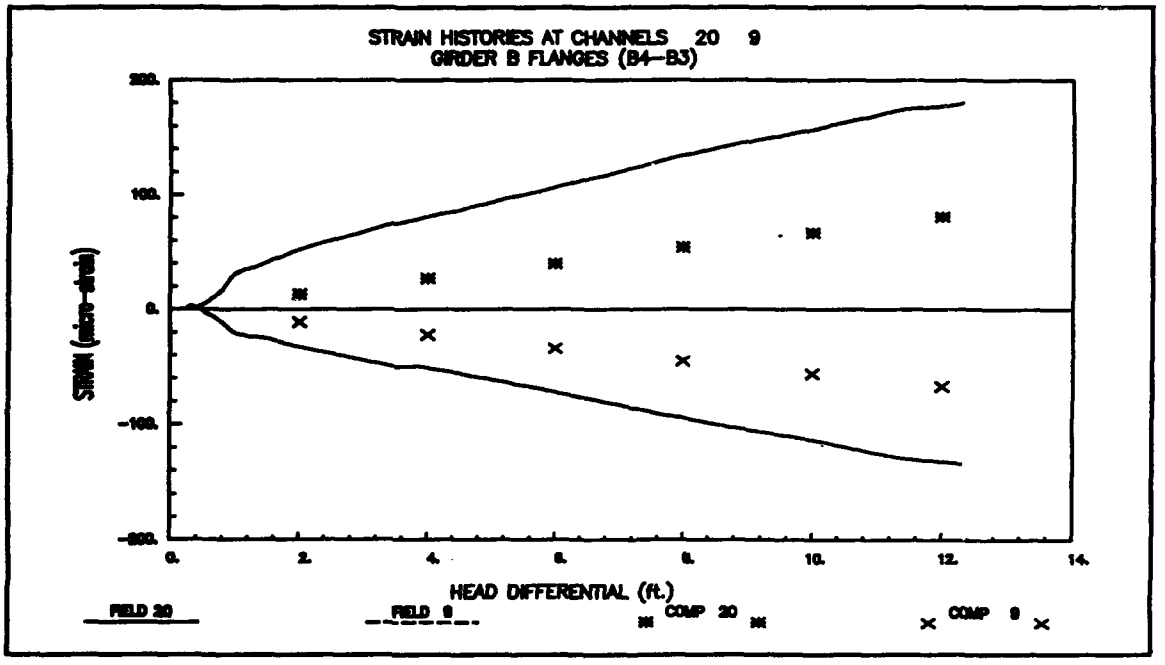

Figure B6. Locks 27 strain histories - Test 272B (SET2-27), Channels 20 and 9

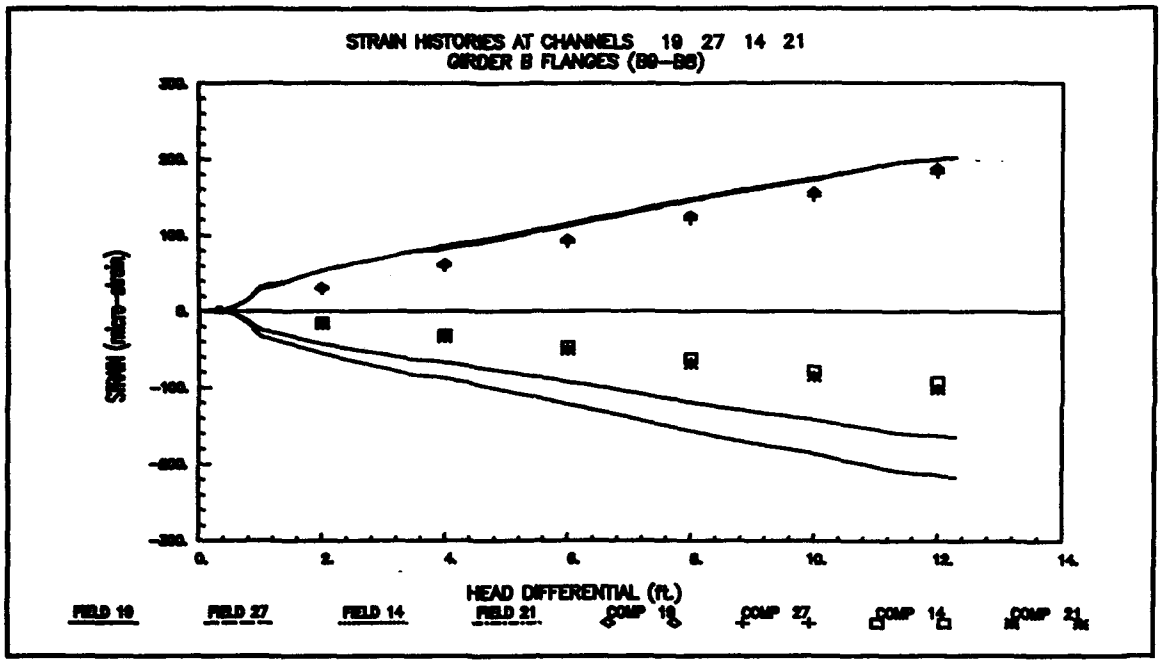

Figure B7. Locks 27 strain histories - Test 272B (SET2-27), Channels 19, 27, 14, and 21

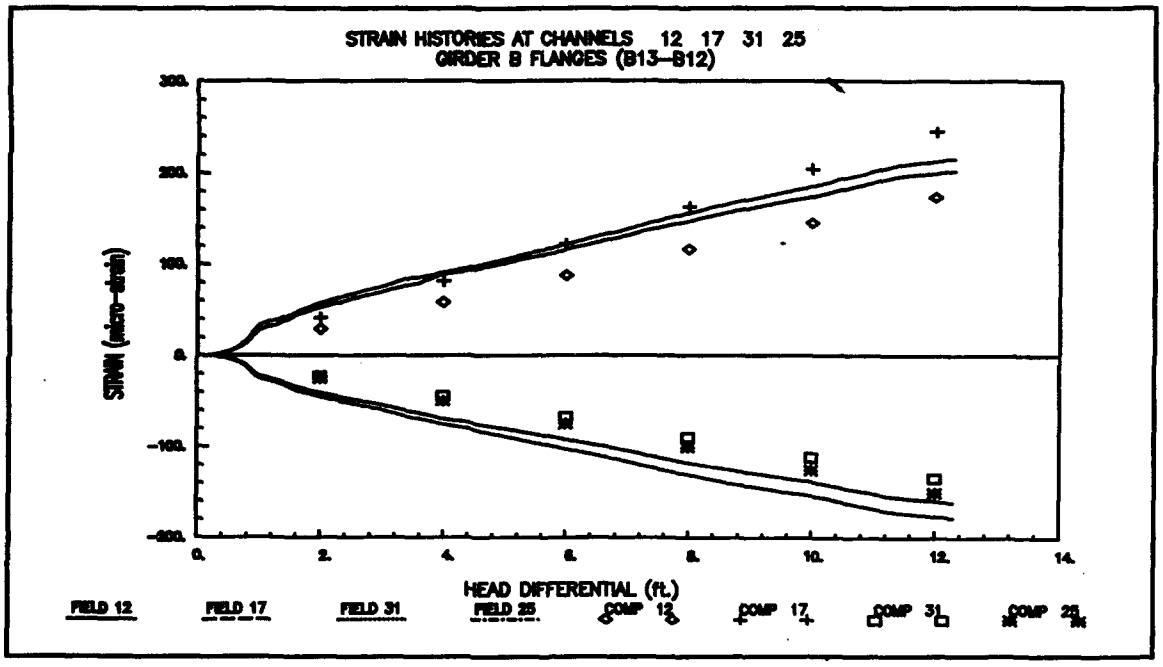

Figure B8. Locks 27 strain histories - Test 272B (SET2-27), Channels 12, 17, 21, and 25

Locks 27 Strain Data (Test 271C; SET1-27)

For the chamber drop Test 271B, chamber level position indicator marks were not reliable (main text, Chapter 2, Field Notes), and it was not possible to accurately correlate the data with the level of head differential. Therefore, the experimental data based on the results of the chamber fill Test 271C are presented here. The data for the chamber fill test were established at the maximum head differential. Therefore, to compare results based on increasing values of head differential, the data shown in Figures B9 through B16 were adjusted to reflect a datum position of zero head differential.

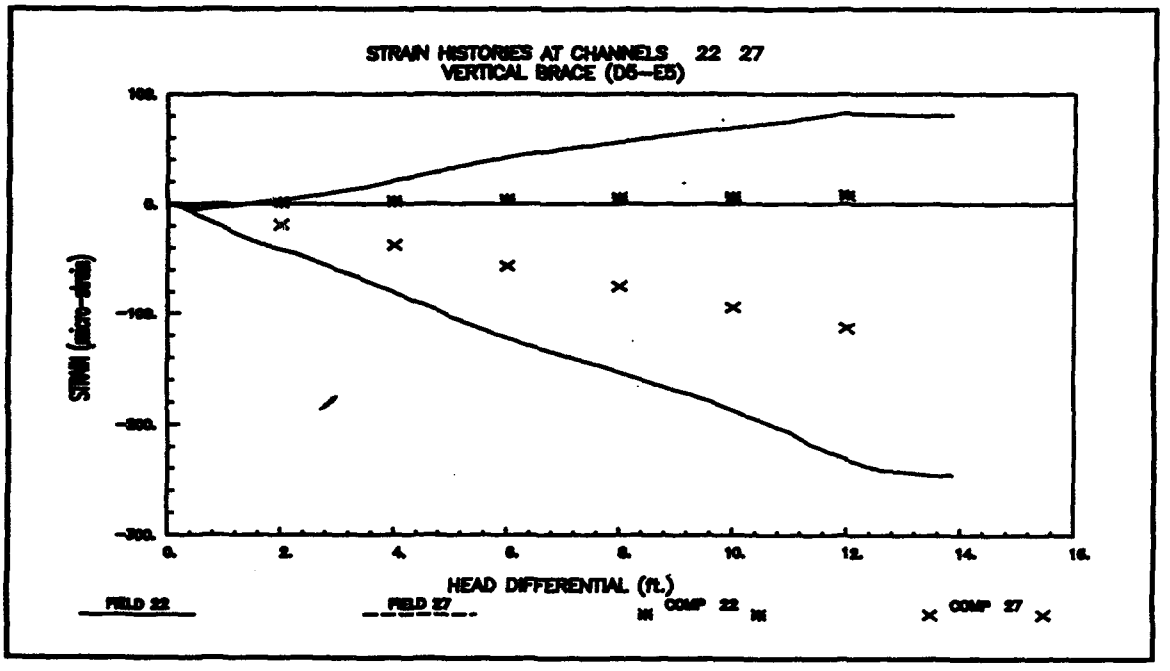

Figure B9. Locks 27 strain histories - Test 271C (SET1-27), Channels 22 and 27

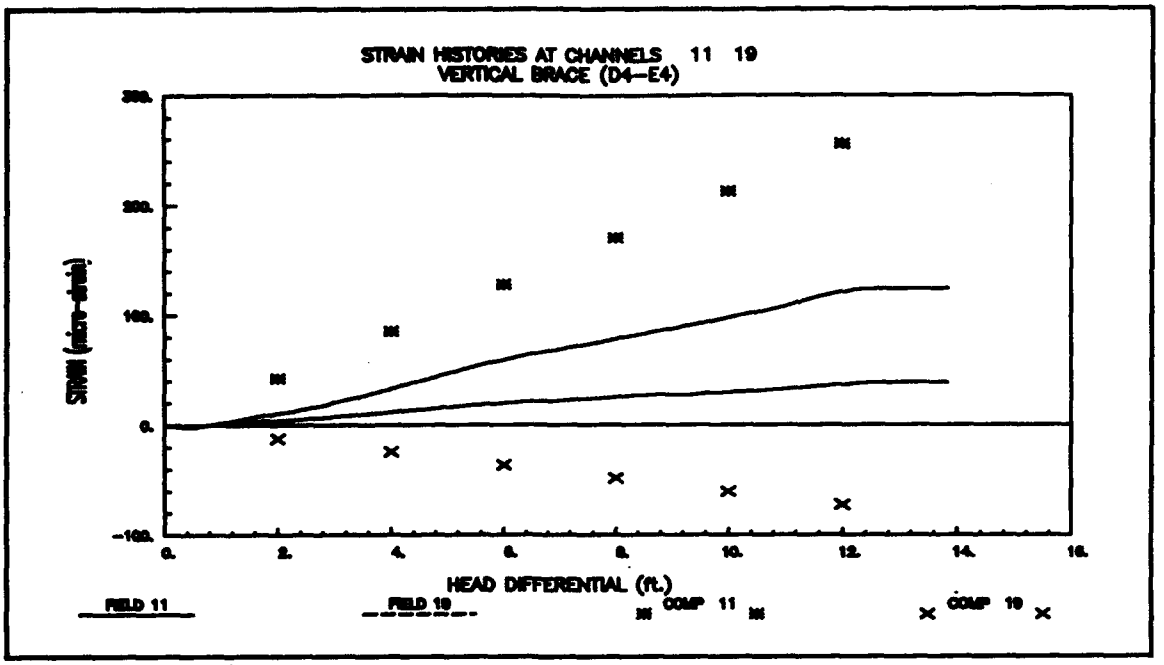

Figure B10. Locks 27 strain histories - Test 271C (SET1-27), Channels 11 and 19

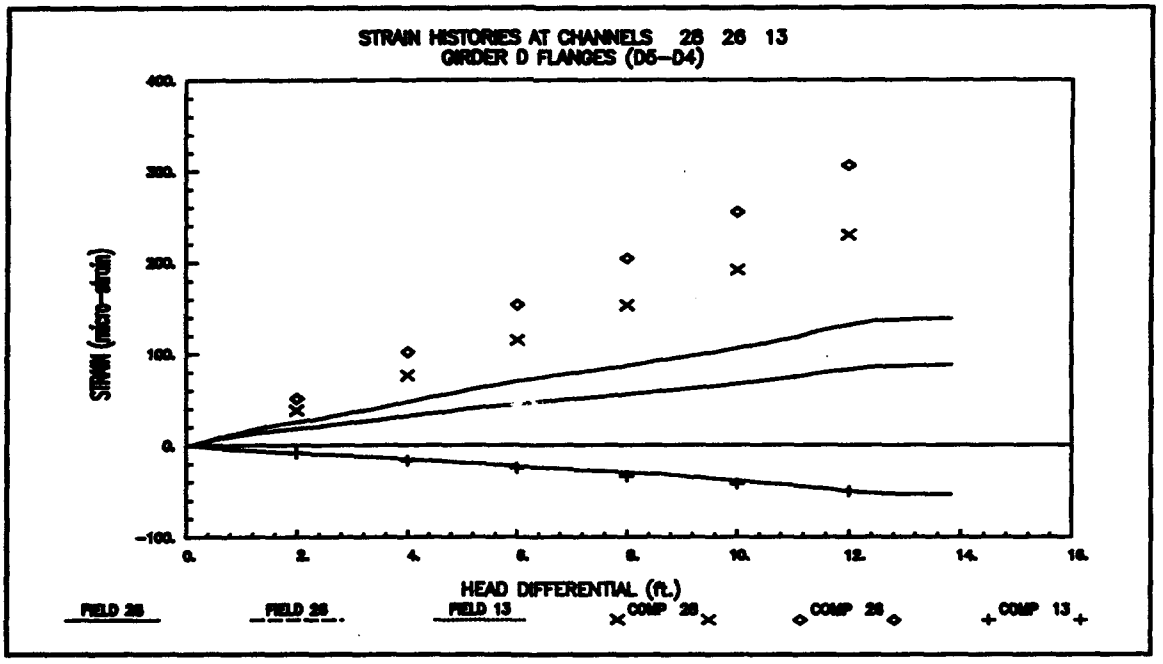

Figure B11. Locks 27 strain histories - Test 271C (SET1-27), Channels 28, 26, and 13

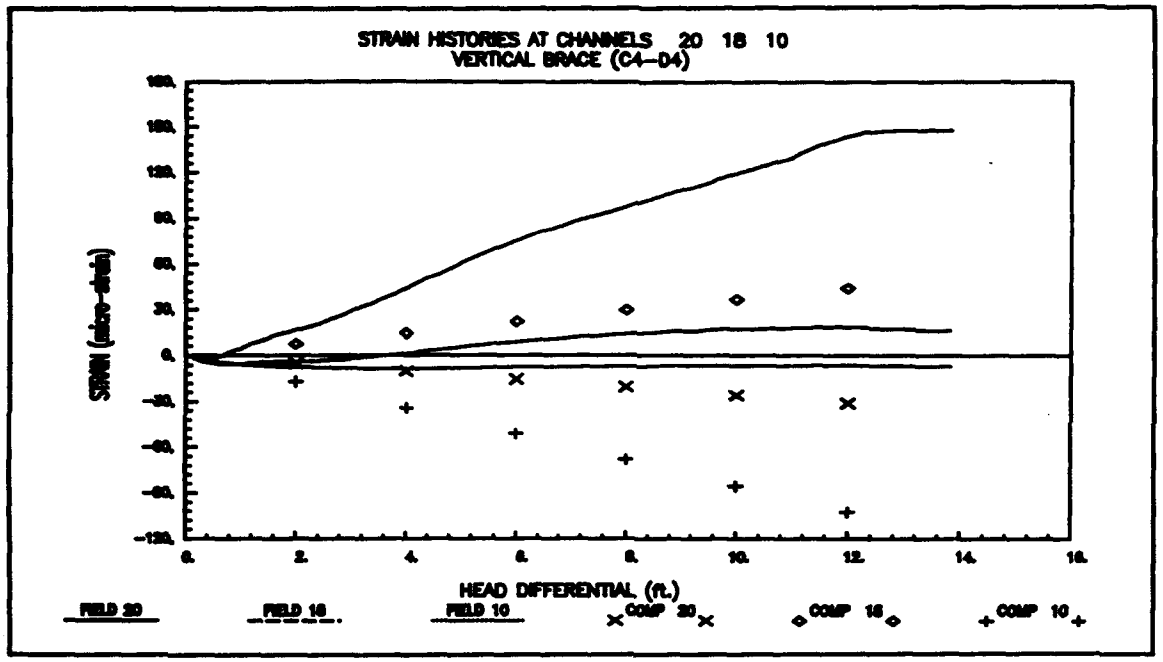

Figure B12. Locks 27 strain histories - Test 271C (SET1-27), Channels 20, 18, and 10

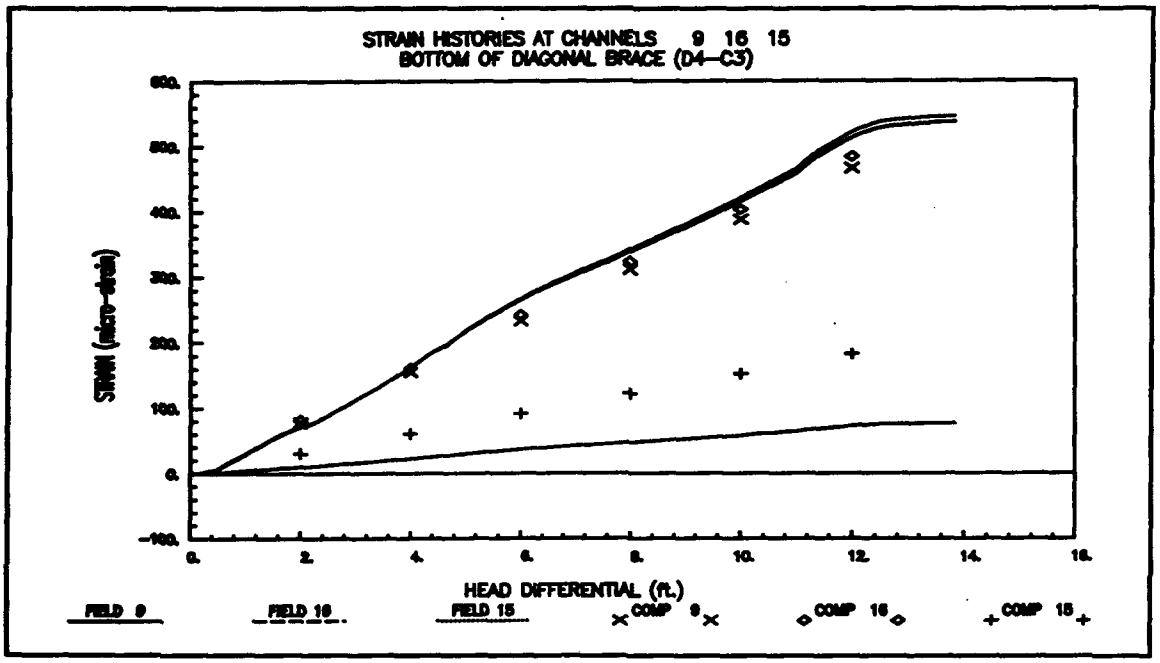

Figure B13. Locks 27 strain histories - Test 271C (SET1-27), Channels 9, 16, and 15

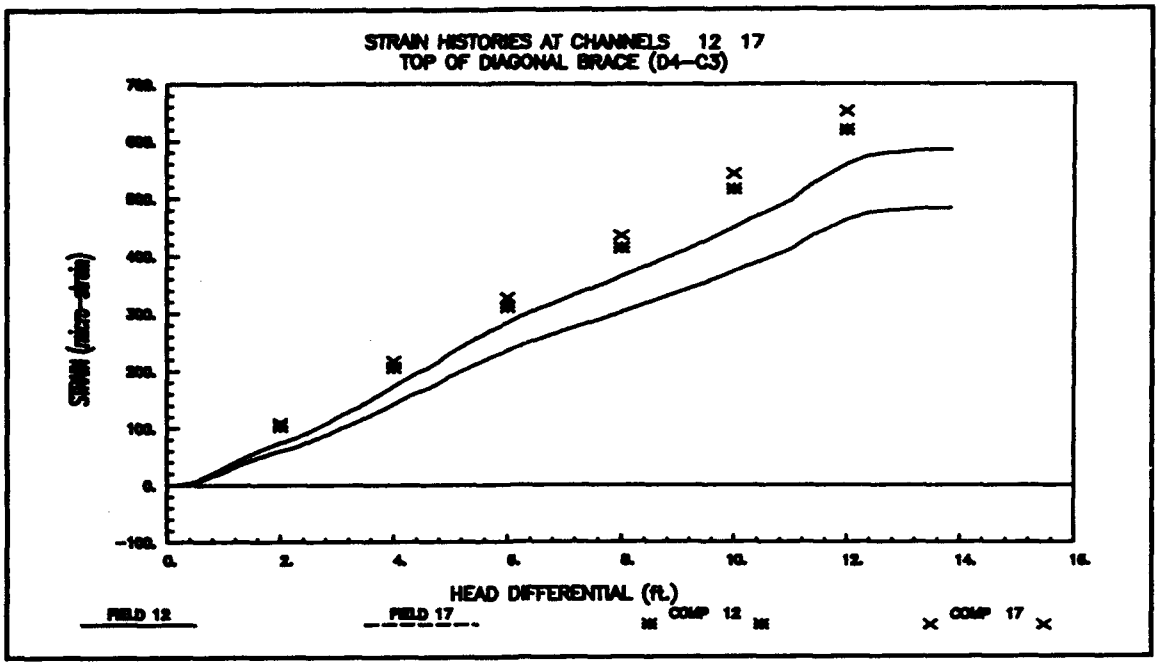

Figure B14. Locks 27 strain histories - Test 271C (SET1-27), Channels 12 and 17

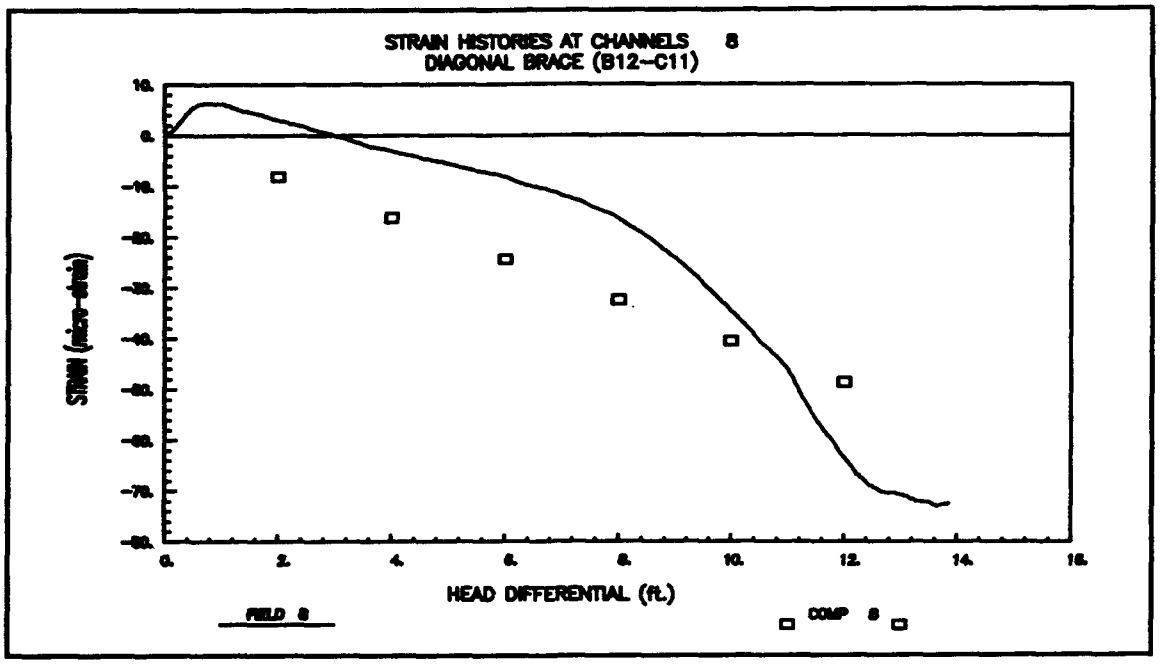

Figure B15. Locks 27 strain histories - Test 271C (SET1-27), Channel 8

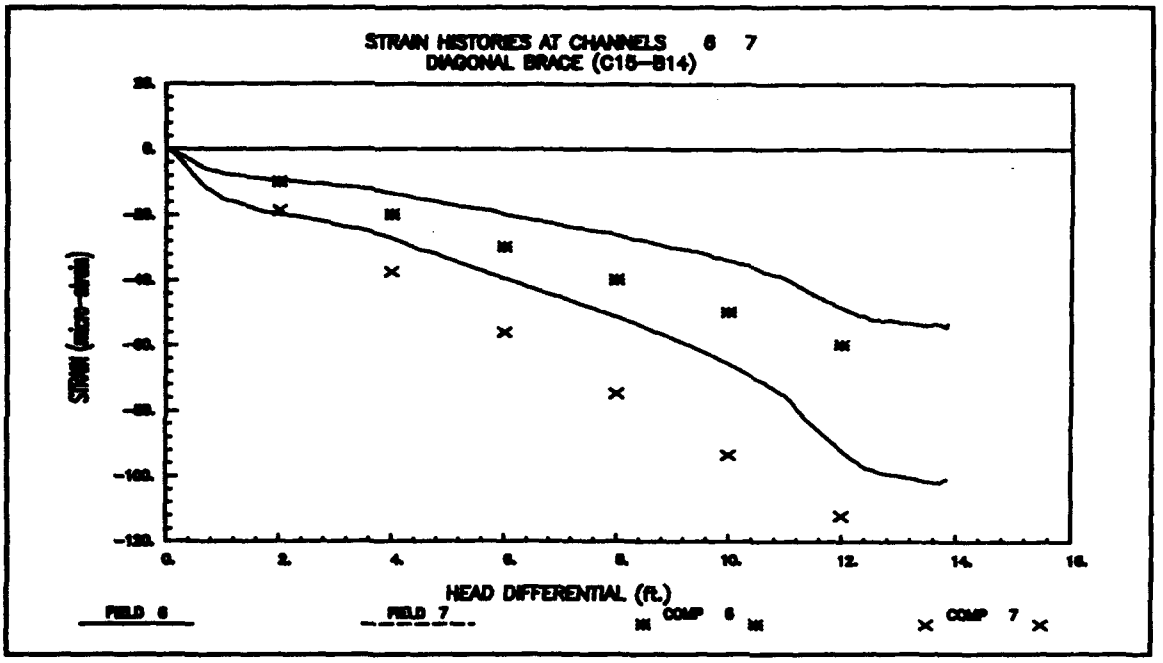

Figure B16. Locks 27 strain histories - Test 271C (SET1-27), Channels 6 and 7

Locks and Dam 26 Strain Data (Test 261A; SET1-26)

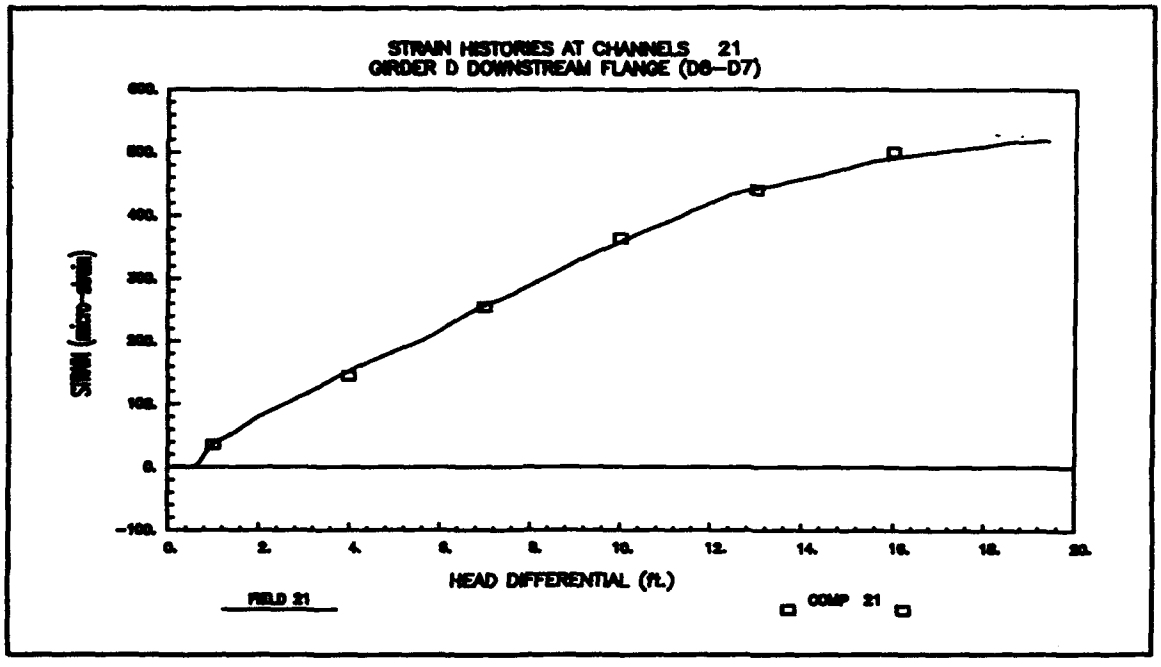

Figure B17. Locks and Dam 26 strain histories - Test 261A (SET1-26), Channel 21

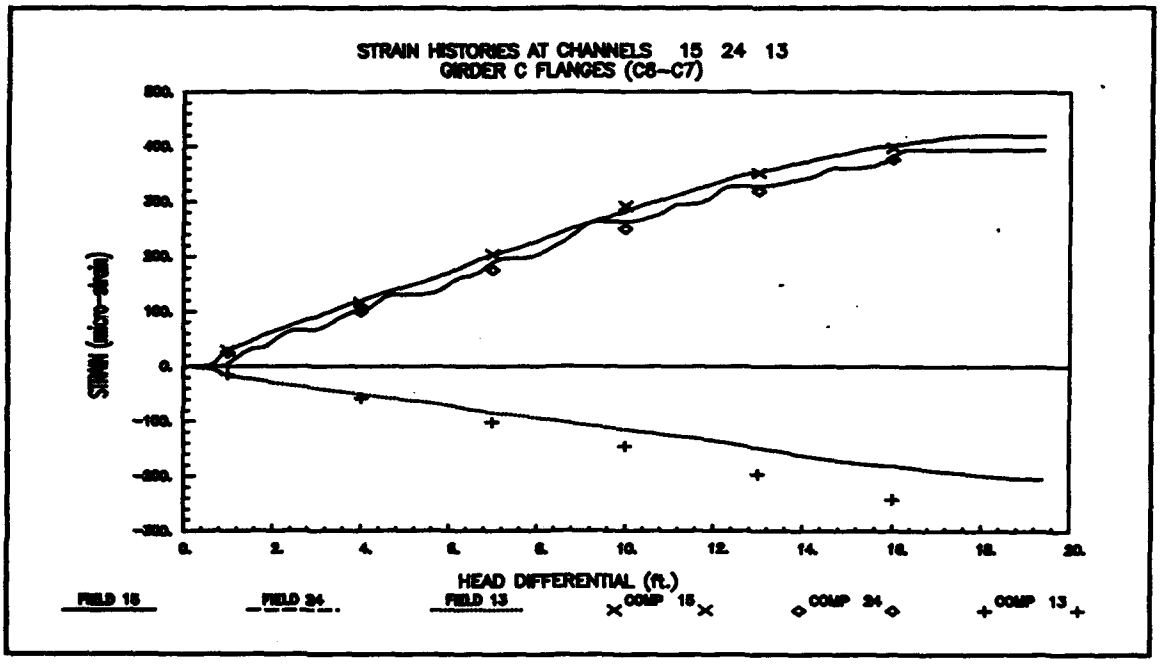

Figure B18. Locks and Dam 26 strain histories - Test 261A (SET1-26), Channels 15, 24, and 13

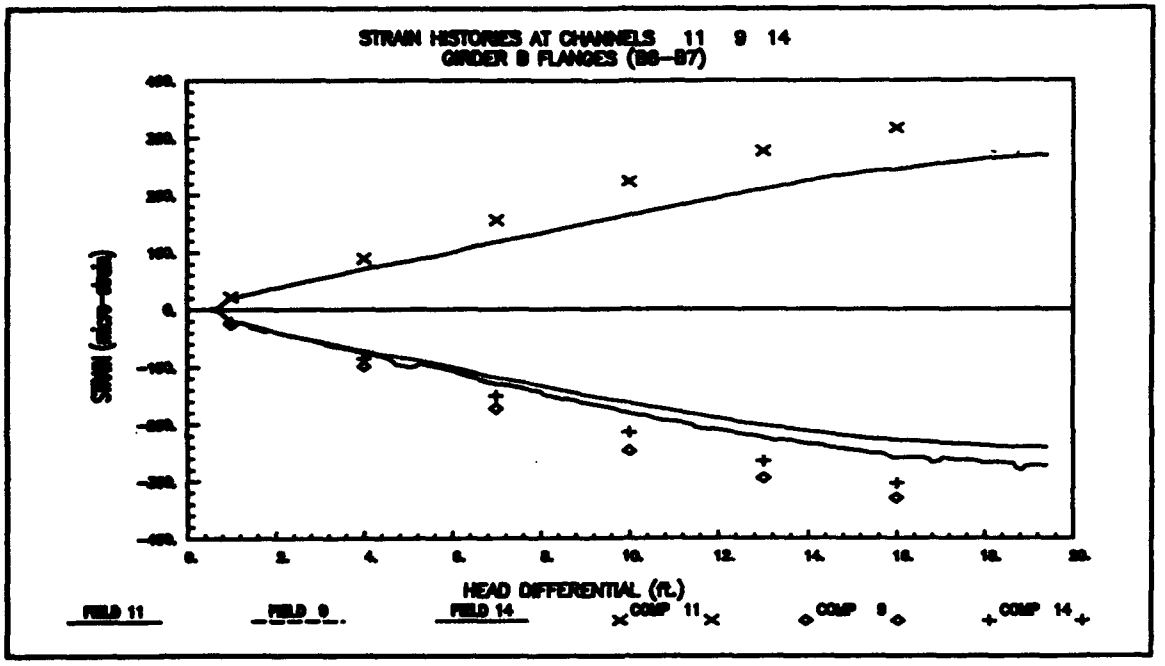

Figure B19. Locks and Dam 26 strain histories - Test 261A (SET1-26), Channels 11, 9, and 14

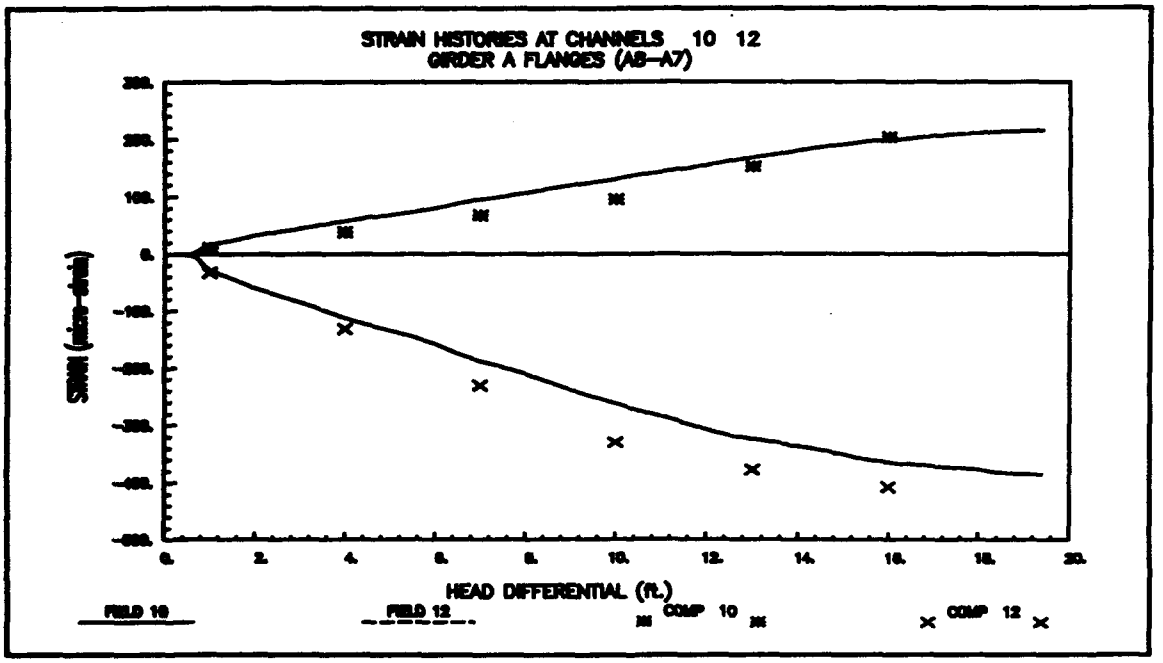

Figure B20. Locks and Dam 26 strain histories - Test 261A (SET1-26), Channels 10 and 12

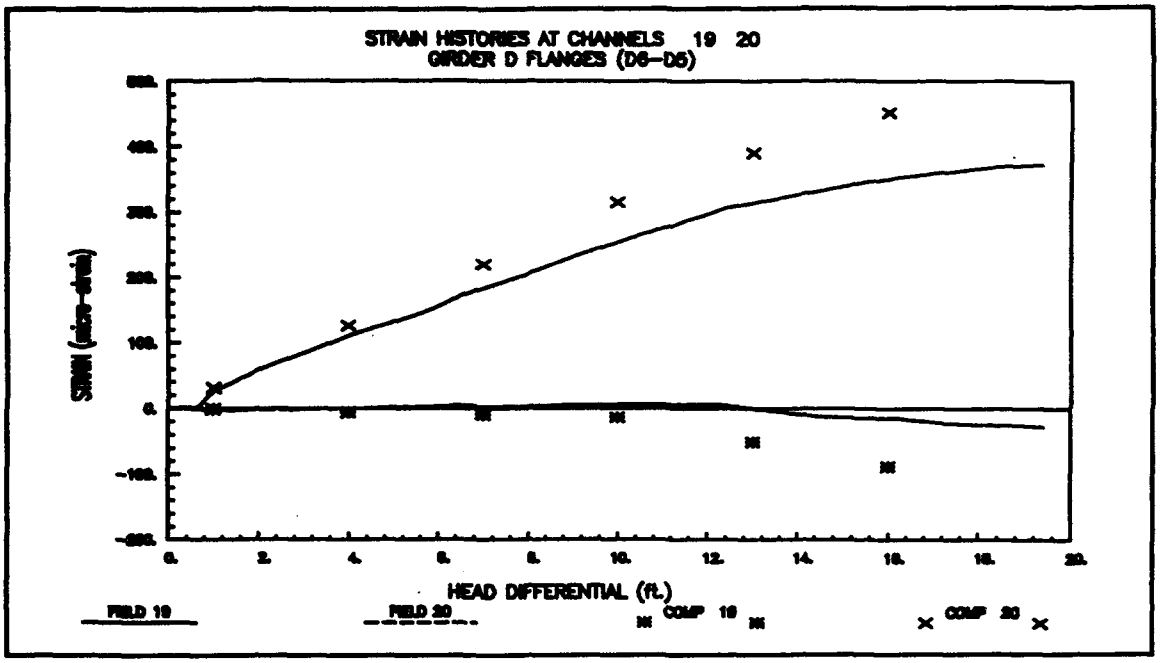

Figure B21. Locks and Dam 26 strain histories - Test 261A (SET1-26), Channels 19 and 20

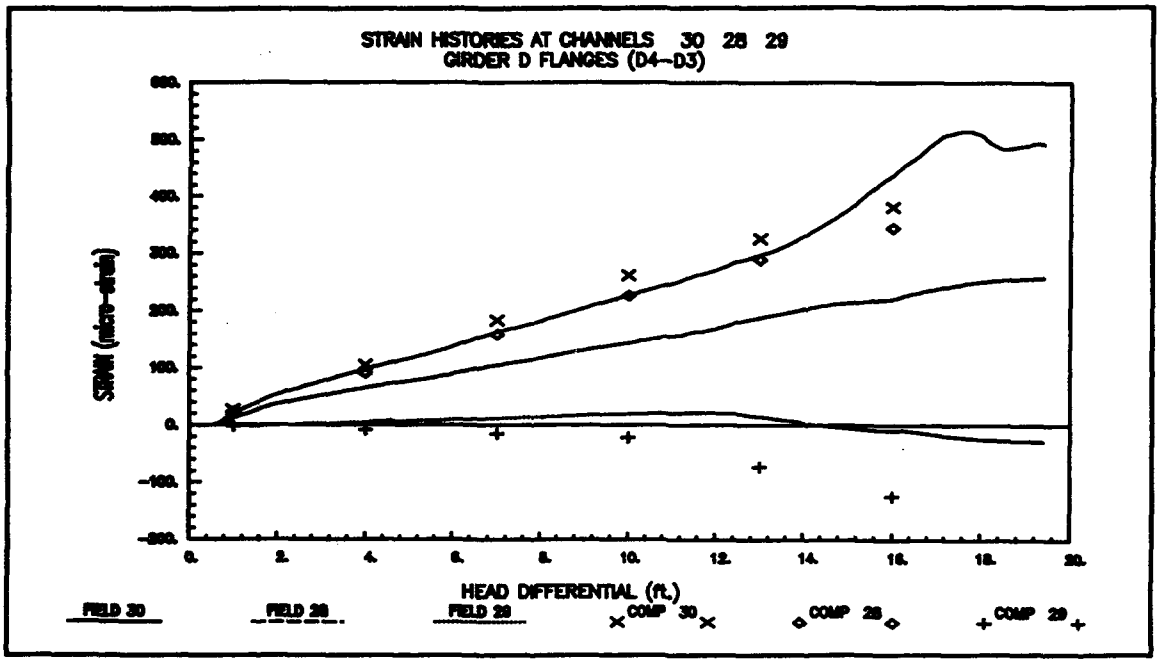

Figure B22. Locks and Dam 26 strain histories - Test 261A (SET1-26), Channels 30, 28, and 29

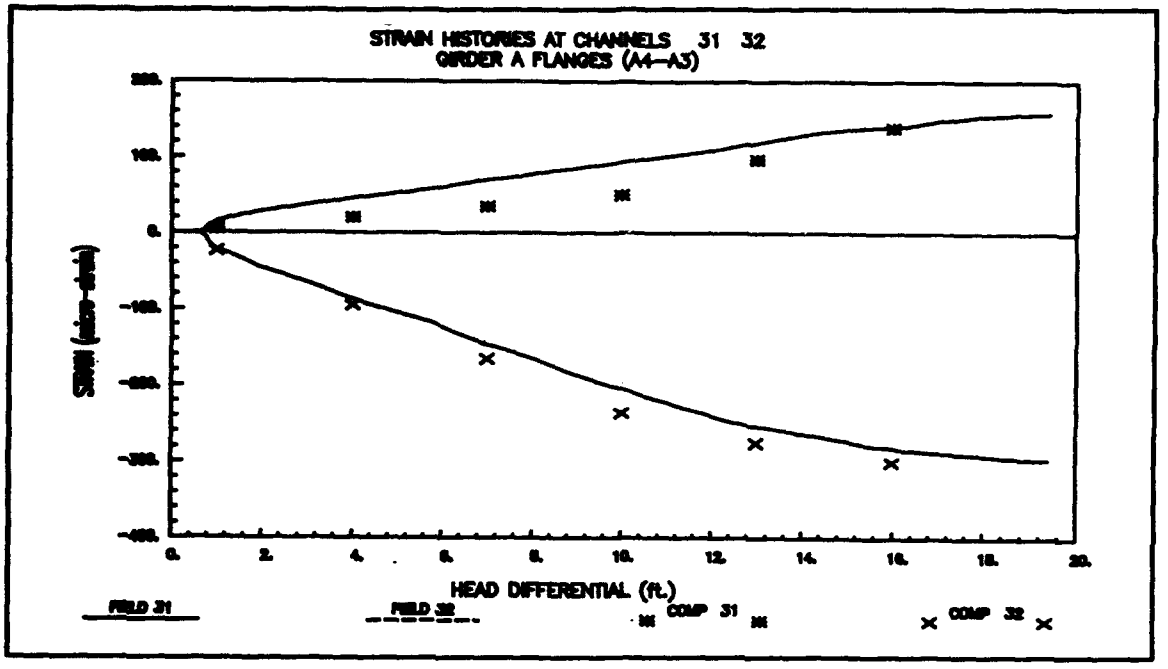

Figure B23. Locks and Dam 26 strain histories - Test 261A (SET1-26), Channels 31 and 32

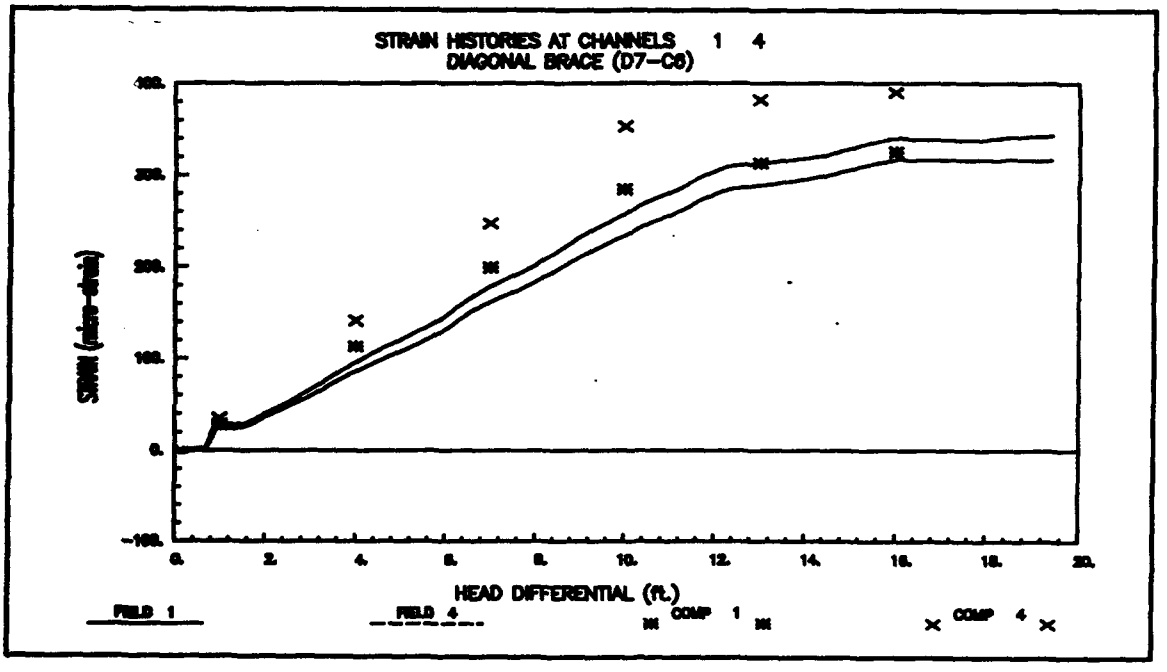

Figure B24. Locks and Dam 26 strain histories - Test 261A (SET1-26), Channels 1 and 4

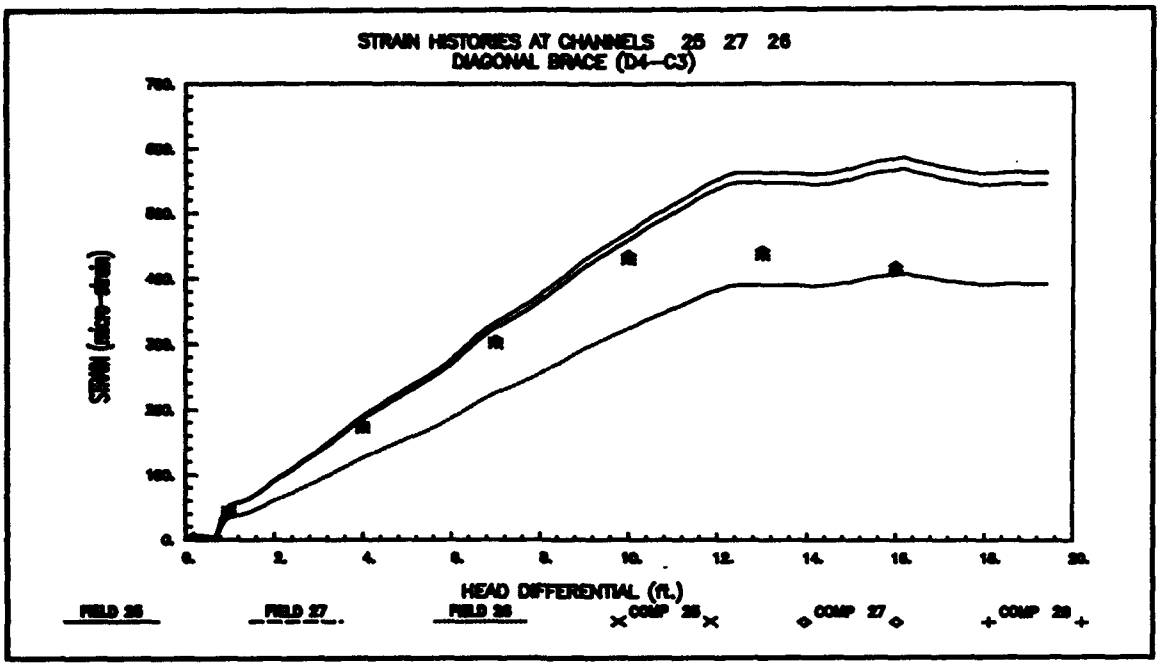

Figure B25. Locks and Dam 26 strain histories - Test 261A (SET1-26), Channels 25, 27, and 26

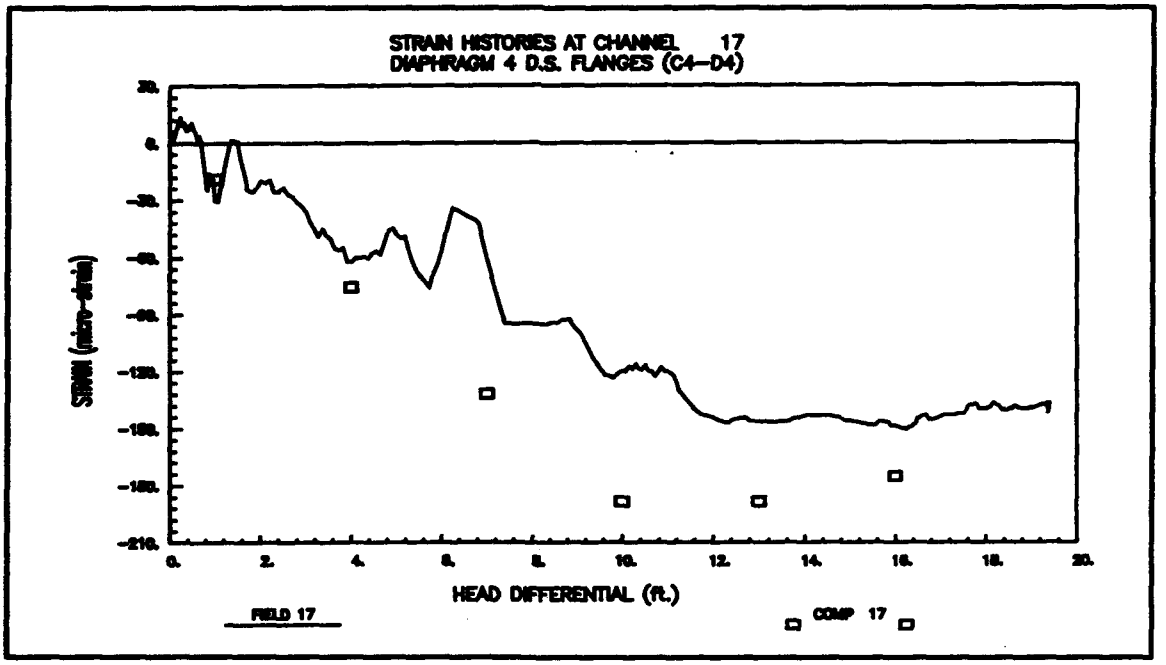

Figure B26. Locks and Dam 26 strain histories - Test 261A (SET1-26), Channel 17

Locks and Dam 26 Strain Data (Test 262B; SET2-26)

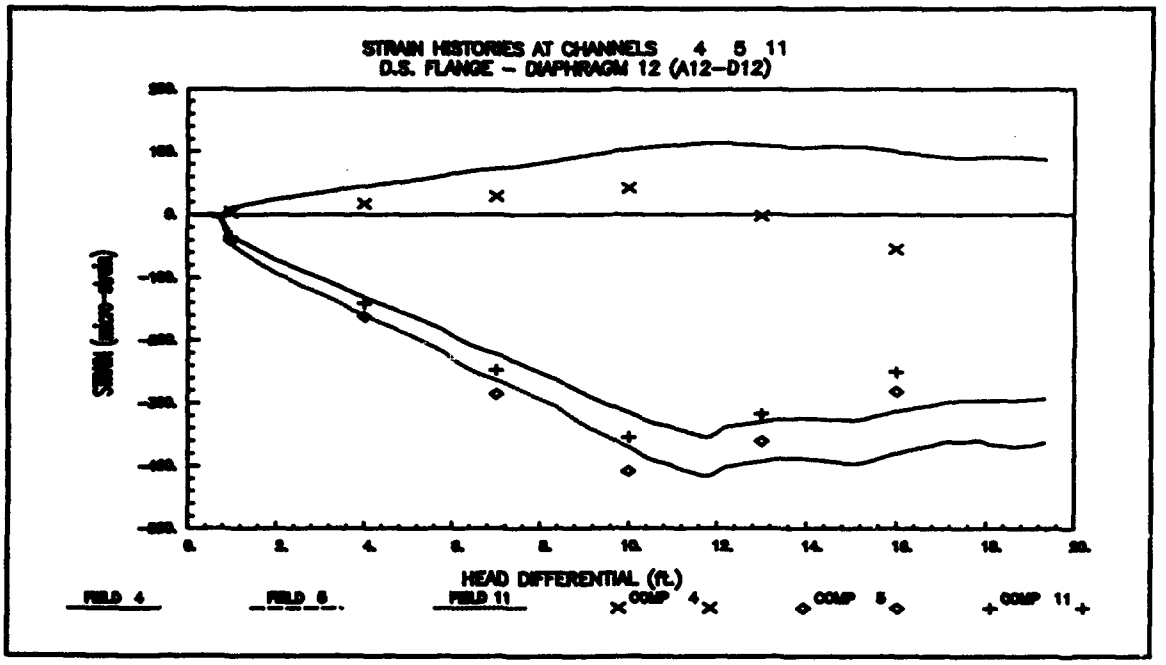

Figure B27. Locks and Dam 26 strain histories - Test 262B (SET2-26), Channels 4, 5, and 11

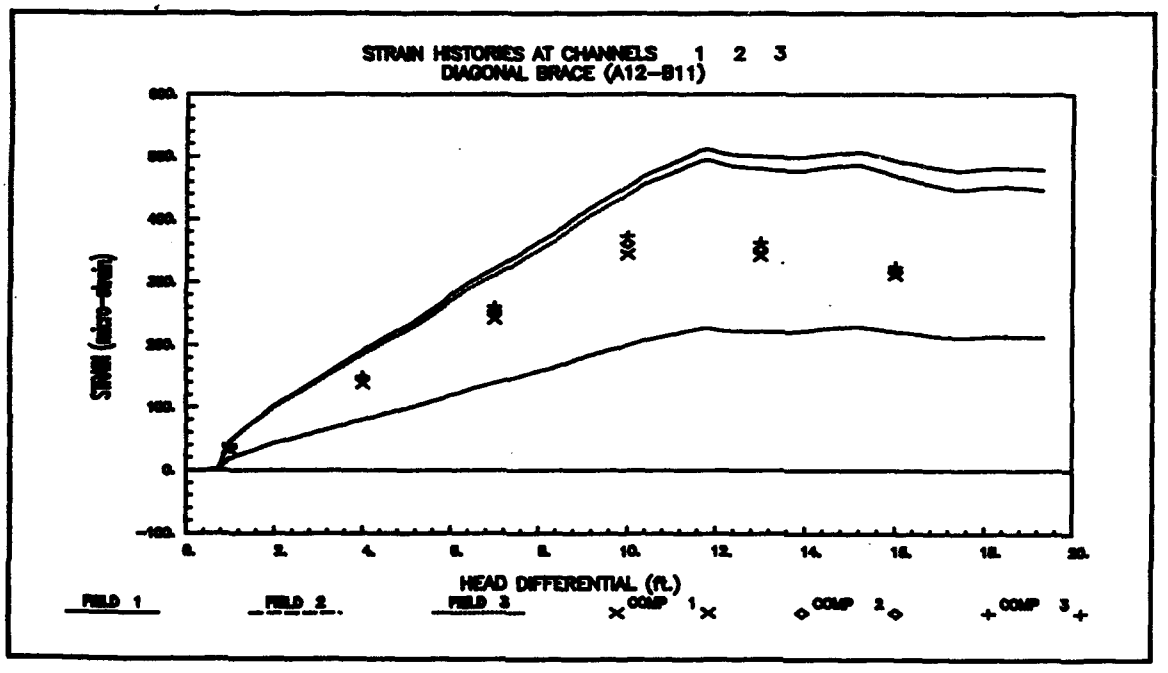

Figure B28. Locks and Dam 26 strain histories - Test 262B (SET2-26), Channels 1, 2, and 3

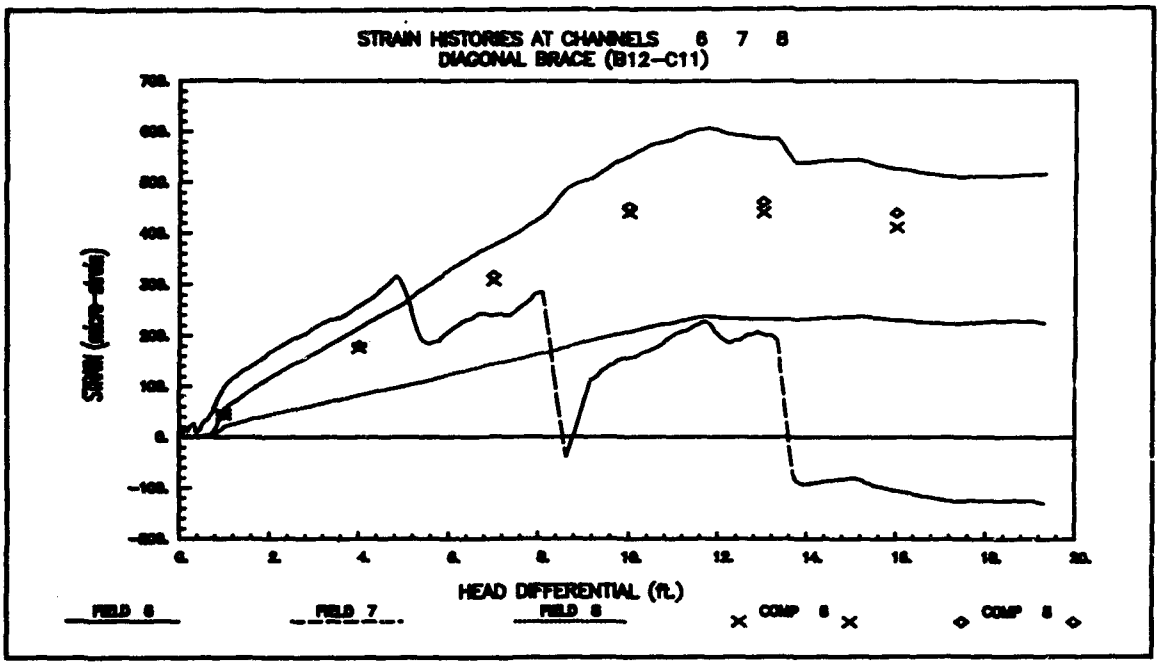

Figure B29. Locks and Dam 26 strain histories - Test 262B (SET2-26) (gage slippage on channel 7), Channels 6, 7, and 8

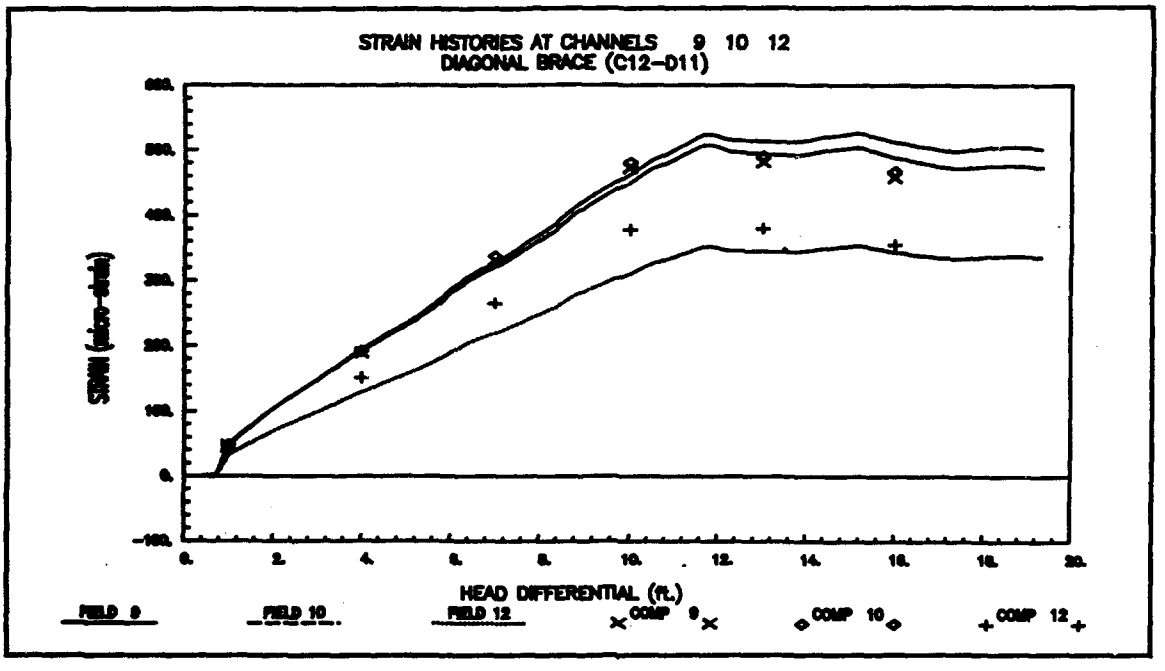

Figure B30. Locks and Dam 26 strain histories - Test 262B (SET2-26), Channels 9, 10, and 12

REPORT DOCUMENTATION PAGE

Form Approved
OMB No. 0704-0188

Public reporting burden for this collection of information is estimated to average 1 hour per response, including the time for reviewing instructions, searching existing data sources, gathering and maintaining the data needed, and completing and reviewing the collection of information. Send comments regarding this burden estimate or any other aspect of this collection of information, including suggestions for reducing this burden, to Washington Headquarters Services, Directorate for Information Operations and Reports, 1215 Jefferson Davis Highway, Suite 1204, Arlington, VA 22202-4302, and to the Office of Management and Budget, Paperwork Reduction Project (0704-0188), Washington, DC 20503.

1. AGENCY USE ONLY *(Leave blank)*	2. REPORT DATE	3. REPORT TYPE AND DATES COVERED
	June 1994	Final report

4. TITLE AND SUBTITLE
Field Testing and Structural Analysis of Vertical Lift Lock Gates

5. FUNDING NUMBERS
WU32641

6. AUTHOR(S)
Brett C. Commander, Jeff X. Schulz, George G. Goble, Cameron P. Chasten

7. PERFORMING ORGANIZATION NAME(S) AND ADDRESS(ES)
Bridge Diagnostics, Inc., 5398 Manhattan Circle, Suite 280, Boulder, CO 80303;
U.S. Army Engineer Waterways Experiment Station, 3909 Halls Ferry Road, Vicksburg, MS 39180-6199

8. PERFORMING ORGANIZATION REPORT NUMBER
Technical Report REMR-CS-44

9. SPONSORING/MONITORING AGENCY NAME(S) AND ADDRESS(ES)
U.S. Army Corps of Engineers
Washington, DC 20314-1000

10. SPONSORING/MONITORING AGENCY REPORT NUMBER

11. SUPPLEMENTARY NOTES
Available from National Technical Information Service, 5285 Port Royal Road, Springfield, VA 22161.

12a. DISTRIBUTION/AVAILABILITY STATEMENT
Approved for public release; distribution is unlimited.

12b. DISTRIBUTION CODE

13. ABSTRACT *(Maximum 200 words)*

The objective of this study was to measure the behavior of vertical lift lock gates experimentally and to develop modeling and analysis procedures for the evaluation of existing gates and design of new gates. In this study, lift gates at Mississippi River Locks 27 and Locks and Dam 26 were investigated. The gates were instrumented and tested under various loading conditions and analytical models were developed to simulate structural response of each.

Substantial structural response data were obtained with minimal impact on normal lock operation. Based on experimental strain data obtained during the field tests, it was determined that the analytical (finite element) models provided reasonably accurate predictions of the general behavior. Experimental and analytical data comparisons provided quantitative information on lift gate behavior and loading conditions. Through data comparisons for the Locks 27 lift gate, it was concluded that: 1) one of the seals did not exist; 2) an unknown amount of frictional resistance exists between the bottom sill and bottom of the leaf; and 3) for this case, a dynamic load model (Figure 54) is most appropriate for simulation of hydrostatic head differential loading. Through the Locks and Dam 26 study, it was verified that the downstream bracing members are primarily affected by vertical loading, and a probable cause for cracking of downstream bracing members was obtained.

14. SUBJECT TERMS

Analysis	Design	Loading condition
Boundary condition	Evaluation	Modeling
Data comparison	Head differential	Strain

15. NUMBER OF PAGES
81

16. PRICE CODE

17. SECURITY CLASSIFICATION OF REPORT	18. SECURITY CLASSIFICATION OF THIS PAGE	19. SECURITY CLASSIFICATION OF ABSTRACT	20. LIMITATION OF ABSTRACT
UNCLASSIFIED	UNCLASSIFIED		